Determining Mechanism Used by Bacteria to Evade Bactericidal Conditions, By the Way of Resistance and Persistence

A DISSERTATION

SUBMITTED TO THE FACULTY OF THE GRADUATE SCHOOL

OF THE UNIVERSITY OF MINNESOTA

BY

Lev Ostrer

IN PARTIAL FULFILLMENT OF THE

REQUIREMENTS

FOR THE DEGREE OF

DOCTOR OF PHYLOSOPHY

Advisor: Arkady Khodursky, PhD

February 2020

Acknowledgements

I would like to acknowledge my family, without their support I do not think I could have made it. Especially, I would like to thank them for their patience and putting up with all the late nights, missed celebrations and general absence in favor of research. The phrase "I live on bacterial schedule "at this point has become synonymous in my family with "experiments are taking longer than expected".

I also would like to thank my advisor Dr. Arkady Khodursky for giving me ample opportunities to peruse my own hypotheses, no matter how farfetched they had seem at the time. Because of the freedom and support provided by my advisor, I have learned to be a more independent as a scientist, and for that I will always be grateful. During our meetings, he taught me to temper my expectations and "not to bite of more than I can chew" as well as to be the harshest critic of my own work. I will fondly look back to the times when we would start discussing data, and will inevitably end up swapping jokes and life anecdotes. Looking back, all I can say is thank you for both the stern hand that guided me and the freedom and support that you have provided over the years.

Also I would like to thank my class mates and coworkers that I had privilege working alongside with. Despite always being busy, I cannot think of a single person who wasn't willing to help when asked for. This sort of comradery is hard to find, and I hope that in the future I will meet more amazing people like that.

Lastly, I would like to thank my girlfriend Yabing Yang. Though we had some rough times, she was the one to help me realize that there is a world outside the lab, and dragged me kicking and screaming into the twenty-first century. She was my outlet for many frustrations over failed experiments while also being subjected to endless excited

proclamations about the future projects. She taught me how to tame my scientific oversharing and to better read my audience, an invaluable skill in both science and everyday life.

Dedication

This thesis is dedicated to trillions of bacteria that put their lives on the line to make this research possible.

Table of Content

List of tables

List of Figures

Chapter 1

Introduction

Antibiotic resistance:

Drug resistance was described in the same manuscript that first chronicled the discovery of penicillin (1). Consequently, medical and scientific communities were made aware of drug resistance prior to the first infection ever being cured by an antibiotic. Following the discovery and clinical use of penicillin, the rate of drug discovery first outpaced the rise in subsequent drug resistance for clinically used therapeutics. By the 1980s however, fewer and fewer new antibiotics were being developed and therefore ease of public's access to antibiotics caused drug resistance to get out of control and to become a major public health concern. For the last four decades antibiotic resistance across all microbial pathogens has been rising steadily. Currently, nearly 30% of common pathogens are resistant one or more antibiotics (2, 3). Based on the current trends, it has been predicted that by 2050 more people would die from common microbial infections than from cancer or HIV/AIDS (4). The ramifications of widespread drug resistance are far beyond individual illnesses. Surgical procedures would carry enormous risks for acquiring post-operation incurable infections. Food supply will be greatly diminished, since farmed animals rely heavily on antibiotics for improved growth and survival. Undoubtedly, by compromising healthcare and the food supply, antibiotic resistance will have a major negative effect on world economy, at which point there is no telling the full extent of the damage widespread drug resistance may inflict.

The focus of my thesis is to address the impeding threat of antibiotic resistance by studying mechanism and strategies used by microbes to avoid death. Tackling the expansive and impending problem of antibiotic resistance can be broken down into individual aims: i) finding an efficient way to kill pathogenic bacteria, ii) predicting

resistance before it renders drugs ineffective, and iii) limiting the occurrence of chronic infections. Each of the following thesis chapters address these obstacles posed by drug-resistant bacteria.

Bactericidal vs. bacteriostatic drugs

Antibiotics are small molecules capable of preventing growth or killing microorganisms. These small molecules largely target four key processes bacteria need to proliferate; cell wall biosynthesis (β-lactams and vancomycin), protein synthesis (aminoglycosides, folate inhibitors and macrolides), transcription (rifampicin) and DNA synthesis (quinolones and fluoroquinolones). Antibiotics can be categorized into two major groups: bactericidal those that kill, and bacteriostatic those that inhibit growth without killing bacteria. A drug may be considered bactericidal if: the minimal bactericidal concentration (MBC), a concentration of the drug at which 99.99% of bacteria dies, is less than four times the minimal inhibitory concentration (MIC), a concentration of the drug at which bacteria growth is fully inhibited. Bactericidal drugs are mostly comprise of, but not limited to, DNA and cell wall synthesis inhibitors. Bacteriostatic antibiotics, on the other hand, are predominantly protein synthesis inhibitors. Bacteriostatic antibiotics work by hindering microbial growth, and though they may have some bactericidal activity, they are not sufficiently potent to classify as bactericidal.

Bactericidal drugs, such as β-lactams and fluoroquinolones, were historically preferred over bacteriostatic antibiotics, and are currently used to treat more serious infections such as meningitis and endocarditis (5). One advantage of bactericidal drugs is the rapid

killing of the intended bacterial target. The kill rate of a bactericidal antibiotic is proportional to the doubling time of a bacteria (6). In some cases, as with fluoroquinolones, kill rate may be as fast as 10% of the doubling time (7). Such rapid killing helps to restrict the emergence of antibiotic resistance. For example, patients treated with the bactericidal antibiotic penicillin against *Streptococcus pyogenes* have never developed a β-lactam resistant *S. pyogenes* mutants (8, 9). In contrast, treatment of the same pathogen with bacteriostatic macrolides resulted in 15% of clinical isolates gaining resistance (10). The act of killing bacteria also prevents phenotypic adaptation, such as differential expression of *omp* (porins) (11, 12). Additionally, bactericidal drugs can target slow-growing cells. High toxicity, even at low concentrations, assures that every available target would be exploited by the drug, leading to bacterial death. This is especially true for fluoroquinolone family of drugs that have a toxic effect at nanomolar concentrations.

Bactericidal antibiotics also have several major drawbacks. Some data indicates that use of bactericidal compounds has been linked to rapid release of endotoxins and cells wall particles, leading to a worsening proinflammatory response, edemas and septic shock (13). The consequences of using bactericidal antibiotics may also include permanent changes to human and animal microbiomes, resulting in the susceptibility to stomach cancer and infections by opportunistic pathogens (14). Pseudomembranous colitis which is caused by an opportunistic pathogen *Clostridium difficile* is the best illustration of the significant damage that prolonged exposure to bactericidal antibiotics can impose on a microbiome. The overuse of bactericidal drugs, primarily fluoroquinolones (15) causes major devastation microbial gut community. The transiently exposed ecological niche is

then taken up by the pathogen. During infection, *C. difficile* covers large portions of intestine in biofilms, preventing host nutrient absorption and causing diarrhea and in some cases, death (16). According to the 2015 report by the center for disease control, *Clostridium difficile* infections caused over 15000 deaths that year and the number is on the rise (17). Lastly, the rapid killing exhibited by bactericidal drugs can be a duel edged sword; while it prevents resistance via adaptation, it also provides the necessary pressure to select for drug resistant mutants. Hence, following the treatment, resistant mutants will have no competition from wild type cells and are likely to become the new dominant strain.

Unlike bactericidal antibiotics, bacteriostatic antibiotics are those that do not kill, but instead inhibit growth. These typically include ribosome and folate synthesis inhibitors (18, 19). These antibiotics work together with human/animal immune systems to clear an infection. Collateral damage to a human/animal microbiome is also limited, as most host bacteria are not killed (20). Bacteriostatic antibiotics have been shown to avoid the release of endotoxins, by inhibiting protein synthesis, consequently preventing sepsis (13). Reliance on the immune system to kill a pathogen and to clear the infection, however, poses a problem for treating the infections in areas of the body with no/limited access to immune cells. For this reason, for example an infection of gallbladder is never treated with bacteriostatic antibiotics (21). Another complication with bacteriostatic drugs is a higher rate of drug resistance. Suboptimal dosing, improper administration of drugs or premature discontinuation of therapy exposes a much larger population of bacteria to conditions known to select for resistance.

In some cases the same antibiotic may be either bactericidal or bacteriostatic, depending on the target species. Two such drugs showing species-dependent effects are rifampicin and chloramphenicol. Rifampicin has been shown to be bactericidal in Gram-positive bacteria, while bacteriostatic in Gram-negative (22). In addition, *Haemophilus influenzae* and *Streptococcus pneumoniae* are killed by the generally bacteriostatic drug chloramphenicol (23, 24).

Broad and narrow-spectrum antibiotics

Narrow- and broad-spectrum antibiotics are differentiated based on the range of bacteria that can be affected by the drugs. By targeting a specific pathogen, narrow-spectrum antibiotics do not expose commensal bacteria to selective pressure induced by broad-spectrum antibiotics. This helps to preserve patient's microbiome and limits emergence of new resistant isolates. Narrow-spectrum antibiotics such as vancomycin and isoniazid (which target staphylococcal and mycobacterial cell wall biosynthesis, respectively) are used for non-immediate life-threatening infections. A major limitation of narrow-spectrum antibiotics is that in order to be effective, prior knowledge of a pathogen is required. Hence, narrow-spectrum antibiotics cannot be used to treat unknown pathogens and non-specific infections. The use of narrow-spectrum drugs may also be limited due to lack of diagnostic equipment, such as in rural communities, developing and underdeveloped countries.

Broad-spectrum antibiotics, such as fluoroquinolones, are used to treat rapidly progressing infections (if the species of bacteria is unknown), for prophylaxis (such as after surgery), in cases where bacteria developed resistance to narrow-spectrum antibiotics and as a part of combination therapies. However, this group of drugs, even in after a short (7 day) course, have been shown to permanently alter microbiomes (25). The microbiomes become a reservoir of antibiotic resistant strains within commensal populations (26). Because use of broad-spectrum antibiotics does not require prior knowledge of a pathogen to be effective, this group of drugs is commonly misused and overprescribed, contributing to a rapid rise in antibiotic resistance worldwide. The number of clinically isolated strains resistant to fluoroquinolones and broad-spectrum penicillins have quintupled from 1998 to 2008 (27), with nearly 30% of all clinical isolates now being resistant to quinolones. Versatility and power of bactericidal broad-spectrum antibiotics is what made them an irreplaceable tool in the fight against bacteria, but at the same time qualities that made these drugs so great are now a major force behind widespread antibiotic resistance.

Combination therapies

For millions of years bacteria used antibiotics for carving out ecological niches. Evolutionarily, antibiotics produced by bacteria not only served role as a deterrent, but also a way of communication between different microbial species (28). Many soil-dwelling bacteria have an immense capacity for secondary metabolite production (29). Occasionally, superclusters of multiple antibiotic pathways are co-localized and co-expressed in species from the phylum of actinobacteria. One example of such behavior is well illustrated by *Streptomyces clavuligerus*. This particular soil dweller has been shown

to produce cephamycin C (a β-lactam) and clavulanic acid (β-lactamase inhibitor) from adjacent gene clusters (30). Similar drug combinations, such as amoxicillin with clavulanic acid, are used today to treat human infections. The general consensus, however, is that in most cases monotherapy should be the primary course of action (31). With proper dosing, single antibiotics are sufficient to clear most infections without incurring resistance. The exceptions to this monotherapy rule are; infections that are known to quickly develop resistance, rapidly progressing infections and severe infections that require long-term treatment (32). In these cases, specific combination drug therapy is recommended and often used, consisting of at least one bactericidal antibiotic and a number of bactericidal or bacteriostatic drug. At a glance this approach may seem counterintuitive, since most bacteriostatic drugs would slow down cells growth thus eliminating drug targets for the bactericidal drugs. However, certain antibiotic combinations have been shown to have synergy. One example of synergy is between aminoglycosides that target the ribosome and cause incorporation of misfolded proteins into cell membranes and β-lactams that disrupt cells wall synthesis (18). Together these drugs accelerate lysis and improve killing. Another widely used drug combination is trimethoprim with sulfonamides. By targeting the same pathway of folate synthesis, these antibiotics work together to inhibit thymine and methionine synthesis, causing both protein synthesis arrest and DNA damage via thymine starvation. A bit of a strange, yet favored antibiotic combination is rifampicin and fluoroquinolone (33). This antibiotic cocktail has had a great success in treating MRSA and TB (33, 34). However, the nature of the synergetic interactions between these drugs is not fully understood. Some suspect that during the SOS response induced by fluoroquinolones, bacteria experience

morphological changes, such as bloating or filamentation. With rifampicin inhibiting transcription, normal filamentation cannot take place, resulting in septal wall disruption (35). The malformed sections of the cell wall eventually contribute to membrane leakiness and results in effective killing. Another possibility is that with rifampicin, any and all stress response signaling is inhibited, further contributing to bacteria's inability to deal with stress induced by quinolones. Despite the general success of multidrug therapies in slowing down emergence of new drug resistant strains, the past three decades have seen a major increase in the emergence of multi drug-resistant (MDR) and extensively drug-resistant (XDR) pathogens (2). The rise in frequency of multidrug resistant infections begs the question: How is it possible to develop resistance with several enzymes being inhibited simultaneously?

Drug resistance mechanism

Antibiotic resistance is a natural occurrence that has preceded our discovery of antibiotics by millions of years (36, 37). The low concentration of antimicrobials produced in the wild, combined with long-term exposure promotes evolution of resistance, and in this way, antibiotic biosynthesis and antibiotic resistance co-evolved over centuries. As one example of such co-evolution, researchers were able to discover vancomycin resistance genes in a thirty thousand-year-old permafrost sample (36). There are a number of strategies bacteria can utilize to escape death when exposed to an antibiotic. Most bacteria have some basic level of intrinsic resistance afforded to it by its structural and fictional characteristics. For example, a difference in a structural feature such as microbial cell wall can have a drastic effect on susceptibility of bacteria to some families of drugs. For this reason, β-lactams are most effective against Gram-positive bacteria and

to a lesser degree Gram-negative species, while member of Mycoplasma genus remain completely unaffected by this family of drugs. However, intrinsic resistance on its own is often not enough to assure survival. Microbes have at least three additional avenues to foster resistance to antibiotics; i) drug target mutation, ii) drug inactivation, and iii) decreasing the ratio of drug to drug target (38). While drug inactivation is a major contributor to antibiotic resistance, my thesis will focus on the remaining two areas of antibiotic resistance.

Cellular drug target mutations

Mutation of a target enzyme usually affords the largest protection against a specific antibiotic. The classic example is penicillin and penicillin binding proteins (PBPs). During cell wall biosynthesis, peptidoglycan (a polymer that makes up the cell wall) is deposited in layers outside the plasma membrane. In order to give the cell wall structural rigidity and to prevent disassembly, parallel strands of peptidoglycan are crosslinked by PBP. During crosslinking, PBP removes a D-Alanine residue from one of the components of peptidoglycan chain and replaces it with a covalent bond on the parallel strand. β-lactams structurally mimic the D-Ala—D-Ala peptide moiety, and by entering the catalytic cleft of PBPs forms a covalent bond with active site serine. The resulting complex is hydrolyzed extremely slowly, thus effectively inhibiting the enzyme. Penicillin resistance can be achieved with single mutations in or around the active site of PBPs, which prevents β-lactams from inhibiting the enzymes (39).

Antibiotic resistance mutations can also prevent access of the drug to the active cite. Examples of such modifications occur during acquisition of rifampicin resistance (40). Rifampicin is a bacterial RNA polymerase inhibitor that functions by blocking the

DNA/RNA channel formed by the β-subunit of RNA polymerase and consequently inhibiting RNA elongation. Channel blocking is only effective during early stages of elongation and only occurs within the synthesis of the first three bases of newly synthesized mRNA. The interaction between RNA polymerase and rifampicin is dependent on 12 amino acid residues that help to anchor the drug in place (40) in front of the active site (Fig. 1-1). Depending on the mutated residue, different levels of rifampicin resistance can be achieved. The majority of mutations associated with rifampicin resistance are confined to RNA polymerase β-subunit regions-I (505-537 amino acid residues (aa)) and/or region-II (562-575aa).

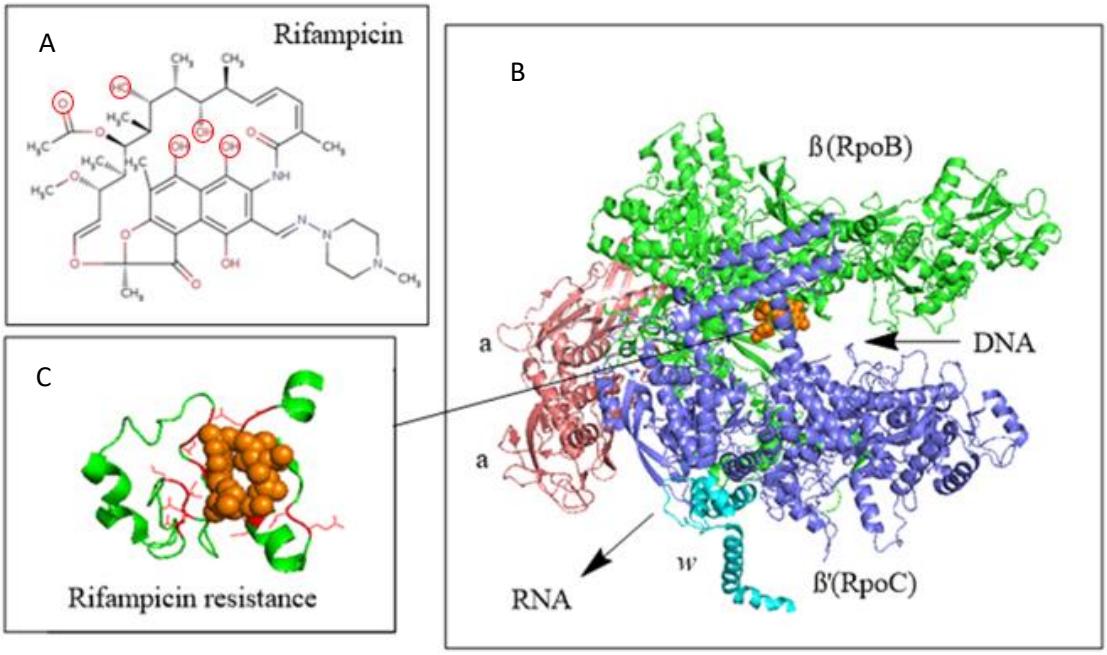
A
Rifampicin
B
ß(RpoB)
a
a
DNA
RNA
w
ß'(RpoC)
C
Rifampicin resistance

D

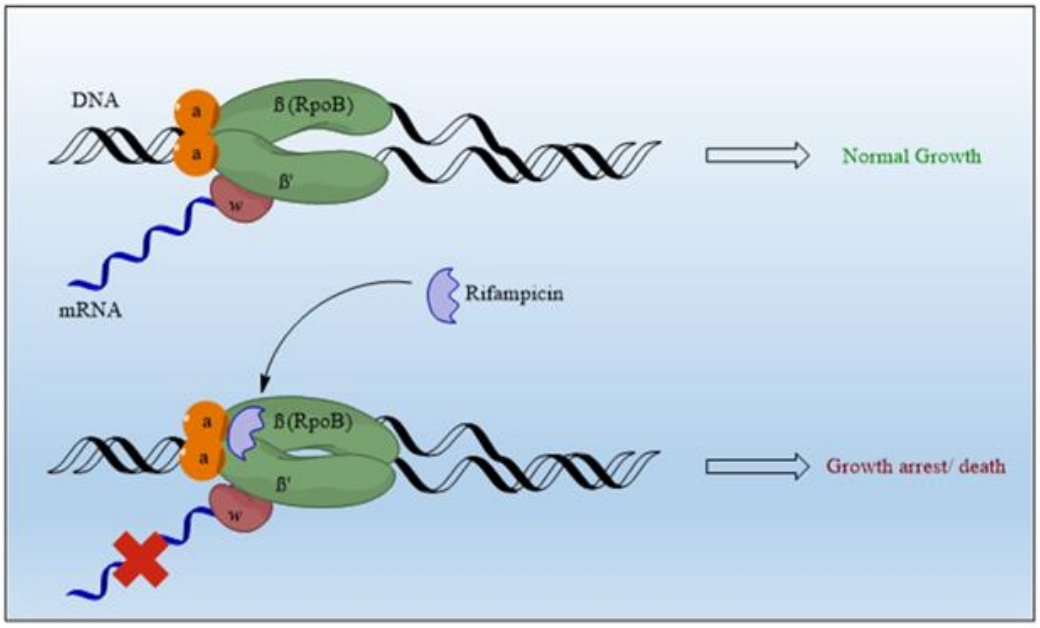
DNA
a
a
ß(RpoB)
ß'
w
Normal Growth
mRNA
Rifampicin
a
a
ß(RpoB)
ß'
w
Growth arrest/ death

Figure 1-1: Mechanism of rifampicin action and resistance: (**A**) Shows rifampicin molecule with red circles indicating oxygen atoms that help to from hydrogen bonds with RNAP β-subunit in order to block transcription. Some of the oxygens highlighted can interact with several residues. (**B**) Depicts a 3.8Å crystal structure of RNA polymerase, with rifampicin effectively blocking DNA/RNA channel (Molodtsov et.al, 2017).The arrows indicate the directionality of transcription, with active site located just past the rifampicin (shown in orange). (**C**) Is a magnified view showing key amino acid residues (505-537 and 562-575) that when mutated confer rifampicin resistance (40). (**D**) Is a cartoon representation of RNA polymerase action, with RNAP holoenzyme depicted in green, rifampicin in purple and DNA/RNA in black and blue respectively.

Mutations in drug targets provide the greatest levels of resistance, but in order to withstand bactericidal activity of more powerful antibiotics, additional mutations are sometimes needed. One such example is ciprofloxacin, a widely used broad-spectrum antibiotic and a member of fluoroquinolones family. This drug efficiently kills bacteria by inhibiting type II topoisomerases (DNA gyrase and topoisomerase IV) (41). The gyrase function is to introduce DNA supercoiling, while topoisomerase IV performs decatenation at the end of DNA replication (42). Unlike type I, type II topoisomerases alleviate supercoiling by introducing a DNA double-stranded break followed by re-legation (42). Ciprofloxacin inhibits the DNA-gyrase/topoisomerase IV complex by forming a DNA-gyrase/topoisomerase IV-ciprofloxacin complex, which consequently prevents DNA re-ligation step from taking place (Fig.1-2). Ultimately, progressing replication forks collide upon reaching inhibited complexes converts DNA within the frozen complex in to a non-ligatable from and eventually dislodging the complex, exposing a double-stranded breaks (43, 44). Since most bacteria lack an efficient way to repair this type of DNA damage, killing occurs rapidly and efficiently. As mentioned above, most pathogens contain both enzymes. This means that in order for bacteria to

gain clinical level of resistance (resistance to antibiotic at a concentration used to treat specific infection), mutations must occur in both targets. When ciprofloxacin binds its target, the drug interacts with two residues: (*E. coli* based amino acid positions) Ser-83 and Asp-87 gyrase subunit A (GyrA), and Ser-80 and Glu-84 of topoisomerase subunit A (ParC) (45). This region is referred to as quinolone resistance determining region (QRDR). Hence, to achieve clinical level of resistance as little as two and in some cases as many as four residues must be mutated.

A

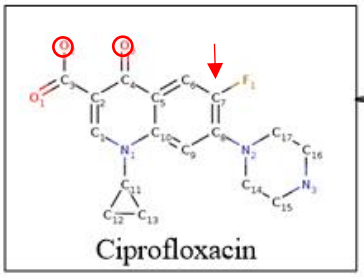
Ciprofloxacin

B

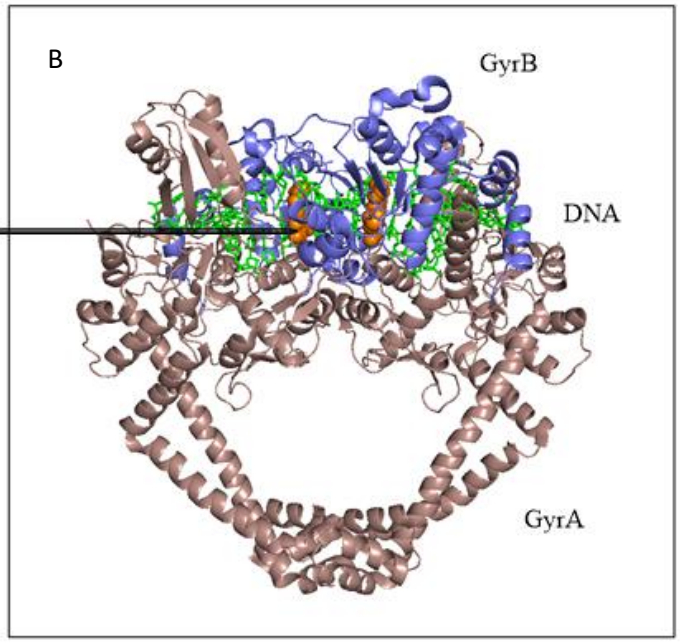
GyrB
DNA
GyrA

C

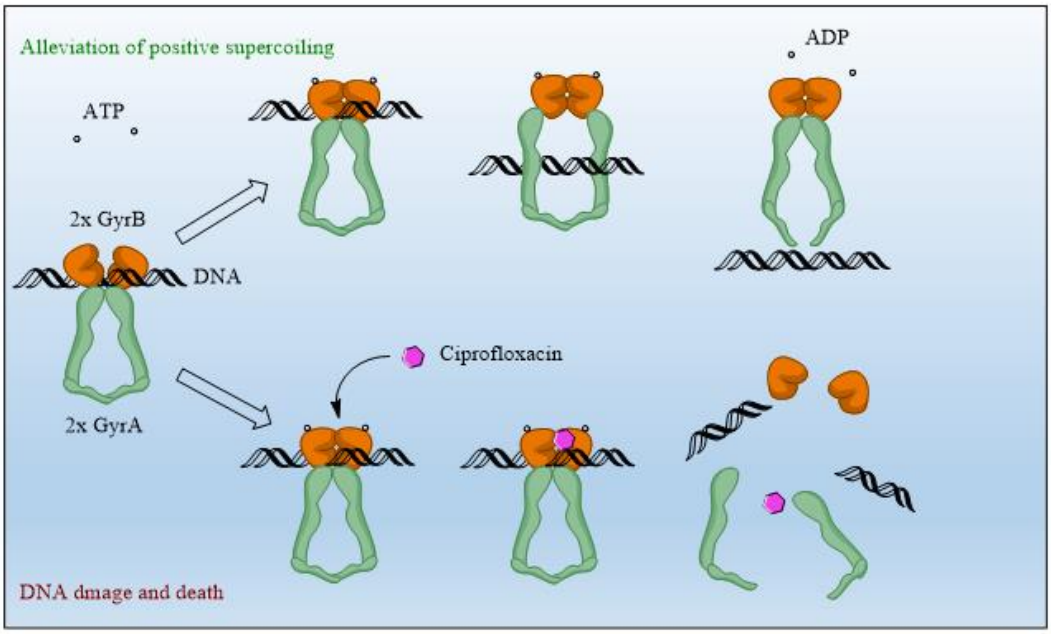
Alleviation of positive supercoiling
ATP
ADP
2x GyrB
DNA
Ciprofloxacin
2x GyrA
DNA dmage and death

Figure 1-2: Mechanism of quinolone action: (**A**) Showing a ciprofloxacin molecule, two oxygens indicated by red circles play an important role in orienting quinolones into the right position while according to Mustaev et.al., C-7 carbon ring (indicated by the red arrow) interacts with the enzyme. (**B**) A crystal structure showing gyrase-DNA complex inhibited by ciprofloxacin. Quinolones can only interact with an enzyme after enzyme-DNA complex has been formed. (**C**) Is a cartoon representation of gyrase action and inhibition of gyrase by ciprofloxacin. Without the drug enzyme uses two ATP to introduce staggered double stranded cuts, while forming a covalent bond with DNA. This is followed by an introduction of a negative supercoil and relegation. In presence of the drug quinolone binds the at the cleavage site, preventing re-ligation. A collision with a replication fork dislodges complex, resulting in double-stranded break.

Based on rates of spontaneous mutagenesis, the chances of generating a quadruple mutant is one in 10^{28}. However, during an infection not all cells are exposed to the same concentrations of drug. Physical environment such as biofilms, mucus, tubercles, implants and bone may create barriers to drug diffusion, resulting in microenvironments with lowered drug concentration. A gradual change in drug concentration is conducive for resistance to emerge and become fixed in a population one mutation at a time (46, 47). The need for bacteria to possess several mutations in order to reach clinical levels of resistance presents an opportunity. If mutations follow a hierarchy, then a mutational path can be determined. Using the first mutation in the chain it would be possible to detect drug resistance before it reaches clinical levels.

Antibiotic target concentration

Another strategy bacteria uses to escape antibiotic-mediated death is to lower the drug-to-target ratio. This can be done by i) removing the drug from the target or ii) removing the target. The job of removing toxic substances from the cell wall to efflux pumps. There are five efflux pump families; the major facilitator superfamily (MFS), the ATP-binding cassette superfamily (ABC), the small multidrug resistance family (SMR), the resistance-

nodulation-cell division superfamily (RND) and the multi antimicrobial extrusion protein family (MATE) (48). Due to their relevance to this thesis, RND and MATE families will be further discussed. The best studied RND pump is AcrA/B TolC multicomponent proton/drug antiporter (49). What sets RND pumps apart from the other pump families, is that lipophilic and amphiphilic antibiotics (tetracycline, β-lactams, fluoroquinolones and others) are secreted out of the cell, instead of into the periplasmic space (50). Production of these pumps is highly regulated at several levels. AcrA/B are directly repressed by AcrR, an upstream local repressor (Fig. 1-3B). Global level expression of both *tolC* (an outer membrane part of the pump) and *acr* components are regulated via MarA and SoxS activators, which themselves are under regulation of MarR and SoxR repressors (51). Mutations in RND regulatory pathways result in RND pump overexpression, substantially improving bacterial resistance to several antibiotics.

MATE efflux pumps are symporters. However, in addition to protons, MATE efflux pumps can also use sodium ions to remove molecules from the cytosol. MATE efflux pumps transport antibiotics into the periplasm in contrast to RND pumps that export material outside the cell (Fig. 1-3C). MATE pumps have a high affinity to quinolones and fluoroquinolones (52), yet these pumps are not expressed during exponential growth and thus do not normally contribute to changes in the corresponding drugs' MICs/MBCs. One of the pumps belonging to the MATE family is MdtK. This particular pump is predicted to be under the control of σS and σ24 transcription factors (Fig. 1-3A). Both sigma factors are associated with stress conditions and are not expressed during active growth (53, 54). Overexpression of MdtK provides a moderate level of resistance (2-3-fold

increase) to quinolones (55). This member of MATE efflux pumps will be discussed in later chapters.

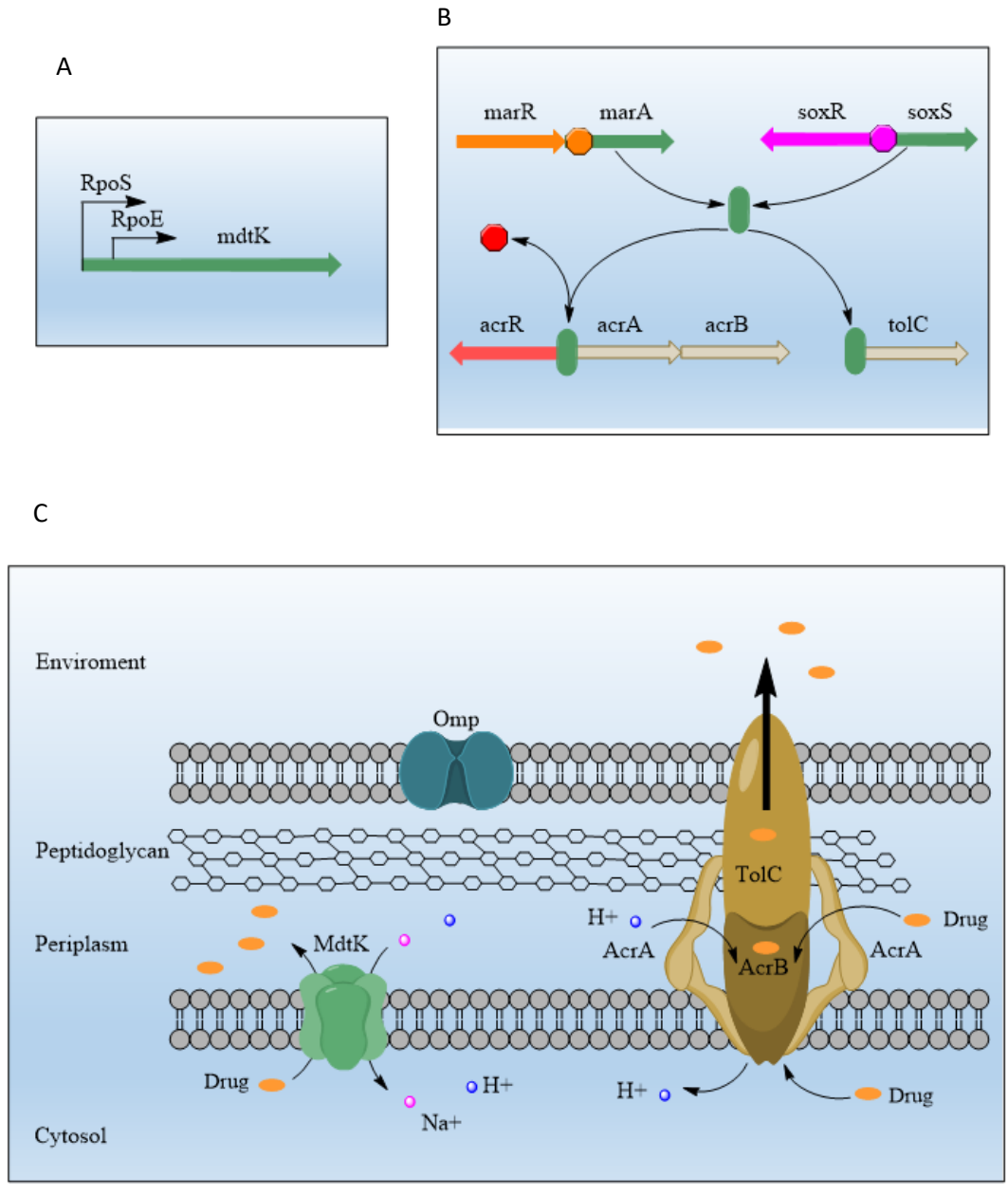

Figure 1-3: Regulation and functionality of RND and MATE efflux pumps: (**A**) Shows proposed transcriptional regulation for MdtK, one of the pumps from the MATE family of efflux pumps. (**B**) Multiple tears of transcriptional regulation of AcrA/B, TolC RND efflux pump, requiring removal of three perpressors and presence of two activators in order to initiate transcription. (**C**) A cartoon representation of RND, MATE and Omp. RND pumps used H+ to move wide range of antibiotics from both the periplasmic space and the cytosol out of the cell. Mdtk (MATE efflux pump) is a symporter that can used both Na+ and H+ to move quinolones from the cytosol to periplasmic space. Omp(s) facilitate non-specific diffusion and are located on the outer membrane.

Elimination of drug targets in bacteria occurs through resource reallocation during growth state transitions in response to environmental changes. The most common example occurs after cells reach stationary state. Due to the lack of cellular targets in non-growing cells, bacteria can become thousands of times more resilient to nearly all antibiotics compared to their exponentially growing state. Though technically not considered resistance since elimination of essential enzymes or drug targets substantially retard or even completely eliminates growth, this strategy substantially improves ability of bacteria to survive extreme antibiotic stresses. A more accepted term for this phenomenon is called persistence (56).

Bacterial persistence

Definitions of persistence tend to vary, but in a broader sense persistence can be defined as a dormant or dormant-like state where bacteria are highly resilient to lethal levels of stress. Persistence has been documented in many living organisms, including both eukaryotes and prokaryotes. Persistence is closely tied to adaptation and the ability of an organism or cell to handle stress. This mode of survival is highly beneficial in most cases, allowing for repopulation of decimated biomes and survival in rapidly changing

environments. The type of persistence discussed in this thesis will specifically address persistence of pathogenic bacteria in response to bactericidal antibiotics.

Resistance and persistence historically have been viewed as drastically different concepts (57) despite achieving the same goal of surviving antibiotic exposure. A key difference that exists between resistance and persistence is; resistant bacteria can proliferate in the presence of antibiotic, while persistent isolates cannot. Inability to proliferate, however, does not imply death. Persisters promote survival by simply waiting out the stress, before re-infecting the host. High persistence among pathogens often results in chronic infection. During such an infection, bacteria are susceptible to treatment. However, re-infection by a small sub-population of survivors occurs following antibiotic withdrawal. The cycle of re-infection and treatment continues until resistance develops. Consequently, chronic infections serve as a major reservoir for developing newly emerging MDR strains (58, 59).

Metabolic dormancy within a sub-population is believed to manifest improved survival by indiscriminately eliminating drug targets. Thus, persistence is not drug specific nor dependent on drug concentration or duration of exposure to a drug (60). While metabolic inactivation has been well documented as the benchmark behavior of persister cells, many questions aimed at understanding mechanisms of persistence still remain unanswered. Questions listed below are some major queries still being asked in the field of persistence. In later chapters of my thesis I will be touching upon the first two questions, while more substantially addressing the later questions posed below.

Question 1: *Is persistence a distinct physiological state from stationary state?* At a first glance, much evidence would suggest that persister cells are stationary cells. The lack of

growth or division and expression of σS (a transcription factor associated with stationary state) (61) in persister cells suggests that stationary state and the persister state are one in the same. Additionally, forced arrest of bacterial growth via starvation or through exposure to a bacteriostatic drug, significantly increases persistence (62). Further supporting the notion that persister cells are stationary is the observations of exponential increase in persister frequency as population transition into stationary state. However, here lies the problem. If persister cells are stationary cells, then it would stand to reason that in stationary state all cells should be persisters, but that is not the case. For example, in *E. coli*, the persistence rate when treated with ciprofloxacin is only 0.1-1.0% of stationary cells (63), suggesting that the persister state is different than stationary state (64). Further supporting the notion of distinctive states are the observations that slowed growth in exponential steady-state culture increases persistence. The exponential steady state implies that all cells in a population are proliferating and thus are not stationary, yet the number of persisters in such culture may be increased hundreds fold, depending on degree of slowing (65, 62). Though the question remains unanswered with substantial evidence to support both notions, persistence is likely a distinct state that shares some features with stationary state cells.

Question 2: *Is persistence induced in response to stress or is it a constant byproduct of growth?* The inducibility of persistence is another point of controversy. Appearance of persisters under all types of bactericidal treatments would suggest that persistence is intrinsic to any bacterial population (66). Thus, persisters must be formed spontaneously prior to bactericidal antibiotic treatment (67). However, some evidence contradicts this notion. One example is the induction of persistence via toxin-antitoxin systems such as

with the toxin TisB that gets induced by ciprofloxacin via the SOS response (68). This particular type II toxin induces persistence by decreasing membrane potential and forcing cells into dormancy before it can be killed. Yet knocking out any of the individual toxin-antitoxin pairs does not eliminate persistence (66), suggesting a more complex signaling network. Provided that persistence may be triggered in a number of ways, it is likely that multiple stress responses can activate metabolic dormancy using any and all of 36 known toxins-antitoxins (in *E. coli*) (69). Compelling data on both sides of the argument imply that both may be true, where some persister cells are formed spontaneously prior to drug exposure, while others are induced by a stress response. It is also worth mentioning that the rate of antibiotic killing vs the rate of bacterial adaptation may be a determining factor in inducibility of persistence. With fast-killing drugs, inducible persistence may not have enough time to trigger, while slow-acting antibiotics would be more effective at inducing persistence.

Question 3: *Given intrinsic nature of persistence, what pathway(s) may be responsible for inactivation of premature metabolic dormancy associated with the persister state?* One of the most common types of stress experienced by bacteria is starvation. Surviving stress imposed by long-term starvation is reliant on the ability of bacteria to effectively transition in and out of a metabolically dormant state. One of the main regulators of the starvation response is guanosine tetraphosphate (ppGpp). Indeed, deletion of RelA or SpoT, enzymes responsible for ppGpp synthesis, results in a significant loss of persistence (70). Many toxin-antitoxin pairs work by triggering the ppGpp signaling cascade. A classic trigger of this cascade is caused by the HipA toxin (Fig.1-4) (71). The toxin works by phosphorylating glutamyl tRNA synthetase that prevents recharging of

the tRNA with glutamate. As a result, bacteria experience nutrient starvation in the presence of glutamate. An inducible starvation activates SpoT (a stringent response sensor) changing SpoT's activity from degradation to synthesis of ppGpp (72). The alarmone signal is further amplified by a RelA, a homolog of SpoT, until cells transition into a non-growing state. At its maximum ppGpp concentration reaches 10 times the basal level (73). At this point ppGpp acts to change transcriptional activity of RNA polymerase, and facilitates exchange of transcription factors from σ70 to RpoS (74). This transcriptional shift eventually leads to dormancy and increased persistence. A large number of pathways are regulated by ppGpp. For this reason, knockout experiments may be complicated by a number of unexpected consequences. Moreover, with so many pathways effected by ppGpp, pinpointing the one or more pathways responsible for persistence may prove challenging. With that said, the general theme across all of the persistence-inducing systems is the ability to trigger central stress responses, leading to dormancy and thus increasing chance of survival.

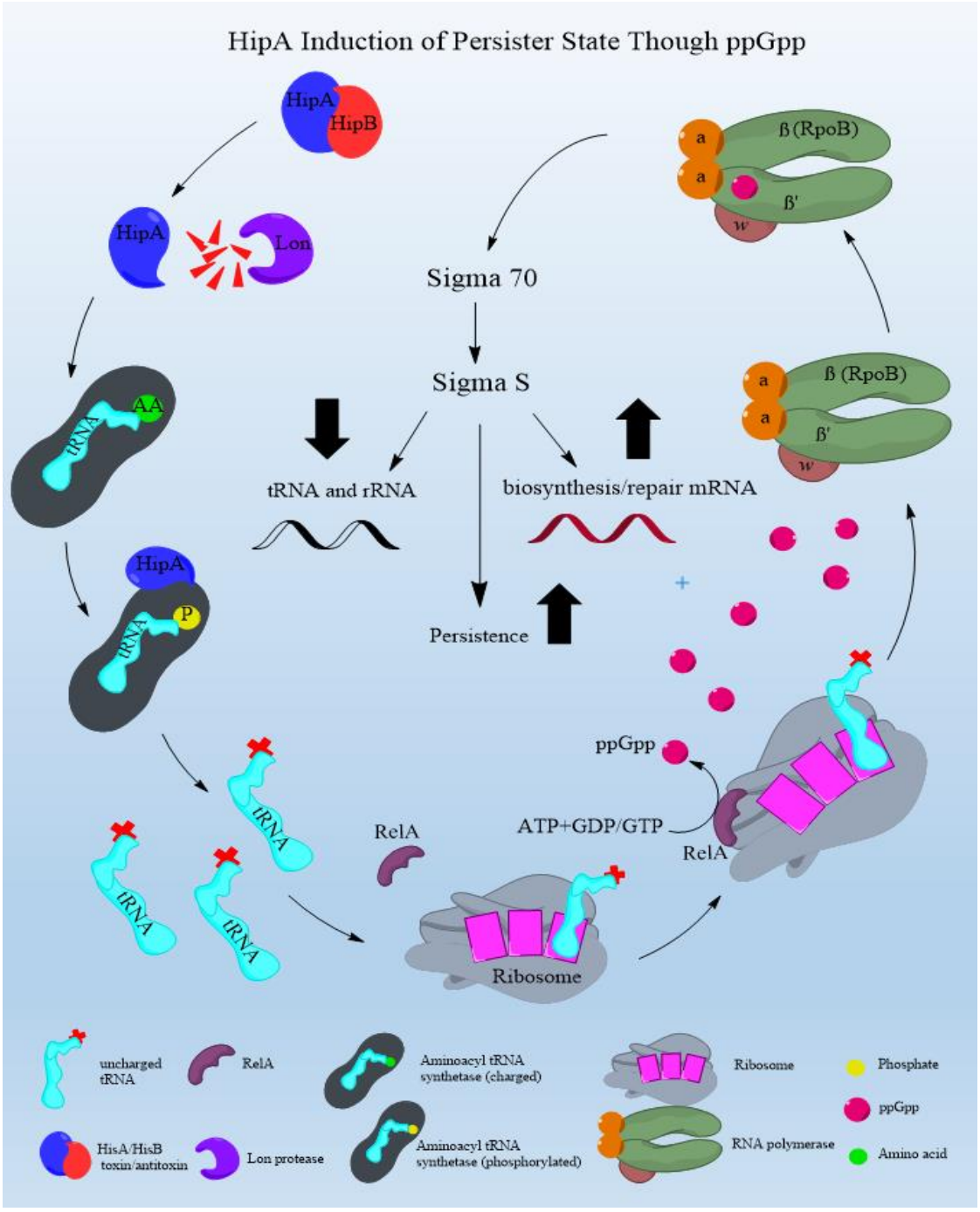
HipA Induction of Persister State Though ppGpp
HipA
HipB
HipA
Lon
Sigma 70
ß (RpoB)
a
a
ß'
w
Sigma S
AA
tRNA
tRNA and rRNA
biosynthesis/repair mRNA
HipA
P
tRNA
Persistence
ppGpp
ATP+GDP/GTP
RelA
RelA
tRNA
tRNA
tRNA
Ribosome
uncharged tRNA
RelA
Aminoacyl tRNA synthetase (charged)
Ribosome
Phosphate
ppGpp
Amino acid
HisA/HisB toxin/antitoxin
Lon protease
Aminoacyl tRNA synthetase (phosphorylated)
RNA polymerase

Figure 1-4: Mechanism of toxin-antitoxin based persistence: Release of toxin though degradation of the antitoxin results in phosphorylation of tRNA synthase. Lack of charged tRNA, causes cell to experience "starvation" triggering ppGpp production. Accumulation of ppGpp causes cells to transition into adaptive phase, and if starvation is not resolved, eventually cells will transition into stationary state. Upon growth arrest, persistence frequency drastically increases. While not all toxins follow this path, all of the known toxins work by rapidly depleting a key resource to induce starvation in presence of nutrients.

Question 4: *If and how does persistence in vitro and in vivo differ from one another?*

Most of what we know about toxin-antitoxins and high-persistence mutants was learned by selecting and studying laboratory-derived strains. Such strains were selected by drastic fluctuations of drug concentrations in optimal environments or by transposon mutagenesis (75, 76). This approach resulted in discovery of many individual toxin-antitoxin systems. Unfortunately, almost none of the high-persistence mutations identified by in vitro experiments are found in clinical isolates, the only exception being *hipA* allele (77). This implies one of two possibilities. The first possibility is that the cost of persistence mutations to the cell is greater than the advantage provided. In other words, high persistence mutants selected in vitro are outcompeted by wild type bacteria in their native environment. The second possibility is that the benefit of in vitro high persistence mutations is limited to the conditions used to select and test the said mutations. In either case, while understanding of microbial physiology gained from laboratory-selected high persistence mutants is invaluable, from clinical perspective these mutations contribute little to the fight against chronic infections. Clinical persistence often relies on completely different mechanisms than high persistence in vitro mutants. Strains isolated from patients with chronic infections typically have mutations in one or more stress

response pathways or rely on dysregulation of intrinsic survival mechanisms such as biofilm formation (78, 79).

Additionally, for an in vitro selected mutant to be considered a "pure persister mutant", it must not have any growth defects (56). The justification for this claim is based on two ideas. First, that slower growth results in the decreased number of drug targets per cell. Loss of drug targets across bacterial population causes a subpopulation of cells that lost enough targets not to be killed by the antibiotic to emerge. Resulting in a greater fraction of bacteria surviving the killing. Second, is that slow-growing cells would be outcompeted in the wild as soon as antibiotic pressure is gone. Indeed, as demonstrated by completion experiments, faster growing cells tend to take over within a few generations. However, the fact that chronic clinical isolates have shown varying degrees of growth defects argues against this notion. This further implies that same mutations that increase persistence frequency and retard growth may have other advantageous traits to allow them to compete on par with non-growth-retarded cells in the wild. The growth retardation of clinically relevant persistence is exemplified by small colony variant (SCV) MRSA, which is responsible for some of the worst chronic MRSA infections. This particular type of multidrug resistant MRSA is difficult to grow under standard lab conditions and has a growth defect of up to 6-9 times slower than the wild type *S. aureus* (80). With such vast differences between in vitro and in vivo persistence, focusing research on clinically relevant isolates may be a more beneficial rout to pursue.

Despite many of the challenges associated with working on persistence, this topic is of most importance, since not only is microbial persistence responsible for millions of chronic infections per year, but treating persistent bacteria with antibiotics carries an

increased risk of developing resistance. In the third chapter of my thesis I will be focusing on characterizing antibiotic resistance mutations commonly seen in clinical isolates, and their contribution to improved persistence.

Thymineless death

Starvation of nutrients typically does not kill bacteria; starvation decreases the relative cellular abundance of drug targets and stops bacterial growth. An exception where nutrient limitation is lethal to bacteria is thymine starvation. A condition where cells are starved for the DNA building block thymine. Thymine starvation can be achieved by knocking out or mutating thymidylate synthase (*thyA*), an enzyme responsible for methylation of uracil to synthesize thymine (81). Thymine starvation is distinct from other nutrient-limiting conditions since bacteria are unable to sense when thymine is absent. In this state, bacteria continue to accumulate biomass, while DNA replication grinds to a halt. This phenomenon is referred to as unbalanced growth (81). The inability to resolve DNA replication blockage eventually results in rapid bacterial death. First identified almost seventy years ago, thymineless death investigations yielded insights into mechanism of DNA replication and repair, as well as served as basis for widely implemented chemotherapies (82, 83). However, despite all the research into thymineless death phenomenon, the mechanism of bacterial killing still remains elusive. Some researchers hypothesize that death is due to irreversible DNA damage exacerbated by DNA repair and the restarting of replication forks (84). However, others attribute thymineless death to the accumulation of reactive oxygen species following DNA damage. (85). Identifying the mechanism that is responsible for thymineless death may

prove invaluable in the development of new antimicrobial agents, especially against pathogens that have developed multidrug resistance.

Final remarks:

In the three main chapters of this thesis, I will be addressing antibiotic resistance, persistence and thymineless death. The antibiotic resistance chapter will focus on determining mutation hierarchy and predicting mutational paths different species of bacteria take to reach clinical levels of fluoroquinolone resistance. The persistence-focused chapter will aim to answer the questions addressed in this introduction by characterizing clinically relevant high-persistence mutants. Finally, the thymineless death chapter will focus on identifying new mechanisms of killing bacteria through search of a new drug target. Altogether, this thesis work attempts to gain insights into strategies bacteria have at their disposal to evade antibiotic-mediated death, while at the same time attempting to offer real world solutions. It is my hope that this body of work, in combination with others' research, will someday usher changes that ultimately will help to reign in the rampant spread of antibiotic resistance.

Chapter 2

Analysis of Mutational Patterns in Quinolone Resistance-Determining Regions of GyrA and ParC of Clinical Isolates

This chapter has already been published as a paper in the journal "International Journal of Antimicrobial Agents" (158). As the first author my primary contributions were to conception and design of the study, as well as drafting of the article and final approval of the manuscript. The second author on the paper R. Khodursky, greatly contributed to data acquisition and analysis. Dr. J. R. Johnson as a third author was very helpful in drafting of the article. The fourth author, Dr. H. Hiasa, as an expert in the field of topoisomerases and quinolones, provided great insights into the best ways to design the study as well as offering a number of critical revisions for the article. Finally, overseeing the entire endeavor was my advisor Dr. A. Khodursky, contributing with his expertise, guidance and knowledge at every step of making this paper a reality.

Abstract

Fluoroquinolone-resistant bacteria pose a major global health threat. Unanalyzed genomic data from thousands of sequenced microbes likely contain important hints regarding the evolution of fluoroquinolone resistance, yet this information lies fallow. We analyzed co-occurrence patterns of quinolone-resistance mutations in genes encoding the fluoroquinolone drug targets gyrase and topoisomerase IV from 36,402 bacterial genomes, representing 10 Gram-positive and 10 Gram-negative species. For 19 species we determined the likeliest routes toward resistance mutations in both targets, and for five species we also determined which mutations are necessary and sufficient to predict fluoroquinolone resistance. Target mutation hierarchy was fixed in all examined Gram-negative species, with gyrase being the primary and topoisomerase IV the secondary quinolone target, and in six of nine Gram-positive species, with topoisomerase IV being the primary and gyrase the secondary target. By contrast, in three Gram-positive species

(*Staphyloccus haemolyticus*, *Streptococcus pneumoniae*, and *Streptococcus suis*), under some conditions, gyrase became the primary and topoisomerase IV the secondary target. The path through individual resistance mutations varied by species. Both linear and branched paths were identified in Gram-positive and Gram-negative organisms alike. Finally, fluoroquinolone resistance could be predicted based solely on target gene quinolone-resistance mutations for *Acinetobacer baumanii*, *Escherichia coli,* and *Staphyloccus aureus,* but not *Klebsiella pneumoniae* or *Pseudomonas aeruginosa*. These findings have important implications for both sequence-based diagnostics and understanding the emergence of fluoroquinolone resistance.

Introduction

Fluoroquinolones are broad-spectrum antibacterial agents used to treat diverse acute bacterial infections, from cystitis to meningitis (86-88). In many relevant bacteria they have two targets, DNA gyrase (gyrase) and topoisomerase IV (topo-IV) (89-91), which are paralogous, type IIA topoisomerases (92-94). Although the structural and biochemical properties of such topoisomerases are highly conserved generally, gyrase and topo-IV have distinctive cellular functions: gyrase introduces negative supercoils, whereas topo-IV decatenates daughter chromosomes (95).

The antibacterial activity of fluoroquinolones is determined by how effectively they inhibit these two targets. Fluoroquinolones stabilize a catalytic intermediate, the topoisomerase-DNA covalent complex, by forming a topoisomerase-fluoroquinolone-DNA ternary complex (89-91). Accumulation of such ternary complexes leads to inhibition of DNA replication and generation of double-strand breaks.

Mutations that render gyrase quinolone-resistant map to a segment of *gyrA* designated the "quinolone resistance-determining region" (QRDR) (96). Likewise, homologous mutations in the QRDR of *parC* render topo-IV quinolone-resistant. Two conserved QRDR amino acid residues that correspond to Ser-83 and Asp-87 in *Escherichia coli* GyrA are hotspots for quinolone resistance-conferring mutations (91, 96, 97). These residues are critically important in quinolone-topoisomerase interactions, as shown by structural analysis of the *Acinetobacter baumannii* topo-IV-fluoroquinolone-DNA ternary complexes (98). Ser-84 and Glu-88 in *A. baumannii* ParC (corresponding with Ser-83 and Asp-87 in *E. coli* GyrA), interact with the *C*-3, *C*-4 di-keto moiety of floroquinolones through the Mg^{2+}-water bridge. No other amino acid residue in either gyrase or topo-IV interacts directly with fluoroquinolones in ternary complexes (98-100).

Mutations in these two topoisomerases' QRDRs greatly diminish the inhibitory activity of fluoroquinolones, thus representing a main cause of fluoroquinolone resistance (91, 96, 97). Bacteria may need to accumulate QRDR mutations in each target gene to render the antibiotic ineffective (45). Indeed, in numerous studies of clinical isolates and laboratory strains categorical fluoroquinolone resistance (per clinical breakpoints) corresponded with mutations in both targets (97).

Individual QRDR mutations can be selected predictably at different antibiotic concentrations (96, 101). However, the routes by which different bacteria evolve quinolone resistance mutations in nature, with drug concentrations varying substantially over time and space, is unknown. Knowledge of possible paths of acquisition of quinolone resistance-conferring mutations conceivably can be used to detect and preempt the development and emergence of clinical resistance.

Genomes of clinical isolates contain a wealth of sequence information that can be used to identify mutational patterns and to develop probabilistic insights into the possible temporal order of antibiotic resistance-conferring mutations in target genes. Here we present the inferred likeliest mutational paths through the QRDRs of gyrase and topo-IV for 19 bacterial species from the PATRIC database, a computational resource and repository for genome sequences of clinical isolates of pathogenic bacteria (102). Furthermore, for 5 species – *A. baumannii, E. coli, Klebsiella pneumoniae, Pseudomonas aeruginosa*, and *Staphylococcus aureus* – we determined which mutations, or combinations thereof, are necessary and sufficient to predict clinical resistance.

Materials and Methods

Rationale

The study focused on those substitutions in gyrase and topo-IV that have been established as genetic determinants of fluoroquinolone resistance. Large data sets allow the evaluation of different combinations of these substitutions, likely dependencies among them, and common recurring patterns. This requires no prior knowledge of the source isolates' fluoroquinolone phenotype, thereby leveraging vast quantities of data from isolates that were collected without a specific focus on quinolone resistance [91.2% of isolates in PATRIC “Bacteria” (103)]. By contrast, the 8.8% of PATRIC "Bacteria" that carry resistant/susceptible labels can be used to determine whether and which topoisomerase substitutions are necessary and sufficient to predict quinolone resistance. Whereas the presence of topoisomerase substitutions implies that bacteria have experienced quinolone selection, their absence in resistant isolates implies the existence of topoisomerase-independent resistance mechanisms.

Species and genome selection

We initially selected all 28 bacterial species with at least 100 PATRIC database isolates (102, 103). The 100-isolate cutoff was chosen arbitrarily to ensure sufficient power for downstream analyses. From this initial set we retained only species with genomes that included both full-length gyrase and topo-IV-encoding genes, and multiple (>1) available mutant variants of either topoisomerase. This yielded 20 species, represented by from 101 (*Streptococcus mutans*) to 10,099 (*Escherichia coli*) genomes each (Table 2-1).

Table 2-1: conditional probabilities.

Bacteria	Number of genomes	Number [1] of mutant genomes	$GyrA^R$ QRDR, %	$ParC^R$ QRDR, %	p($GyrA^R$) given $ParC^R$	p($ParC^R$) given $GyrA^R$	p($ParC^R$) given $GyrA^{wt}$	p($GyrA^R$) given $ParC^{wt}$	Inferred primary target
Acinetobacter baumannii	2456	2147	87.4	82.4	1	0.97	0	0.17	gyrase
Enterobacter cloacae	786	430	54	26	1	0.50	0	0.38	gyrase
Escherichia coli	1098	2178	20.9	14.3	1	0.69	0	0.08	gyrase
Klebsiella pneumoniae	4619	3189	68.3	63.3	1	0.97	0	0.08	gyrase
Neisseria gonorrhoeae	733	408	55.7	49.8	1	0.93	0	0.08	gyrase
Pasteurella multocida	119	54	14.3	6.7	1	0.53	0	0.25	gyrase
Pseudomonas aeruginosa	1684	500	26.4	16.2	1	0.62	0	0.16	gyrase
Salmonella enterica	5763	894	12	1.0	1	0.08	0	0.15	gyrase
Shigella sonnei	971	98	9.1	4.5	1	0.50	0	0.06	gyrase
Vibrio cholerae	638	368	57.7	51.3	1	0.89	0	0.13	gyrase
Enterococcus faecalis	520	80	14.4	15	0.98	1	0.005	0	topo IV
Enterococcus faecium	927	611	64.0	66.0	0.99	1	0.003	0	topo IV

Staphylococcus aureus	5444	4136	73.6	75.6	0.97	1	0.08	0	topo IV
Staphylococcus epidermidis	393	185	45.6	46.8	0.99	1	0.01	0	topo IV
Staphylococcus Haemolyticus [a]	520	168	56.5	59.0	0.99	0.99	0.02	0.009	preferred topo IV [2]
Streptococcus agalactiae	931	20	0.97	1.5	0.57	1	0.01	0	topo IV
Streptococcus mutans [b]	101	2	2	0	NA	0	0	0.02	gyrase
Streptococcus Pneumoniae [c]	7663	74	0.2	0.7	0.2	0.85	0.008	0.0003	preferred topo IV [2]
Streptococcus pyogenes	343	22	1.5	6.4	0.23	1	0.05	0	topo IV
Streptococcus suis [d]	693	40	4.2	4.5	0.71	0.76	0.02	0.01	preferred topo IV [2]

QRDR, quinolone resistance-determining region; ^{R}, resistant; ^{wt}, wild-type; topo-IV, topoisomerase IV.

[1] – Non-redundant count of genomes containing mutations in at least 1 out of 4 QRDR loci

[2] – rules 1 and 3 are not met; only a mutational preference can be inferred. The relative preference can be estimated by the ratio $p(ParC^{R}|GyrA^{wt}) \div p(GyrA^{R}|ParC^{wt})$: 0.008 ÷ 0.0003=2.2 for S. haemolyticus, 27 for *S. pneumoniae*, and 2-fold for *S. suis*.

[a] – 2 genomes (1% of all genomes with mutant QRDR) had resistant GyrA with wt ParC QRDR, carrying the same substitution GyrA S84L

[b] – GyrA S81L was the only substitution type

[c] – 2 genomes (13% of all genomes with mutant QRDR) had resistant GyrA with wt ParC QRDR: one carried S81Y substitution and another - S81F.

[d] – 7 genomes (24% of all genomes with mutant QRDR) genomes had mutant GyrA with wt ParC QRDR: 5 contained ParC S81G and 2 - ParC S79R substitutions

Data processing and analysis

Analysis was done in R (cran.r-project.org/). After removal of putatively duplicate genomes with the same identifier, other potentially duplicated entries were removed by consolidating sequences that had identical nucleotide variations in *gyrA*, *gyrB*, *parC*, and *parE*, and had the same sequencing center or completion time. The putatively unique nucleotide sequences of *gyrA*, *gyrB*, *parC*, and *parE* were translated, the resulting amino acid sequences were aligned in 2-dimensional arrays by species, and residues in each row and column were compared to the corresponding wild-type reference sequence. The resulting logical array was used in subsequent analysis. We evaluated the degree of (dis)similarity between the original and mutant amino acid in each position using BLOSUM100 (104), which is most suitable for comparing amino acid changes in identical proteins.

Substitution frequency was calculated as the number of substitutions per position divided by the total number of substitutions in a protein alignment, including only substitutions that scored ≤ 2 per BLOSUM100, which identifies dissimilar amino acid substitutions between otherwise identical proteins.

Observed amino acid variations could be described by type, i.e., how different was the substitute amino acid from the original, and variation frequency at a given position. To evaluate observed amino acid substitutions, we examined all previously described substitutions in GyrA and ParC that individually could confer quinolone resistance (see references in Supplemental File 1), and found that the highest BLOSUM100 score associated with such a substitution was 2, for Glu→Gln. Positions in which substitutions scored ≤ 2 could be coarsely divided into two categories: relatively infrequent (< 1% of

all observed substitutions in a protein alignment) and relatively frequent (≥ 1% of all observed substitutions).

Estimating independence between QRDR substitutions in GyrA and ParC

Independence was evaluated using a chi-squared statistic, in which $X^2 = \frac{(expected-observed)^2}{expected}$. The number of *expected* co-occurrences between substitutions in gyrase and topo-IV QRDRs was determined as:

$frequency_{Gyrase} \times frequency_{Topo-IV} \times N$, where $frequency_{Gyrase}$ and $frequency_{Topo\text{-}IV}$ are frequencies of substitutions in the first or second QRDR positions of GyrA and ParC, respectively; and *N* is the total number of aligned sequences (Fig. 2-1). The number of *observed* co-occurrences included all instances in which ≥ 1 substitution in one QRDR co-occurred in the same genome with ≥ 1 substitution in the other QRDR. P-values were estimated from the X^2 distribution, with 1 degree of freedom.

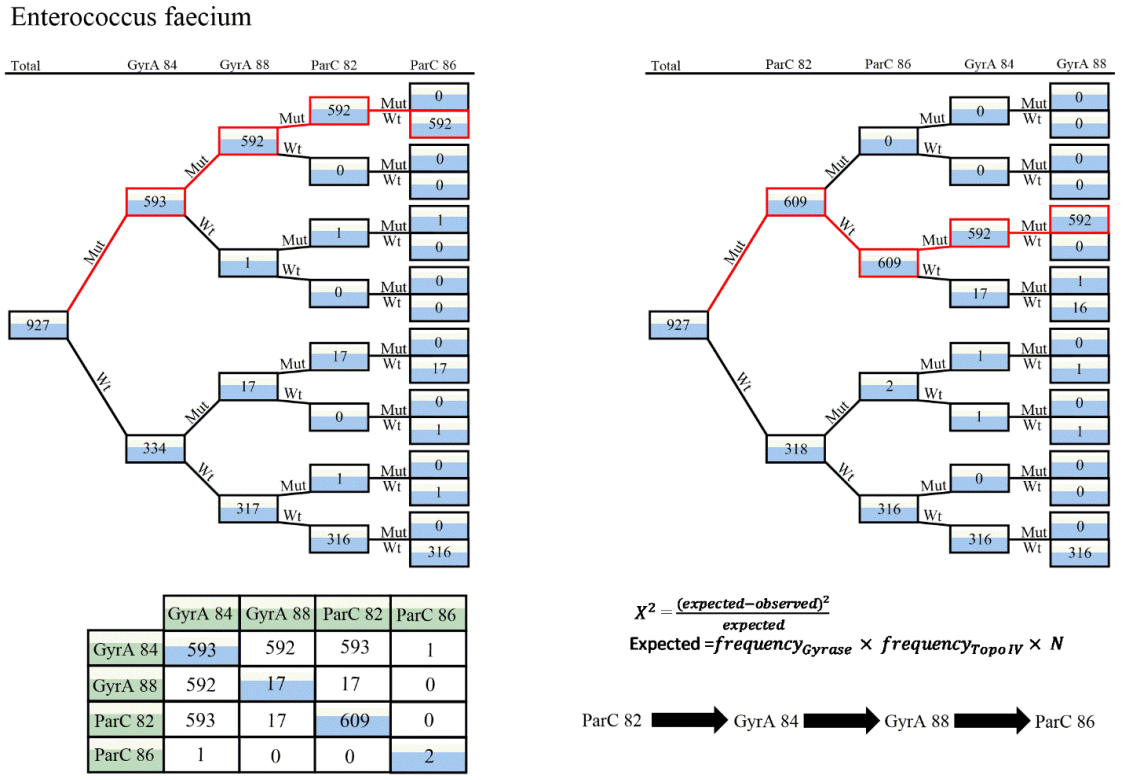

	GyrA 84	GyrA 88	ParC 82	ParC 86
GyrA 84	593	592	593	1
GyrA 88	592	17	17	0
ParC 82	593	17	609	0
ParC 86	1	0	0	2

Figure 2-1: Visualization of statistical analysis used to determine the order of QRDR mutations: Using enumerated trees shown above, we were converted into Chi square tables. Form the four QRDR positions, we were able to generate 6 possible pairs (white fields in the table below). Using chi-square formula most significantly associated mutation pairs were determined based on the smallest P values.

Probabilistic approach to defining the sequence of mutations and gene targets

Let event A correspond to mutating one topoisomerase, gyrase or topo-IV, and event B to mutating the other topoisomerase, to a resistant form, where the resistant form of an enzyme carries substitutions in either or both QRDR positions and the parental, susceptible form carries substitutions in neither.

If event A necessarily precedes event B, then in a sample for which each member has undergone event B, each member must also have undergone event A. The reverse, however, does not hold: in a sample for which each member has undergone event A, only a fraction (or none) of the members may have undergone event B, which occurs at a frequency equal or greater than 0 but less than 1, depending on other conditions. Furthermore, any members that have not undergone A also should not have undergone B; whereas, any members that have not undergone B may have undergone A or not. In other words, observing event A is necessary but not sufficient to observe B, and observing B is sufficient but not necessary to observe A. Thus, the formal rules for A preceding B are:

$$p(A|B) = 1 \qquad (1)$$
$$p(B|A) < p(A|B) \qquad (2)$$
$$p(B|A') = 0 \qquad (3)$$
$$p(A|B') > p(B|A') \qquad (4),$$

where A´ and B´ are subsets of elements in which the event A, or B, has not been observed. The existence of just a single element for which event B can be observed without event A, i.e., not meeting rule (3), would disprove the above relationship. However, if all 4 rules are met, the relationship can provisionally be considered true (although a future disproving exception still could occur).

Results and Discussion

1. The consensus landscape of QRDRs can be reduced to only two positions in both GyrA and ParC

Substitutions conferring quinolone resistance are found frequently in the QRDRs of the GyrA and ParC subunits of gyrase and topo-IV (95-97). Since these regions are defined for only a handful of species, we examined all variants in the N-termini (1-200 aa) of GyrA and ParC in all bacterial species in the PATRIC database that are represented by > 100 isolates/genomes and that have both gyrase and topo-IV. In most of these species, we observed amino acid variations in multiple positions along the N-terminus in both subunits. However, for all but four examined species, substitutions in only two positions, corresponding to the canonical *E. coli* GyrA Ser83 / GyrA Asp87 dyad, had a frequency ≥ 1% (Supplemental File 1).

Moreover, recurring changes across all examined species occurred only in the positions corresponding to *E. coli* GyrA83 and 87; in no other position (adjusted for protein-specific coordinates) did changes occur in the genomes of more than 2 species. Thus, we focused further comparative analysis on this canonical QRDR dyad.

2. Delineating the targeting order from QRDR mutational patterns

First, we assessed whether substitutions in the GyrA and ParC QRDRs co-occur more frequently than expected by chance. For this we calculated a Chi-squared statistic for the 19 species-specific genome sets (of 20 total) that contained QRDR mutations in both gyrase and topo-IV, excluding only *S. mutans* because the available genomes contained no ParC QRDR mutations. For all 19 species, the null hypothesis of independence

between the substitutions in the two QRDRs could be rejected with very high confidence (all P values $\leq 3.6 \times 10^{-26}$). This dependence provides a basis for examining conditional probabilities, which in turn can be used to infer the chronologic sequence of mutational events.

If genomes with a resistance mutation in one topoisomerase also always have one in the other, and the converse is not true, then the mutation(s) in the latter presumably is (are) necessary for the mutation in the former to occur. To test for such a strict relationship between the resistance mutations in the two topoisomerases in the study population, we counted instances of co-occurrences of QRDR mutations in each of the 20 genome sets. With these counts we determined conditional probabilities of observing *gyrA* resistance mutations in genomes with resistant *parC*, i.e., $p(GyrA^R|ParC^R)$, and of observing *parC* resistance mutations in genomes with resistant *gyrA*, i.e., $p(ParC^R|GyrA^R)$ (Table 2-1).

For 16 of 20 genome sets, the necessary condition was satisfied. Specifically, for all 10 analyzed Gram-negative species, resistance mutations in gyrase were prerequisite for resistance mutations in topo-IV, as evidenced by $p(GyrA^R|ParC^R) = 1$ while $p(ParC^R|GyrA^R) < 1$. By contrast, for 6 of 10 analyzed Gram-positive species, resistance mutations in topo-IV were prerequisite for resistance mutations in gyrase, as evidenced by $p(ParC^R|GyrA^R) = 1$ while $p(GyrA^R|ParC^R) < 1$. For the remaining 4 Gram-positive species, including *S. haemolyticus*, *S. mutans*, *S. pneumoniae*, and *S. suis*, resistance mutations in topo-IV vs. gyrase had no prerequisite relationship in either direction.

Next, we determined relative preference order for resistance mutations in each of the species. For this we calculated conditional probabilities of observing mutant gyrase in genomes with wild-type topoisomerase, $p(GyrA^R|ParC^{wt})$, and vice versa,

$p(ParC^{R}|GyrA^{wt})$ (Table 2-1, columns 8 and 9). The ratio of such probabilities, with the larger probability in the numerator, yields the estimate of relative preference in mutation order. For the above 16 genome sets, the ratio had 0 in the denominator, resulting in an infinity (Table 2-1). That means that the preference order in these species is absolute, i.e., in natural environments, quinolone resistance in the 16 species evolves through mutations in one topoisomerase, the primary target, at a time. In 3 of the 4 remaining species, which had genomes with a resistant gyrase but a wild-type topo-IV, the relative preference order was not absolute, but varied between 2-fold and 27-fold (Table 2-1 footnotes). Lastly, the *S. mutans* genome set, which contained only 2 mutant genomes, had resistance substitutions in GyrA but not in ParC, suggesting a preference for GyrA, unlike the other examined Gram-positive species.

The observed relative preference in mutation order can be interpreted as reflecting species-specific targeting preferences for whichever fluoroquinolones the study isolates were exposed to that selected the observed mutations. As such, the above results support the following conclusions. First, for the 16 species with an absolute targeting preference, either the natural drug exposure conditions the isolates experienced did not vary enough to switch the targeting order, or the targeting order depends solely on intrinsic properties of the two topoisomerases (105. 106), not specific drug or context-related factors (107). Since *in vitro* the targeting preference for at least one of these 16 species (*S. aureus*) may differ by quinolone agent (108), the quinolones to which the bacteria were exposed likely did not include those chemical structures that could elicit a change in targeting order (109, 110); alternatively, fixation of mutations corresponding to an alternative targeting order occur less readily with naturally occurring than experimental drug exposure.

Second, since in streptococcal species different fluoroquinolones can preferentially target either topo-IV or gyrase (109), presumably *S. pneumoniae*, *S. suis*, *S. haemolyticus*, and (by extension) *S. mutans* were exposed to fluoroquinolones that can preferentially target Gram-positive gyrase.

In principle, in bacteria that carry two paralogous, type II topoisomerases, quinolones should inhibit both enzymes. However, the two enzymes are too distinct for most fluoroquinolones to target them equivalently at a given drug concentration. This results in differential targeting, whereby one enzyme is targeted at lower drug concentrations, and the other enzyme only at higher concentrations. Such differential targeting is reflected in the sequential emergence of resistance mutations in QRDRs of the two enzymes during experimental evolution (45, 101, 111, 112). By contrast, in natural isolates such sequential emergence of resistance cannot be demonstrated readily. Indeed, the only way to demonstrate sequential or preferential order of antibiotic targeting in nature may be through analysis of hierarchical mutational patterns. Furthermore, even without experimental data, our counting approach can be used to predict primary and secondary fluoroquinolone targets, and their relative preference, in any sample with a sufficiently large number of mutations. Accordingly, we can uniquely postulate that gyrase is the primary target in *P. multocida*, *V. cholerae*, and *S. sonnei*, whereas topo-IV is the primary target in *S. agalactiae*, *S. hemolyticus*, and *S. epidermidis*.

3. Delineating the order of individual QRDR substitutions

The simplest order in which individual mutations may emerge en route to resistance may correspond to the relative frequencies of individual mutations in surveyed samples. However, if individual mutations are dependent on each other, then the likeliest path to a

multiple (e.g., double, triple, quadruple) mutant corresponds to a chain of conditional mutational events with the highest probability. Delineation of paths through individual mutations requires knowledge of the first mutation, because the direct path has the same likelihood as its inverse (113). Once the primary, or preferred, target enzyme is established, the identity of the first element in such a chain is narrowed to one of the two QRDR positions in the primary target. The 4 QRDR positions in each species yield 6 possible pairs; we determined in which of the 6 possible pairs a mutation in one position was significantly associated with a mutation in the other position (at $P < 0.001$). Significant pairs (Supplemental File 1) were used to calculate conditional probabilities, which in turn were used to calculate the probabilities of corresponding multiple mutants. The likeliest mutational paths were the longest possible paths with the highest expected probability of occurrence (Table 2-2, last column).

Table 2-2: Prevalence of individual substitutions and their combined paths.

Bacteria		GyrA		ParC		Quadrupole-mutant			Most probable mutation path(s)
		Pos1	Pos2	Pos1	Pos2	Expected	Observed	O : E [1]	
Acinetobacter baumannii [a]	Pos	**81**	**85**	**84**	**88**				C88←**A81**→C84
	Fr	0.87	0.004	0.82	0.03	8.9x10^{-05}	0	0	
Enterobacter cloacae	Pos	**83**	**87**	**80**	**84**				**A83**→C80→A87→C84
	Fr	0.54	0.2	0.26	0.006	0.00018	0.001	7	
Escherichia coli	Pos	**83**	**87**	**80**	**84**				**A83**→C80→A87→C84
	Fr	0.21	0.15	0.14	0.06	0.00026	0.06	220	
Klebsiella pneumoniae	Pos	**83**	**87**	**80**	**84**				C84←**A83**→C80→A87
	Fr	0.68	0.34	0.63	0.03	0.001	0.0004	0.09	
Neisseria gonorrhoeae	Pos	**91**	**95**	**87**	**91**				**A91**→C87→A95
	Fr	0.56	0.54	0.50	0.02	0.003	0.003	1	
Pasteurella multocida	Pos	**88**	**92**	**84**	**88**				**A92**→C88; **A88**→C84
	Fr	0.14	0.31	0.07	0.2	0.0006	0	0	

Pseudomonas aeruginosa	Pos	**83**	**87**	**87**	**91**				C91←**A83**→C87→A87
	Fr	0.26	0.05	0.16	0.005	1.1x10^{-05}	0	0	
Salmonella enterica	Pos	**83**	**87**	**80**	**84**				C84← **A83**→C80→A87
	Fr	0.12	0.04	0.009	0.001	5.5x10^{-08}	0	0	
Shigella sonnei	Pos	**83**	**87**	**80**	**84**				**A83**→C80→C84→A87
	Fr	0.09	0.06	0.05	0.004	9.4x10^{-07}	0.004	4379	
Vibrio cholerae [b]	Pos	**83**	**87**	**85**	**89**				**A83**→C85
	Fr	0.58	0	0.51	0	0.29	0.51	2	
Enterococcus faecalis	Pos	**84**	**88**	**82**	**86**				A88←**C82**→A84→C86
	Fr	0.14	0.006	015	0.02	2.2x10^{-06}	0	0	
Enterococcus faecium [c]	Pos	**84**	**88**	**82**	**86**				**C82**→A84→A88→C86
	Fr	0.64	0.02	0.66	0.002	2.0x10^{-05}	0	0	
Staphylococcus aureus [c]	Pos	**84**	**88**	**80**	**84**				**C80**→A88→C84→A84
	Fr	0.74	0.08	0.76	0.36	0.017	0.081	5	
Staphylococcus epidermidis	Pos	**84**	**88**	**80**	**84**				**C80**→A84→A88→C84
	Fr	0.47	0.12	0.47	0.26	0.007	0.078	12	
Staphylococcus haemolyticus	Pos	**84**	**88**	**80**	**84**				**C80**→A84→C84
	Fr	0.57	0.02	0.59	0.1	0.0007	0	0	
Streptococcus Agalactiae [d]	Pos	**81**	**85**	**79**	**83**				A85←**C79**→A81→C83
	Fr	0.0096	0.001	0.015	0.006	1.0x10^{-09}	0	0	
Streptococcus Pneumoniae [d]	Pos	**81**	**85**	**67**	**71**				A85←**C67**→ A81→C71
	Fr	0.002	0.0003	0.007	0.002	6.4x10^{-12}	0	0	
Streptococcus pyogenes [b]	Pos	**81**	**85**	**79**	**83**				**C79**→A81
	Fr	0.01	0	0.06	0	0.0009	0.015	16	
Streptococcus suis	Pos	**81**	**85**	**79**	**83**				**C79**→A85→A81
	Fr	0.04	0.01	0.04	0.003	6.2x10^{-08}	0	0	

[1] - rounded to the nearest integer

[a] – Substitutions in GyrA85 were not significantly associated with substitutions in any other position. Hence the path goes through only three positions: GyrA81, ParC84 and ParC88.

[b] - Only the frequencies related to a double mutant could be ascertained.

[c] - Although a quadruple mutant has not been observed, each pairwise transition was highly significant.

[d] - Although a triple mutant has not been observed, each pairwise transition was highly significant.

We found that every path involves a switch from the primary to secondary target after the first mutation, i.e., two consecutive initial mutations within one QRDR are unlikely, in agreement with in vitro data (114). We identified two main types of paths toward a multi-mutational quinolone-resistance genotype. The first type of path, which gives the longest possible path, is linear. These mutations occur in a fixed hierarchical sequence; mutation in an invariant primary target positions is followed by a mutation in an invariant secondary target position, which in turn is followed by either another switch, e.g., in *E. coli*, **GyrA83**→ParC80→GyrA87→ParC84 (where → indicates direction of the path) or a repeat mutation in the secondary target, e.g., in *S. epidermidis*, **ParC80**→GyrA84→GyrA88→ParC84. The second type of path is branched: the primary mutation is followed by either of two mutations in the alternate target (possibly followed by an invariant subsequent mutation in the primary target), e.g., in *A. baumannii*, ParC88←**GyrA81**→ParC84, or in *E. faecalis*, GyrA88←**ParC82**→GyrA84→ParC86. By contrast, in three samples, *P. multocida*, *V. cholera*, *S. pyogenes*, the mutational path was limited to only two sequential mutations.

We also examined the occurrence of mutants carrying mutations in all 4 QRDR positions, which likely result from the highest selective pressure on the topoisomerase targets. Only 6 (32%) of 19 species-specific datasets, for 5 Gram-negative and 1 Gram-positive organisms, contained such quadruple mutants (Table 2-2). Such mutants were strikingly over-represented in *E. coli* and *S. sonnei* (Supplemental File 1).

Each of the characteristic QRDR mutations is likely selected for at a different range of antibiotic concentrations and becomes fixed in a population due to largely unknown interactions between genetic and environmental factors. Unlike the gene target order, the order of individual mutations may not be strictly, mechanistically prescribed. For example, in GyrA the Asp87 → Asn substitution increases the MIC for multiple quinolones almost as much as the Ser80 → Leu substitution (96). Thus, whether individual QRDR mutations follow any particular order was of significant interest. We searched for the likeliest sequence of individual QRDR mutations in 19 species and found that mutational paths, although conserved within a given species, were not characteristic of large groups of bacteria; even some closely related species, e.g., *E. faecium* and *E. faecalis*, had different paths through the QRDRs of the two targets. If on average all pathogenic bacteria are under comparable selective pressure in nature, then the observed between-species variability in mutational paths and the abundance of quadruple mutants can be attributed to species-specific intrinsic and environmental differences in how the bacteria adapt to antibiotic challenges and the physiological effects of accumulating mutations.

4. Necessary and sufficient mutational predictors of resistance in clinical isolates

In the genome sets for *Acinetobacter*, *Escherichia*, *Klebsiella*, *Pseudomonas*, and *Staphylococcus* ≥ 5% of genomes per set were labeled as resistant or susceptible, i.e., associated with MICs above or below current clinical resistance breakpoints for a given fluoroquinolone agent (Table S2-1).

Having delineated the primary targets and the most probable mutational paths, we assessed which mutations are necessary, and which mutations and their combinations are sufficient, to predict reliably fluoroquinolone resistance (See Supplemental File 1 for details).

We found that the primary target mutations are necessary for predicting fluoroquinolone resistance in *A. baumanii*, *E. coli*, and *S. aureus* (Table 2-3). By contrast, for *K. pneumoniae* and *P. aeruginosa*, the absence of a primary QRDR mutation does not signify drug susceptibility. Specifically, despite lacking the expected QRDR mutations, more than 27% and 14% of *K. pneumoniae* isolates were resistant to ciprofloxacin and levofloxacin, respectively, and more than 14% of *P. aeruginosa* isolates were resistant to levofloxacin (Table 2-3), implying the existence of one or more QRDR-independent quinolone resistance mechanisms. The mechanism(s) is(are) also likely to be topoisomerase-independent, because the genomes of resistant isolates lacked other gyrase or topo-IV mutations.

We found that, in considering only the four canonical QRDR mutations, a single primary mutation suffices to predict ciprofloxacin resistance in *A. baumanii*, *K. pneumoniae*, *P. aeruginosa*, and *S. aureus* (Table 2-4). By contrast, two mutations, one each in the primary and secondary target are needed to predict levofloxacin resistance in *A. baumanii*, *K. pneumoniae*, and *P. aeruginosa*. Finally, at least three mutations are needed

to predict ciprofloxacin resistance in *E. coli*, which agrees with experimental evidence that such a combination is required to surpass the CLSI MIC breakpoint for fluoroquinolone resistance (115).

The fact that bacteria adapt along multi-mutation paths even when categorical resistance can be fully predicted by mutations at a single position, e.g., for *A. baumannii* and *S. aureus* with ciprofloxacin, implies that the drug concentrations to which organisms are exposed in the relevant natural selection environment may significantly exceed the established clinical breakpoint concentration. Multiple, including as-yet-unknown, mechanisms other than the canonical QRDR mutations (e.g., surveillance and maintenance of DNA integrity) can contribute to high fluoroquinolone MICs (116, 117). However, at least in *A. baumanii*, *E. coli*, and *S. aureus*, such mechanisms are acquired and disseminated by strains that already have relevant underlying QRDR mutations.

Thus, our analysis showed that genomic data can be mined for biologically meaningful genetic patterns (e.g., quinolone-resistance-conferring mutations in gyrase and topo-IV) even in the absence of relevant metadata (e.g., fluoroquinolone MICs or resistance status). Furthermore, some binary phenotypes of clinical bacterial isolates, here fluoroquinolone resistance, can be predicted by one, two, or three point mutations, which could dramatically simplify the development of reliable diagnostic tools.

Table 2-3: Is a primary QRDR mutation necessary for quinolone resistance?

Bacteria	Antibiotic	Mutation [a]	NPV [b], %	False negative rate [c], %	Necessary, Yes or No
Acinetobacter baumannii	Ciprofloxacin	GyrA81	99.7	0.3	Y
Acinetobacter baumannii	Levofloxacin	GyrA81	100	0	Y
Escherichia coli	Ciprofloxacin	GyrA83	97.6	2.2	Y
Klebsiella pneumoniae	Ciprofloxacin	GyrA83	78.6	27.3	N
Klebsiella pneumoniae	Levofloxacin	GyrA83	87.4	14.1	N
Pseudomonas aeruginosa	Ciprofloxacin	GyrA83	95.7	4.5	Y
Pseudomonas aeruginosa	Levofloxacin	GyrA83	87.2	14.4	N
Staphylococcus aureus	Ciprofloxacin	ParC80	98.8	1.2	Y

[a] – including all possible combinations of the indicated primary mutation with three other QRDR mutations with.

[b] – negative predictive value: a fraction of sensitive isolates that do not carry the corresponding mutation. For example, 97.6% of *E. coli* isolates that were sensitive to ciprofloxacin did not carry mutations in the GyrA83 position.

[c] – a fraction of false negatives among resistant isolates, $\frac{FN}{TP+FN}$. For example, 2.2% of *E. coli* resistant isolates did not carry mutations in the GyrA83 position.

Table 2-4: Sufficiency of the primary mutations and their combinations.

Bacteria	Antibiotic	Mutations and combinations	PPV [a], %	FPR [b], %	Sufficient: Yes or No
Acinetobacter baumannii	Ciprofloxacin	A81	100	0	Y
		A81-C84	100	0	Y
	Levofloxacin	A81	18.1	12.5	N
		A81-C84	100	0	Y
Escherichia coli	Ciprofloxacin	A83	12.1	6.9	N
		A83-C80	49.4	0.3	N
		A83-C80-A87	99.8	0.08	Y
Klebsiella pneumoniae	Ciprofloxacin	A83	100	0	Y
		A83-C80	100	0	Y
	Levofloxacin	A83	41.6	2.0	N
		A83-C80	100	0	Y
Pseudomonas aeruginosa	Ciprofloxacin	A83	100	0	Y
		A83-C87	100	0	Y
	Levofloxacin	A83	88.1	2.1	N
		A83-C87	100	0	Y
Staphylococcus aureus	Ciprofloxacin	C80	98.6	1.3	Y
		C80-A84	100	0	Y

[a] – positive predictive value, calculated for the exclusive sets containing indicated mutations and combinations: a fraction of resistant isolates that carry the corresponding mutation(s).

[b] – a fraction of false negatives among resistant isolates, $\frac{FP}{FP+TN}$.

Supplemental:

Recurring positions found outside of the canonical QRDR dyad

In *E. coli* and *S. enterica* an additional substitution occurred at ParC Ser57 (Thr57 in *Salmonella*). However, previous work found that this substitution alone does not contribute to quinolone resistance (118). Likewise, in *S. aureus,* although a substitution at GyrA Ser85 increases quinolone MICs (119), here in 100% of instances this substitution co-occurred with substitutions at GyrA Ser84. Finally, in *E. cloacae*, substitutions at GyrA Leu128, which have not been described previously, always co-occurred with substitutions in GyrA Ser83.

Cataloging QRDR substitutions

All previously described substitutions in GyrA and ParC that individually could confer quinolone resistance could be found in the following references, (101, 111, 120-124,125-136).

Assessing necessary and sufficient predictor mutations

Assuming that ≥ 95% of the resistant and susceptible designations for individual isolates in the PATRIC database are accurate, the mechanism of resistance mediated by a target mutation can be deemed necessary if that mutation is absent in ≥ 95% of susceptible samples, whereas a mutation, or combination of mutations, can be deemed sufficient to cause resistance if the mutation(s) is present in ≥ 95% of resistant samples. The former can be determined as a fraction of true negatives, a ratio of the number of susceptible genomes that do not carry the mutation to the number of all genomes, susceptible and resistant, that do not carry the mutation. This ratio, $\frac{TN}{TN+FN}$, is also known as the negative

predictive value, or NPV. The latter can be determined as a fraction of true positives among all the genomes that carry the mutation, independent of whether they belong to resistant or susceptible isolates. This fraction, $\frac{TP}{TP+FP}$, is also known as the positive predictive value, or PPV.

Test of independence of QRDR substitutions

Acinetobacter baumannii: three pairs of substitutions were significantly dependent: GyrA81-ParC84 (p-value = 1.4 x 10^{-9}), GyrA81-ParC88 (p-value = 2.3 x 10^{-5}). and ParC84 and ParC88 substitutions were mutually exclusive (p-value = 8.1 x 10^{-8}). Mutation in GyrA85 is not associated with any other mutations.

Enterobacter cloacae: Substitutions in positions GyrA83, GyrA87 and ParC80 were highly significantly dependent (with the highest p-value for GyrA83-GyrA87 pair of 3.1 x 10^{-13}.) However, substitutions in ParC84 were not significantly associated with any other position.

Escherichia coli: all six pairwise positions of amino acid were highly significantly associated (the highest p-value for the Chi-squared statistic is for the association between substitutions in GyrA83 and ParC84 is 7.7 x 10^{-378}.)

Klebsiella pneumoniae: All pairwise combinations of substitutions showed highly significant dependency, and ParC80 and ParC84 were mutually exclusive with a p-value for a corresponding Chi-squared statistic of 1.3 x 10^{-20}. Thus, the likeliest mutational path was branched at GyrA83.

Neisseria gonorrhoeae: 3 pairs of substitutions showed highly significant dependence: GyrA91-GyrA95 (p-value = 2×10^{-32}), GyrA95-ParC87 (p-value = 2.2×10^{-32}), and GyrA91-ParC87 (p-value = 7×10^{-30}.) The occurrence of ParC91 was not significantly dependent on any other QRDR substitutions.

Pasteurella multocida: only two pairs of substitutions were highly significantly dependent, GyrA88-ParC84 (p-value = 4.2×10^{-8}) and GyrA92-ParC88 (p-value = 1.0×10^{-7}.) However, there couldn't be drawn a contiguous path through more than 2 mutations.

Pseudomonas aeruginosa: three pairs of substitutions were significantly dependent, GyrA83-ParC87 (p-value = 5.0×10^{-120}), GyrA87-ParC87 (p-value = 4.9×10^{-7}), GyrA83-ParC91 (p-value = 8.0×10^{-4}.)

Salmonella enterica: Substitutions in positions GyrA83, GyrA87, ParC80 were highly significantly pairwise dependent (with the highest p-value for GyrA83-GyrA87 pair of 2.9×10^{-5}.)

Shigella sonnei: all possible pairwise combinations of amino acid substitutions were highly significant, with the highest p-value of 1.5×10^{-9} for a corresponding Chi-squared statistic for GyrA83-ParC84 pair.

Vibrio cholerae: only one, highly associated pair of substitutions could be observed in the dataset: GyrA83-ParC85 (p-value = 7.0×10^{-24}.)

Enterococcus faecalis: 4 out of 6 pairs of substitutions showed highly significant associations: GyrA84-ParC82 (p = 4.2×10^{-78}), GyrA84-ParC86 (p = 4×10^{-9}), ParC82-ParC86 (p = 1.2×10^{-6}) and GyrA88-ParC82 (p = 0.0001).

Enterococcus faecium: 3 pairs of substitutions were highly dependent: GyrA84-ParC82 (p-values = 1.1×10^{-24}), GyrA88-ParC86 (p-value = 4.1×10^{-6}), GyrA84-GyrA88 (p-value = 0.006), resulting in C82→A84→A88→C86 as the most probable path to a possible quadrupole mutant.

Staphylococcus aureus: Substitutions in all 6 possible pairwise combinations of mutations were highly dependent on each other, with the highest p-value of 1.5×10^{-9} for GyrA88-ParC80 pair.

Staphylococcus epidermidis: amino acid substitutions in all six possible pairs were highly associated, with the highest p-value of 9.9×10^{-8} recorded for a corresponding Chi-squared statistic of the GyrA88-ParC80 pair.

Staphylococcus haemolyticus: substitutions at 3 positions were significantly associated: GyrA84-ParC80 (p = 3 x 10-11), GyrA84-ParC84 (p = 0.002), ParC80-ParC84 (p = 0.005).

Streptococcus agalactiae: 3 pairs of substitutions showed highly significant association: GyrA81-ParC79 (p-value = 1.0×10^{-77}), GyrA81-ParC83 (p-value = 7.4×10^{-16}), GyrA85-ParC79 (p-value = 9.6×10^{-16}.)

Streptococcus pneumoniae: Substitutions in GyrA81-ParC67, GyrA85-ParC67, and GyrA81-ParC71 were highly pairwise dependent (with the highest p-value for GyrA81-ParC71 pair of 3.4×10^{-35}.)

Streptococcus pyogenes: Only one pair, GyrA81-ParC79, of substitutions was observed in the set of 343 genomes, and the co-occurrence of the two substitutions was not random (p-value = 0.0001.)

Streptococcus suis: Substitutions in 3 pairs, GyrA81-ParC79 (p-value = 7.9×10^{-74}), GyrA81-GyrA85 (p-value = 4.6×10^{-40}), GyrA85-ParC79 (p-value = 2.2×10^{-37}), were highly dependent on each other.

Table S2-1. Resistant and sensitive subsets.

Bacteria[1]	Total number genomes	Ciprofloxacin		Levofloxacin	
		Sensitive	Resistant	Sensitive	Resistant
Acinetobacter baumannii	2456	52	400	21	199
Escherichia coli	10099	1255	437	NA[2]	NA
Klebsiella pneumoniae	4619	174	180	218	142
Pseudomonas aeruginosa	1684	110	52	295	221
Staphylococcus aureus	5444	746	243	NA	NA

[1] – other 14 bacterial sets had fewer than 1% of quinolone-labeled genomes.

[2] - less than 5% of the total number of genomes are in the labeled subset ("sensitive" + "resistant") for this antibiotic.

Chapter 3

Identification and characterization of pleiotropic high-persistence mutations in the beta subunit of the bacterial RNA polymerase

This chapter is a manuscript that has been submitted to the journal "*Molecular Microbiology*" and is currently pending review. As the first author on this paper I was heavily involved in design of the study. I had performed all of the experiments described here with exception of principal component analysis (it that was used to identify the most upregulated gene/regulon across different high persistence mutants). I had written large sections of the article as well as contributed to edits and final approval of the manuscript. The second author, Dr. Y. Ji, was very helpful by offering his lab space and expertise in the experiments involving MRSA, as well as providing us with MRSA clinical isolate(s) used in this study. As a corresponding author, Dr. A. Khodursky supervised the entire project, contributing to every step along the way. As for the experiments Dr. Khodursky performed the principal component analysis and generated the figure 3-2A.

Summary:

Antibiotic persistence is a non-heritable trait exhibited by a small fraction of a bacterial population and independent of prior exposure of bacteria to antibiotics. High persistence (hip), however, is a genetic trait that can emerge as a result of antibiotic selection. Here we report the hip phenotype caused by commonly occurring antibiotic-resistance mutations in the *rpoB* gene, encoding the beta subunit of RNA polymerase. Analysis of the mutants revealed that: i) the persistent state depends on the (p)ppGpp transcriptional program and not on (p)ppGpp itself; ii) the hip is associated with increased populational heterogeneity in transcription; and iii) indole overproduction, caused by transcriptional changes in the hip mutants, explains 50-80% of the hip phenotype. We established that the analogous *rpoB* mutations occur frequently in clinical isolates of *Acinetobacter*

baumannii, Mycobacterium tuberculosis and Staphylococcus aureus, and we demonstrated that one of those *rpoB* mutations causes thigh persistence in MRSA.

Introduction:

Exponentially growing bacteria are rapidly killed by fluoroquinolones (63). Only few cells per 100 million can survive the hours-long treatment without acquiring any drug resistance mutations. Such accidental survivors, also known as persisters, serve as the source for bacterial re-population after the antibiotic is withdrawn. The number of survivors may affect the rate and robustness of re-population. Ensuring a sufficient number of survivors in the wake of a bactericidal condition may be viewed as an advantageous genetic trait. However, the survivors are likely to be dormant cells (60, 56, 137), which don't grow and divide in the presence of the antibiotic. Thus, if the improved survival trait cannot provide a growth advantage under the bactericidal condition itself, it was reasoned that the only way it could be selected for is by fluctuating selective pressure from drug to no drug (75). We hypothesized that an increase in the frequency of survivors can be a consequence of persistent selection, where mutations conferring fitness advantage at low antibiotic concentrations can also increase the probability of survival at much higher drug concentrations.

The main tenant of the hypothesis is that a small, population-wide reduction in susceptibility may also lead to a higher persister frequency. That must occur in order for "high persistence" to be a naturally selectable trait in the presence of antibiotics. We chose ciprofloxacin to test this hypothesis because its adaptive landscape is complex, with many mutations reducing susceptibility to the drug by a relatively small margin (138-140). Such low-level resistance mutations provide necessary fitness advantage at

correspondingly low antibiotic concentrations and, if our model is correct, may result in an increased survival frequency at concentrations that are significantly higher than the antibiotic's minimal inhibitory and bactericidal concentrations (MICs and MBCs) against the mutant. In agreement with our prediction, we were able to select mutations that boosted ciprofloxacin MIC only 1.5-3 times while increasing survival frequency at clinical concentrations of the drug by as much as 1,000 times. Two independent selections resulted in two different mutations in the switch region (141,142) of the RpoB subunit. We corroborated the relevance of this observation by finding that similar *rpoB* mutations frequently co-occur with the determinants of quinolone resistance in clinical isolates.

Analysis of transcriptional changes in a switch-region mutant prompted re-evaluation of the (p)ppGpp role in persister formation, which has been a subject of debate (70,143-145) and led to the discovery that at least in *E. coli* and *S. aureus*, resistance to one antibiotic (rifampicin) can cause persistence without cross-resistance. Furthermore, we found that the same mutations are frequent in clinical isolates of *M. tuberculosis*, *A. baumanii* and *S. aureus*.

The dormant state, in which bacteria are recalcitrant to bactericidal antibiotics, can be achieved by a reversible growth inhibition (64,146). Such inhibition depends on growth-affecting factors, positive or negative, crossing the activity threshold (147). We found that *rpoB* hip phenotype is at least in part caused by the activity of indole, which reversibly inhibits growth and cell division in a threshold-dependent manner (148).

Results

High survival frequency is caused by rpoB mutations

We selected mutants with improved survival frequency by incrementally increasing concentration of ciprofloxacin ("Materials and Methods"). Among mutants that were resistant to 250 ng/ml, but not 500 ng/ml, of ciprofloxacin we identified two independent clones with dramatically elevated survival at 4,000 ng/ml. Whole-genome sequencing revealed that each of the mutants contained only two mutations: a *gyrB* mutation (S464Y) and an *rpoB* mutation, one of the mutants carried a substitution in 1279 residue (E–>A) and another in 1304 (M–>R) of RpoB. By comparing with the parent strain, we determined that GyrB S464Y cause an increases in MIC but not in survival frequency (Table 3-1). The RpoB E1279A and RpoB M1304R substitutions increased MIC and MBC_{90} by additional 1.5-2-fold (Table 3-1) while increasing the survival frequency at high drug concentrations by more than 100 times (Fig. 3-1A).

Figure 1A

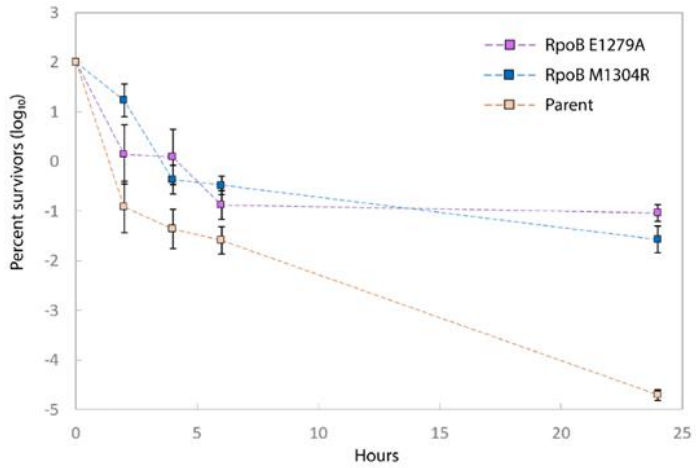

Figure 1B

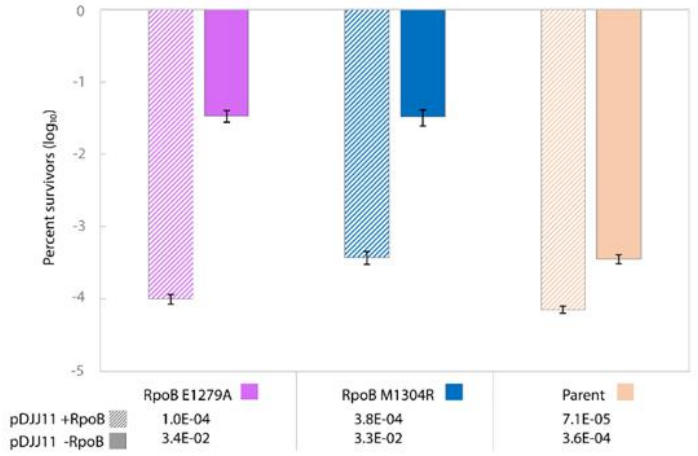

Figure 1C

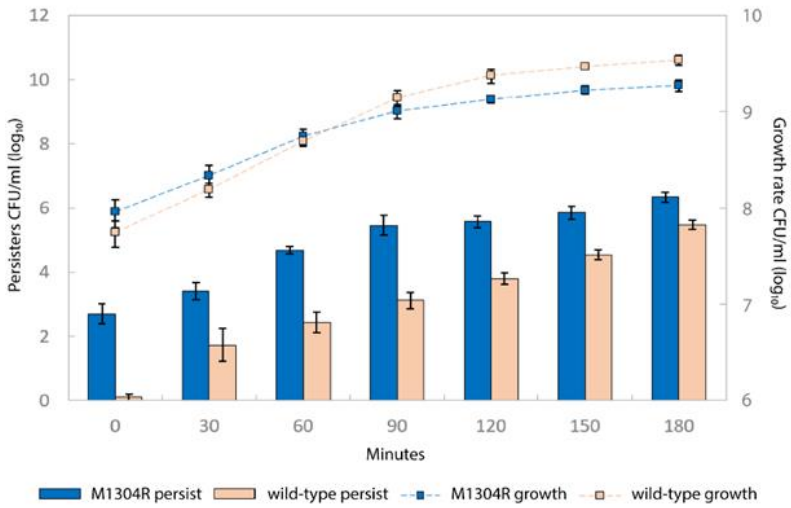

Figure 1D

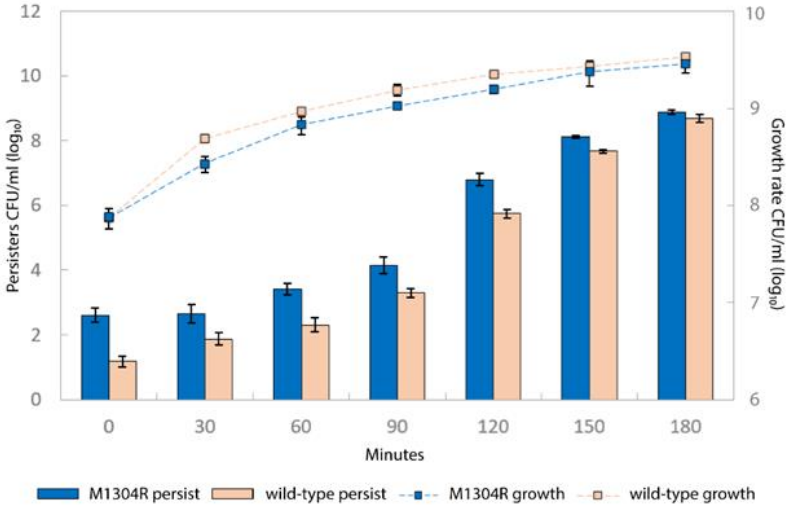

Figure 3-1: Ciprofloxacin-selected *rpoB* mutations confer high persistence phenotype: (**A**) Survival curves in presence of 4µg/mL ciprofloxacin of a parent strain carrying the GyrB S464Y substitution (●) and two RpoB mutants in the same genetic background: RpoB E1279A (●) and RpoB M1304R (●). (**B**) Genetic complementation: RpoB E1279A (●) and RpoB M1304R (●) and GyrB S464Y (●) with a pDJJ11-*rpoB*. (**C**) Comparison of persistence to ciprofloxacin (18h treatment at 1µg/ml) between MG1655 (●) and MG1655 RpoB M1304R (●) along the growth curve. (**D**) Comparison of persistence to ampicillin (18h, 100 µg/ml) between MG1655 (●) and RpoB M1304R (●) along the growth curve.

Table 3-1: MIC/MBC.

	ng/mL ciprofloxacin	
	MIC	MBC90
gyrB S464Y	156.6±12.5	186±17
RpoB 1304	325±10	380±15
RpoB 1279	350±14.3	410±15
RpoB 1275	250±10	300±12
MG1655	15±2	33±2
MG1655 RpoB 1304	25±2	55±4
MG1655 RpoB 533	8.5±1	33±3
Mg1655 Δmdtk	15±2	
MG1655 RpoB 1304 Δmdtk	14±2	

MIC and MBC values of strains with various RpoB substitutions: MIC and MBC were tested in two different backgrounds, the first four strains described are inMG1655 GyrB S464Y background, and the rest are in MG1655. MIC was determined using ~50-300 cell inoculum. MBC90 was determined with 5-8 million cell inoculum in 3ml of media.

We verified that the RpoB M1304R substitution was the cause of the high survival rate phenotype by complementation and transduction. The wild-type *rpoB* expressed from a plasmid fully reversed the phenotype (Fig. 3-1B). Transduction of the allele encoding RpoB M1304R into MG1655 wild-type background increased the survival frequency by a factor of 1,000 (Fig. 3-1C). The survival phenotype was not limited to ciprofloxacin. The strain carrying RpoB M1304R substitution yielded 20-25 times as many survivors as

its parent strain when treated with ampicillin at 100 μg/ml (Fig. 3-1D). The RpoB E1279A mutant had a pronounced growth defect and was excluded from a further analysis.

RpoB M1304R substitution mimics the (p)ppGpp response

Using RNA-seq we identified 379 genes that were differentially expressed (FDR < 0.01) between a strain carrying RpoB M1304R substitution and its parent (Sup. Files 1). These genes represented 116 regulons, which were compiled from RegulonDB and EcoCyc (149, 150). Of the 116, 12 regulons were represented by at least 10 differentially expressed genes and were significantly enriched (hypergeometric test, adjusted p-value < 0.05) (Fig. 3-2 A). Two regulons stood out from the list of significantly enriched sets. First, the set least likely to be overrepresented by chance was the ppGpp regulon (96 genes out of 167 genes in the regulon were differentially expressed between the two strains, FDR < 0.01). Second, the set with the largest per gene variation in transcript abundances was the DksA-ppGpp regulon. These findings raised the possibility that the effect of RpoB M1304R mimics the effect of (p)ppGpp on transcription, including a constitutive upregulation of amino acid biosynthetic genes, which we confirmed for isoleucine (Fig. S3-1).

Figure 2A

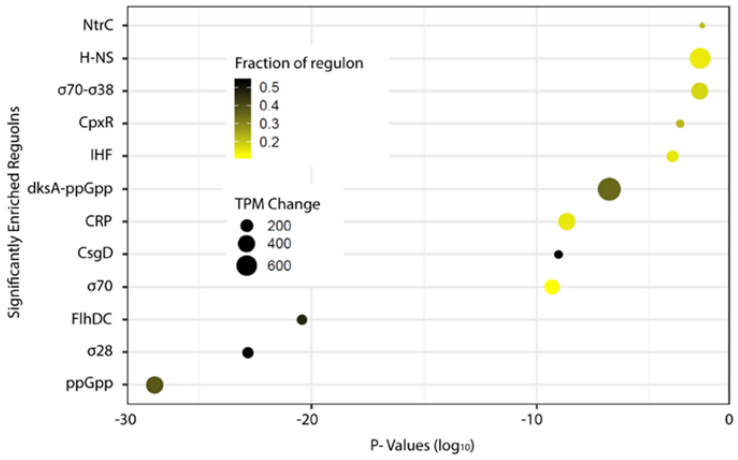

Figure 2B

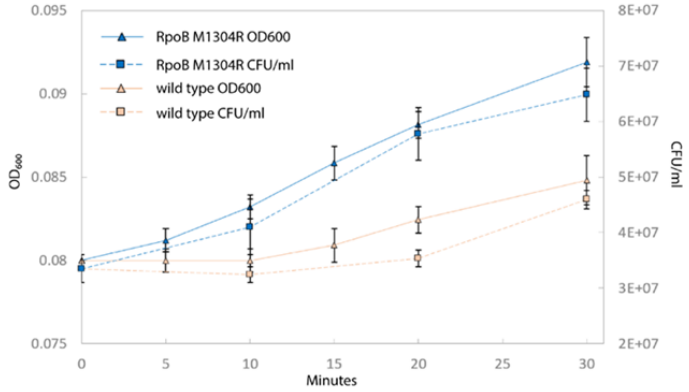

Figure 2C

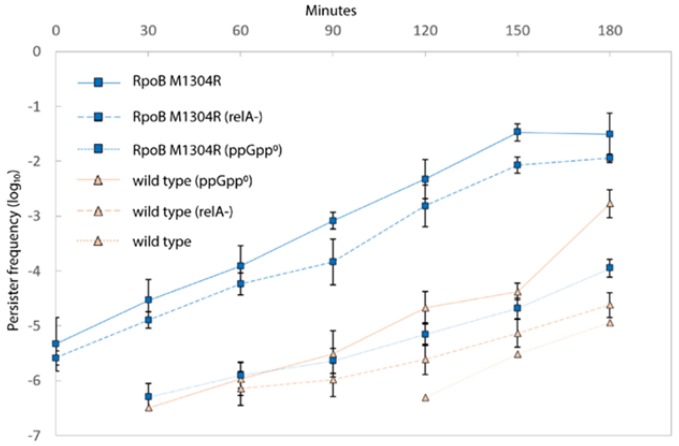

Figure 3-2: The rpoB M1304R substitution mimics (p)ppGpp response: (**A**) Significantly enriched regulons in RpoB M1304R mutant characterized by the fold change and fraction of the regulon effected by the mutation. (**B**) An adaptation lag of Mg1655 parent (●) and MG1655 RpoB M1304R (●) measured in OD_{600} and CFU/ml. (**C**) Ciprofloxacin persistence of RpoBwt(●) and RpoB M1304R (●) in MG1655, *ΔrelA* and *ΔrelA ΔspoT* ($ppGpp^0$) backgrounds.

One of the salient features of the ppGpp-controlled response is an adaptive lag during the amino acid downshift (151, 152). If the transcripts of amino acid biosynthetic genes are upregulated in an amino acid containing medium, then the lag upon the downshift may be shortened. We tested this possibility by comparing the lags of the RpoB M1304R strain and its parent. Upon the downshift, the parent strain exhibited a 20-min delay before resuming growth whereas the mutant started recovering in 5-10 minutes (Fig. 3-2B).

The transcriptional state of the mutant and its accelerated adaptation to the amino acid downshift could result from a constitutive activation of the ppGpp response if the mutant has a higher basal level of ppGpp. We tested this possibility by measuring ppGpp levels. The alarmone abundance was indistinguishable between the parent and RpoB M1304R strains in presence of amino acids (Fig. 3-3A). After 1h amino acid downshift, (p)ppGpp levels increased 10 times over the basal level in both strains (Fig. 3-3B). Thus, the RpoB M1304R substitution either makes RNA polymerase more sensitive to ppGpp or mimics the response in a ppGpp-independent manner.

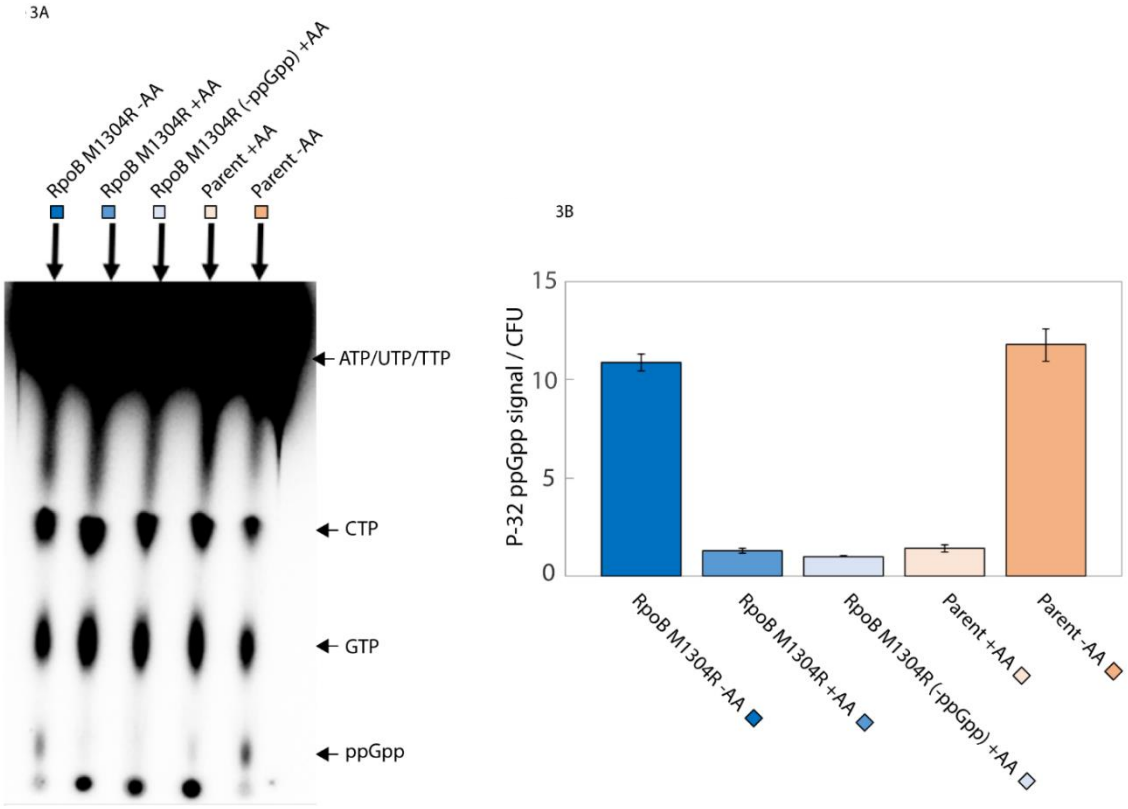

Figure 3-3: ppGpp mimicry is not a result of ppGpp accumulation: (**A**) Radiolabeled ^{32}P nucleotide TLC plate comparing MG1655 RpoB M1304R +/- amino acids, to MG1655 RpoB M1304R ppGpp^0 + amino acids, to MG1655 +/- amino acids. (**B**) Fiji analyzed TLC plate and normalized to corresponding CFU/ml microbial counts: MG1655 RpoB M1304R (●) - AA, MG1655 RpoB M1304R (●) +AA, MG1655 RpoB M1304R ppGpp^0 (●), MG1655 +AA (●), MG1655 –AA (●).

We tested the ppGpp dependence of RpoB M1304R by transducing the mutation into the *relA*$^-$ and *relA*$^-$*spoT*$^-$ (ppGpp^0) backgrounds. While the removal of *relA* alone slightly reduced the frequency of survivors compared to the RpoB M1304R *relA*$^+$ parent, the RpoB M1304R persistence phenotype without ppGpp was similar to that of the wild type MG1655 (Fig. 3-2C). Thus, the *rpoB* persistence mutation, while being dependent on ppGpp for its full effect, makes the basal persistence independent of the alarmone. Such independence, or ppGpp mimicking, can be manifested by phenotypic rescuing of the amino acid auxotrophy of ppGpp^0 mutants (153, 154). However, we found that the RpoB M1304R ppGpp^0 mutant still required amino acids for growth (data not shown).

RpoB stringent mutations cause high-persistence (hip) phenotype

To determine if stringent *rpoB* mutations (153), which are known to rescue the ppGpp^0 auxotrophy, can also rescue the persistence phenotype, we selected rifampicin resistant, *rpoB* stringent mutants in a ppGpp^0 strain ("Materials and Methods") and characterized persistence of one of them, RpoB L533P. While ppGpp^0 yielded no persisters between OD_{600} 0.3 -1.6, RpoB L533P ppGpp^0 had as many persisters throughout the growth curve as wild type MG1655 in the early stationary phase (Fig. 3-4A and B).

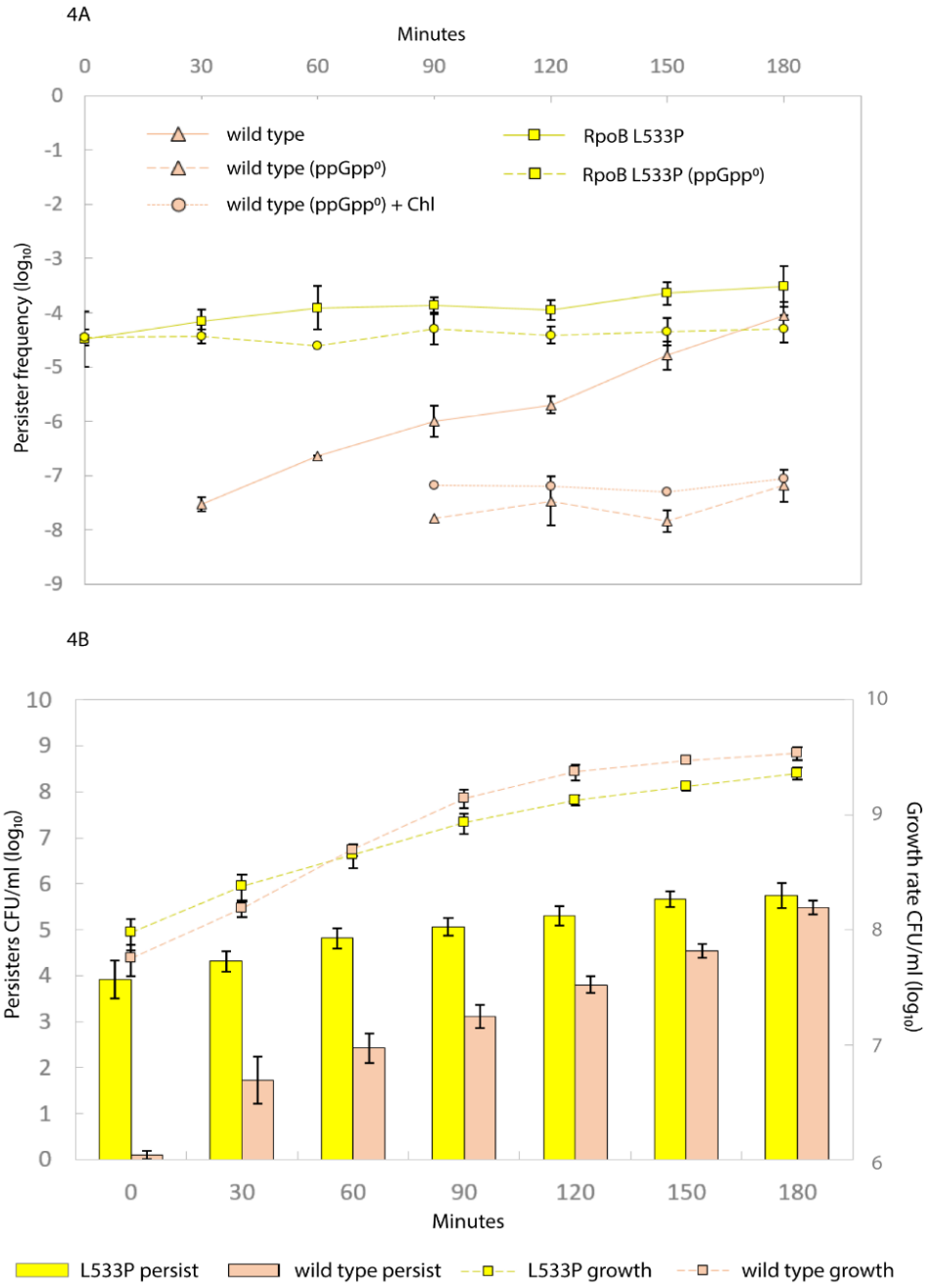

Figure 3-4: *rpoB* stringent mutations confer high persistence phenotype that can't be explained by a slower growth: (**A**) Persister frequency comparison between the MG1655 RpoB L533P (●), MG1655 RpoB L533P ppGpp^0 (●), MG1655 (●), MG1655 ppGpp^0 (●) as well as MG1655 ppGpp^0 (●) slowed with 0.63µg/mL chloramphenicol. The persistence phenotype of stringent mutant is consistently maintained at 1:10,000 -50,000 and is independent of ppGpp.(**B**) Comparison of persistence to ciprofloxacin (18h, 1µg/ml) between MG1655 (●) and MG1655 RpoB L533P (●) along the growth curve. Persistence exhibited by stringent mutant is independent of the growth state.

Interpretation of the persistence data from strains carrying RpoB M1304R and RpoB L533P substitutions is confounded by a relatively slower growth of the two mutant strains (Table 3-2). To estimate the effect of growth rate on persistence, we measured the frequency of persisters in MG1655 at OD_{600} of 0.5 slowed by chloramphenicol to a 22, 27, 30, 35- and 40-min doubling time. Predictably, there was an inverse relationship between growth rate and persister frequency. Yet, when MG1655 was slowed down to the RpoB L533P level, the stringent mutant still yielded over 600 times as many persisters (Fig. S3-2). Additionally, the higher persistence observed in slow-growing cultures could also be a consequence of the ppGpp effect, which controls the growth rate (155), and not of the slow growth itself. To test this, the growth of the $ppGpp^0$ parent was halved by chloramphenicol (Fig. S3-3) and the survival frequency was measured at different points along the growth curve. Slowing down the $ppGpp^0$ had no measurable effect on persistence (Fig. 3-4A), suggesting that ppGpp is required for the effect of growth rate on persistence.

Table 3-2: doubling times

	Doubling time
Strains	Minutes
MG1655	20±1.2
MG1655 RpoB L533P	27.2±2.3
MG1655 RpoB M1304R	25.2±1.4

Growth rates of strains with RpoB substitutions in MG1655 background: Doubling time was determined by CFU/ml.

RpoB high-persistence mutations are found among clinical isolates

We used PATRIC database (102) to determine if the *rpoB* high-persistence mutations occur in clinical isolates. Since in our selection, mutations in *rpoB* followed a *gyrB* mutation, we first analyzed the co-occurrence of *gyrB* mutations known to contribute to quinolone resistance (156, 157) and *rpoB* mutations occurring at or in the vicinity of 1279 and 1304 residues. Sequences were processed and the statistical significance of co-occurrences was analyzed as described in (158). Although we did not find E1279A and M1304R among RpoB sequences of *E. coli* clinical isolates, W1275G and T1286P substitutions did significantly co-occur with D426N and S464Y substitutions in GyrB (Chi-squared test, p-value = 0.002). We introduced the mutation resulting in W1275G substitution into the *E. coli* chromosome. An RpoB W1275G mutant yielded nearly as many persisters as the M1304R strains (Fig. S3-4). We were unable to construct an RpoB1286P strain.

Although rifampicin is not normally used against *E. coli* infections, *rpoB* sequences from 22 clinical isolates carried known Rif^R mutations (159). Three out of the 22 (13.6%) had substitutions in Ser531 residue, which is a known stringent mutation (153) and exhibited high persistence when transferred into MG1655 (data not shown). Coincidently, all three mutations were found in the isolates that also carried known *gyrA* and/or *gyrB* quinolone resistance mutations.

Next, we investigated if stringent mutants can outcompete other Rif^R mutants in presence of bactericidal antibiotics. We selected 104 Rif^R mutants in MG1655 $ppGpp^0$ background,

so that the stringency could be easily confirmed by plating on amino acid-less M9 plates. Out of 104 mutants, 3 were stringent. Following a treatment with ciprofloxacin at 1 μg/ml ("Materials and Methods"), the fraction of stringent mutants increased to 23%, suggesting that stringent mutations can confer competitive survival advantage.

Among the pathogens that are routinely treated by rifampicin, *A. baumannii*, *M. tuberculosis*, and *S. aureus*, the prevalence of the mutations that are homologous to *E. coli* Rif^R stringent was even higher, 96.2%, 23.3%, and 50.9%, respectively. To determine if such mutations can indeed cause high persistence, we investigated the effect of the RpoB S586L substitution in MRSA. Stringent mutants were selected as described in "Materials and Methods". The persister frequency of the RpoB S586L mutant was more than 10,000 times higher than that of the parent in the early exponential phase, and even in the late stationary phase the mutant produced 8 times as many persisters (Fig. 3-5A, B).

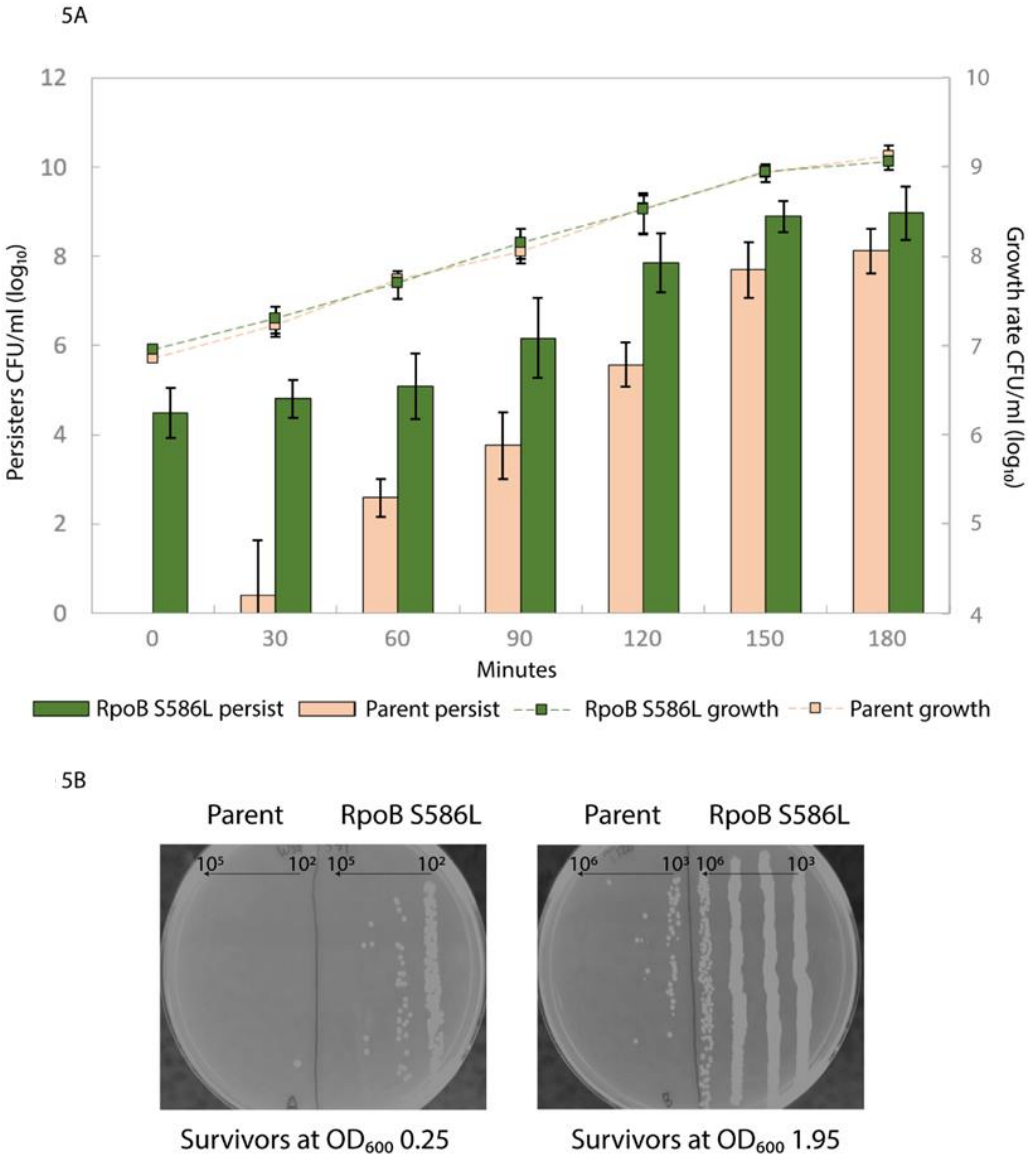

Figure 3-5: An *rpoB* stringent mutation confers high persistence in *Staphylococcus aureus*: (**A**) Comparison of ampicillin persistence (18h, 100µg/ml) between MRSA WCUH29 (●) and WCUH29 RpoB S586L (●). (**B**) Photographs of plates with survivors during exponential phase (*left*) and early stationary phase (*right*), the left side of each plate is the parent, and the right is the *rpoB* stringent mutant. Dilution ranges are shown above the horizontal bars on each plate.

Indole contributes to the RpoB-mediated persistence

To determine if there are any commonalities between the molecular phenotypes of strains carrying RpoB L533P and RpoB M1304R mutations, we compared their transcriptional profiles in wild-type and $ppGpp^0$ backgrounds. Among 697 significantly differentially expressed genes, one operon, *tnaCBA*, stood out as the most upregulated (Sup. File 2). We confirmed activation of the *tnaC* promoter in both *rpoB* mutants by flowcytometry (Fig. 3-6A). Of note, the distribution of the fluorescent signal in the mutants was quantitatively and qualitatively different from that in the parent: not only it was shifted to the up, but it also had two modes, with the second mode representing about 3-5% of all fluorescent counts with about 10-times higher fluorescence than the corresponding mutant average. A *tnaA* knockout in RpoB L533P and RpoB M1304R substitution carrying strains reduced the frequency of persisters by 50% and 80%, respectively (Fig. 3-6B). Concentration of indole in the RpoB L533P and RpoB M1304R cultures was 15 µM and 50 µM, respectively, compared to 0 µM in the parent. However, when we added up to 50 µM indole to a wild-type culture we did not observe any increase in persister formation. When we added indole to a final concentration of 500 µM (a stationary culture equivalent), persistence increased 7-10 times. Given the distribution of the activity of *tnaC* promoter in a population of the *rpoB* mutant cells, it is plausible that only 3-5% of the population produce indole in quantities sufficient to trigger the dormant state, which in turn will happen only in a fraction of that sub-population.

6A

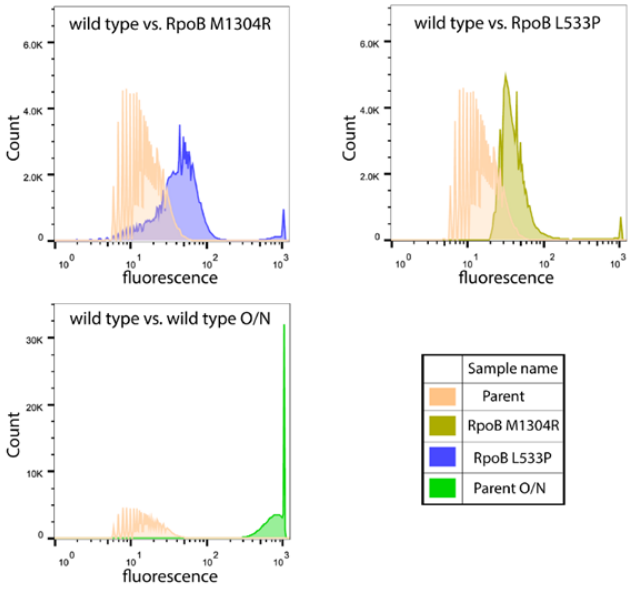
wild type vs. RpoB M1304R
wild type vs. RpoB L533P
wild type vs. wild type O/N
Count
fluorescence
Sample name
Parent
RpoB M1304R
RpoB L533P
Parent O/N

6B

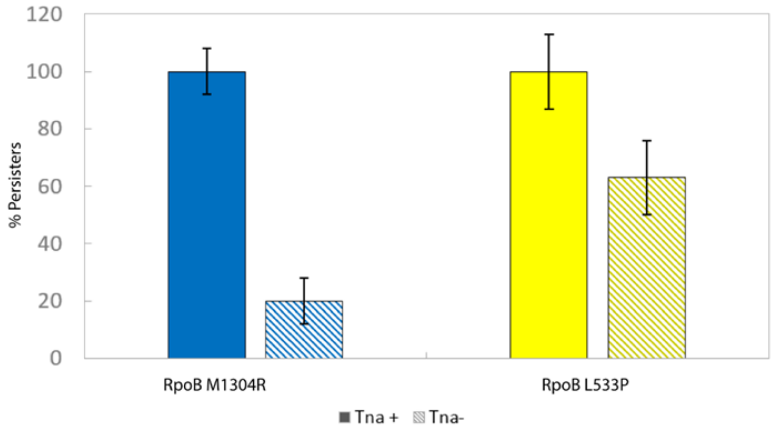
% Persisters
RpoB M1304R
RpoB L533P
Tna +
Tna-

6C

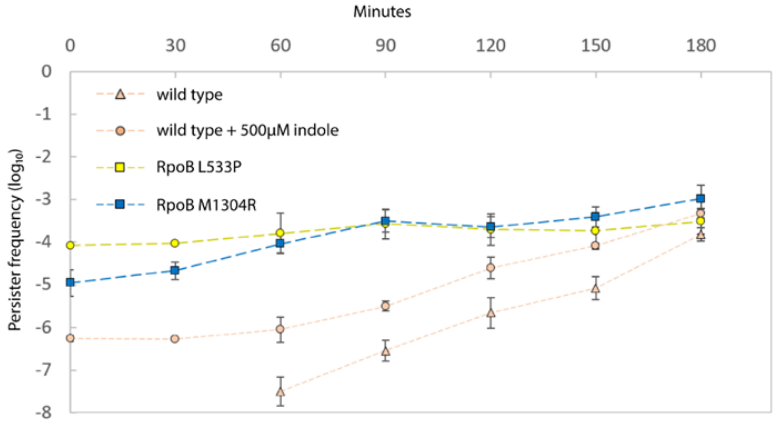
Minutes
wild type
wild type + 500μM indole
RpoB L533P
RpoB M1304R
Persister frequency (log10)

Figure 3-6: The effects of indole on persistence: (**A**) Activation of *tnaC(p)* in MG1655 RpoB M1304R (●) and MG1655 RpoB L533P (●) compared to MG1655(●). The bottom left panel compares the activity of the *tnaC* promoter between exponential and overnight MG1655 cells (●). (**B**) Effect of *tnaA* knockout on ciprofloxacin persistence in MG1655 RpoB M1304R (●) and MG1655 RpoB L533P (●) was measured by averaging percent survival of *tnaA* across 7 time point. (**C**) Ciprofloxacin persistence of MG1655 RpoB M1304R (●), MG1655 RpoB L533P (●), MG1655 (●) and MG1655 + 500µM (●).

Materials and Methods

Bacterial strains and culture conditions

Antibiotics, strains and plasmids used in the study are listed below (supplementary tables S3-1, table S3-2 and table S3-3). Bacteria were grown in LB or MOPS-glucose (E. coli) (Kuroda, 1999), Tryptic Soy Broth / Agar (TSB/TSA) (160) (S. aureus) at 37°C with aeration at 250 rpm. Selection pressure, whenever necessary, was provided by antibiotics at concentrations listed in a table below.

E. coli strains used in this study were all derived from K-12 MG1655 (161). A strain carrying substitution in GyrB S464Y and its derivatives carrying substitutions in RpoB M1304R and E1279A were obtained through stepwise ciprofloxacin selection in liquid medium. The V1275G strain was constructed by replacing the wild type 3'-end of *rpoB* with a fragment carrying the mutation. The mutant fragment was co-amplified with KANR gene and the *rpoB-rpoC* (4184008-4190789) intergenic fragment using rpoBF1, kanR1, rpoBR2, kanR2 primers (Table 3-4) and recombined into the chromosome using λ-Red recombinase (162, 163). Transfer of mutant *rpoB* alleles into the MG1655 wild-type strain was done by P1 phage transductions. ppGpp null mutants were constructed in

two steps: first, a Δ*relA* mutant was constructed by transducing a Δ*relA*::*Kan*^{R} allele from a Keio JW2755 strain (163) into a parent and then a Δ*spoT*::*Cat*^{R} insertion cassette was used to knock out the *spoT* gene in the Δ*relA* strain. The insertion cassette was constructed by amplifying chloramphenicol resistance gene using *spoT*-F and *spoT*-R primers (Table 3-4) with overhangs homologous to flanking regions of the *spoT* gene.

"Stringent" *rpoB* mutants were obtained in ppGpp0 cells, which had been cured of antibiotic resistance cassettes using FLP recombinase, as follows. The culture of a Δ*relA*, Δ*spoT*, *aceB*::Kan^{R} strain was grown from single colonies to OD_{600} of 0.3-0.4; 5 ml of the culture were spun down, resuspended in 1 ml of LB and plated on LB plates with rifampicin at 100 µg/ml. Plates were incubated overnight at 37°C. The following day, colonies were patched onto M9 plates lacking amino acids. Colonies that grew were confirmed to carry *rpoB* "stringent" mutations (164) by sequencing and the "stringent" alleles were transduced into a desired strain using *aceB*::Kan^{R} as a marker.

Spontaneous Rif^{R} mutants were selected by plating 5 x 108 cells of a culture grown to OD600 of 0.4 on LB plates containing rifampicin at 100 µg/ml. Mutations in *rpoB* gene were confirmed by sequencing. Mutant alleles were back-transduced into a desired strain by P1 using aceB::KanR as a *rpoB*-linked, kanamycin-resistant marker. Among Rif^{R} isolates, "stringent" mutants could be identified as smaller colonies. 3 out of 3 "smaller" colonies from each examined plate contained characteristic "stringent" mutations.

A hospital acquired MRSA (WCUH29) was used for this study. S. aureus *rpoB* Rif^{R} mutants were selected by plating a stationary culture of WCUH29 on TSA plates containing 100 µg/ml rifampicin. The following day smaller colonies were patched onto a

fresh TSA plates containing 100 µg/ml rifampicin. The presence of desired "stringent" mutations was confirmed by sequencing the colony PCR products.

Selection

One selection stage consisted of plating a parent strain on LB supplemented with ciprofloxacin at 5x MIC. About 100 colonies were transferred into 3ml LB tubes with the same concentration of the drug and grown overnight. The equivalent of about 10,000 cells were transferred from the O/N cultures into 3 ml LB with ciprofloxacin at 25x MIC for another 16-18 h at 37°C with aeration. 100 µl from tubes without visible growth were transferred into 3ml LB tubes with ciprofloxacin at 5x MIC. The cultures that grew must have resulted from the cells that survived the 25x MIC treatment without being resistant to the 25x MIC concentration of ciprofloxacin. First stage MIC, 5x and 25x MIC were 10, 50 and 250 ng/ml, respectively. Second stage MIC, 5x and 25x MIC were 50, 250 and 1,250 ng/ml of ciprofloxacin, respectively.

Stringent mutant persistence competition assay

Naturally occurring Rif^R mutants were selected for by plating a total of 1X109 MG1655 ppGpp0 cells from a culture grown to OD_{600} of 0.4 in LB onto an LB plate containing 100µg/ml of rifampicin. The following day all of the rifampicin resistant colonies were patched onto fresh LB rif100 plate and M9 plates lacking amino acids (AA-). Frequency of stringent mutations was determined by a ratio of colonies on M9 (AA-) plates over the total rifampicin resistant colonies. All of the rifampicin resistant colonies were then combined into 800 µl of LB and thoroughly mixed. The proportion of stringent mutants in the mixture was determined by a serial ten-fold dilution, plated on both LB and M9 (-

AA). Ten microliters of 800 µl mixture was then inoculated into 30 ml of fresh LB and grown for 8 generations, without ever going above OD_{600} of 0.3. Upon reaching OD_{600} of 0.3 ± 03, culture was treated with 1 µg/ml of ciprofloxacin followed by 18-hour incubation. Prior to plating, treated cells were washed twice with saline. Total persistence was determined as a ratio of CFU/ml of survivors over the CFU/ml count just prior to treatment. Stringent mutant persistence was determined in the same way as total persistence, with an exception of cultures being plated on M9 (AA-) plates. The enrichment ratio was determined as the stringent persister ratio over total persister ratio.

Determining MIC and MBC

MIC and MBC values were determined according to standard protocols (165). Briefly, overnight cultures were diluted 1:1,000 and grown to mid-exponent, OD_{600} of 0.3 ± 0.05. To determine MIC, 500 - 1,000 cells of the mid-exponential culture were inoculated into 2 ml of media with antibiotics at different concentrations. After 18 h incubation at 37°C with aeration, culture ODs were determined and compared to the control culture without antibiotic. Concentrations of antibiotics that inhibited growth by 50%, 90% and 99% or greater were determined. The lowest antibiotic concentration that inhibited growth by at least 99% was chosen as the characteristic MIC of an antibiotic. Coarse ciprofloxacin MICs for different strains were initially tested in the following range of concentrations: 0, 4, 8, 16, 32, 64, 120, 250, 500, 1,000, 2,000 and 4,000. Ampicillin MIC was determined by using the range: 0, 1, 4, 8, 16, 32, 64 and 100 µg/ml. More precise MIC values were obtained by using a finer array of concentrations within a narrower range, which was determined in the coarse MIC assay.

To measure MBC, 5x106 (± 2 106) cells were inoculated into 3 ml of fresh media containing different concentrations of antibiotics. After 18 h incubation at 37°C with aeration, bacteria were serially diluted and plated on LB (TSA for S. aureus) plates. The numbers of surviving CFU/ml were normalized to the number of CFU/ml in the samples immediately prior to the addition of antibiotics. The ranges of concentrations were the same as in MIC assays. The values of MBC_{90}, the concentration at which CFU decreases by 90%, were obtained by interpolation after fitting kill curve data into a polynomial function.

The reported estimates of MIC and MBC, along with corresponding errors, for each strain were obtained from testing at least 3 independent biological samples.

Amino acid downshift assay

Three colonies were picked from LB plate and inoculated into MOPS 0.2% glucose supplemented with 20 L-amino acids, with each amino acid present at a final concentration of 40 ng/ml. Bacteria were grown overnight and sub-cultured into the same medium to OD600 of 0.05 and grown until OD_{600} of 0.35 ± 0.05. Cells were washed three times in MOPS salts buffer and then re-suspended in 20 ml of the nutrient downshift medium (MOPS lacking histidine, leucine, isoleucine, valine, aspartate, and threonine) (151) and grown at 37°C, aerated at 250 rpm. OD_{600} measurements were taken every 5 minutes and serial dilutions were performed every 10 min for one hour. Colonies were counted after 24 h at 37°C on LB plates.

Persistence measurement

Cultures were grown overnight at 37°C in LB to OD_{600} of 2.5-3.5. The following day the O/N cultures were diluted 1:1,000 in fresh media and maintained in early exponential phase by repeated dilution and kept below OD_{600} of 0.3 for at least 10 generation at 37°C with aeration at 250 rpm in the total volume of 30 ml in 150-ml Erlenmeyer flask. For experiments that included the use of indole, freshly prepared indole was added to the cultures for 3-4 generations prior to reaching OD_{600} of 0.3 .Upon reaching an OD_{600} of 0.3 ± 0.03 an aliquot of 3 ml was taken out every 30 min for the next 3 h and inoculated with 1 or 4 μg/ml ciprofloxacin or 100 μg/ml ampicillin, always above 10x MIC for any given strain. Inoculated sample were incubated for 17 h at 37°C aerated at 250 rpm and plated for CFU counts. Persistence was determined as a number of surviving CFU/ml normalized to the CFU/ml counts of untreated samples at the corresponding time points. The same procedure was followed when persistence was measure in bacteria slowed by chloramphenicol or temperature.

(p)ppGpp quantification using TLC

Bacterial strains were streaked out and individual colonies were then inoculated and grown overnight in a complete MOPS medium, supplemented with 0.2% glucose and 20 L-amino acids, with each amino acid present at a final concentration of 40 ng/ml, in a shaker at 250 rpm and 37°C. Overnight cultures were diluted 1:1,000 in 3.8 ml of MOPS and grown to OD600 of 0.3. Cultures were then split into two 1.5 ml tubes and spun down. Half of the samples was resuspended into fresh 3 ml of MOPS supplemented with amino acids, and another half was used to inoculate amino-acid-free MOPS to a starting OD_{600} of 0.15 for all samples. From each sample a 100 μl aliquot was taken to determine CFU/ml by serial dilution. All samples were then supplemented with 20 μCi of P^{32}

orthophosphate. Following 1 h incubation, 200 µl of cell culture was taken and lysed using 40 µl of 10% phosphoric acid. Samples were spun down in the table top centrifuge to remove cell debris and 20 µl of lysate was then spotted on a nitrocellulose TLC plate. Prior to sample application, TLC plate was washed with deionized water and methanol. To mobilize samples, we used a pH 3.5 water-based phosphate buffer (166). Visualization of samples was done using Amersham Typhoon Gel and Blot Imaging system (GE Healthcare Biosciences, Chicago, IL) and the image was analyzed using ImageQuant TL 8.1 and FiJi (64-bit version software) (167).

Single gene expression assay and flow cytometry

Strains were transformed with a pUA66 plasmid carrying a *ilvI*-p:*gfp, hisL*-p:*gfp, tnaC*-p:*gfp* and *mdtK*-p:*gfp* promoter fusion (168). Fresh colonies of confirmed transformants were inoculated into MOPS medium supplemented with 0.2% glucose and 20 L-amino acids, with each amino acid present at a final concentration of 40 ng/ml, and grown overnight at 250 rpm and 37°C. The following day, cultures were diluted 1: 1000 into the fresh, pre-warmed complete glucose-MOPS and incubated for 9-10 generations, without ever going above an OD_{600} of 0.3. A 100 µl aliquots were then taken and diluted 10-100 times in fresh complete glucose-MOPS, immediately prior to flow cytometry. A BD Accuri C6 Flow Cytometer (BD Biosciences, Franklin Lakes, NJ) was used with a FITC optical filter (488 nm excitation 530/533 nm emission) at 14-66 µl/min flow rate. Data was analyzed using FlowJo (BD Biosciences, Franklin Lakes, NJ). The same cultures were also used to measure levels of fluorescence in bulk, using SpectraMax plus-384 plate reader (Molecular Devices, Sunnyvale, CA) and the same excitation and emission parameters as in the flow cytometry experiment. Fluorescence was then normalized to

both OD_{600} and CFU/ml. The same experiment was carried out using glucose-MOPS without amino acids. In the case of *tnaC*-p:*gfp*, experiment was carried out in LB/saline.

Reducing growth rate with chloramphenicol

An overnight culture of MG1655 or MG1655 ppGpp0 was diluted 1:1000 and grown to OD_{600} of 0.3 ± 0.05 in 30 ml of LB at 37°C and 250 rpm. The culture was then split between four flasks at 1 : 20 dilution. Each flask contained a different concentration of chloramphenicol: 0, 0.5, 0.75 and 1 µg/ml in 30 ml LB. Cultures were then adapted to the drug for approximately four generations. Growth rates were measured after cell density reached an OD_{600} of 0.1. Growth curves were reconstructed by measuring a number of CFU/ml every 30 minutes for 3.5 h until the stationary plateau was reached. Exponential growth rates for different concentrations of chloramphenicol were plotted as a function of the drug concentration. The resulting trend line was used to estimate drug concentrations needed to slow down cell growth by a desired amount.

Overnight culture of MG1655 was diluted 1:1,000 fold into flasks containing 0, 0.4, 0.8 and 1.0 µg/ml of chloramphenicol, and grown for 10+ generations until OD_{600} 0.5 was reached. Upon reaching desired concentration, 100µl aliquot was taken to determine the CFU/ml count. The remaining culture was then treated with 1µg/ml ciprofloxacin or 100µg/ml ampicillin for 18 hours. Persistence was determined in the same way as described in "persistence measurement" section of materials and methods. To prevent spontaneously generated stringent mutants due to starvation experienced in the overnight culture of MG1655 ppGpp0 strain, when working with MG1655 ppGpp0, culture was inoculated directly from a freshly streaked out colony.

Whole Genome Sequencing

Isolates were grown overnight from a single colony in LB at standard conditions. DNA was extracted using a Promega Wizard Genomic DNA Purification Kit. Libraries were prepared using a TruSeq Nano library preparation kit. Sequencing was conducted using Illumina HiSeq2500. De-multiplexing was performed using FASTX-Toolkit (http://hannonlab.cshl.edu/fastx_toolkit/index.html). The reads were mapped to the reference genome (GCF_000005845.2_ASM584v2) using Bowtie 2 (169, 170). The SAM files of mapped reads were converted to BAM format and sorted using SAMTOOLS (171). The sorted BAM files were converted to BED files and intersections/mutations with annotated ORF's were enumerated using BEDTOOLS (173). Mutation were identified using Breseq (172) and confirmed using standard Sanger sequencing, using primers listed in supplementary materials (table 3-4).

RNA-seq experiment

Overnight cultures were diluted 1:1,000 in 50 ml of LB and grown for ten generations under an OD_{600} 0.3 at 37°C while shaking at 250 rpm. When an OD_{600} of 0.3 was reached, 10 ml of cultures were transferred into 15 ml conical tubes containing 1.25 ml of the "stop" solution (ethanol v/v 95%, and phenol v/v 5%). "Stopped" cells were spun down and supernatant was removed. Pellets were flash frozen in liquid nitrogen and kept at -80°C until all samples were collected. Pellets were thawed on ice and resuspended in 200 µl of TE buffer containing 20 mg/ml of lysozyme and incubated at 37°C for 10 min. All of the following steps for RNA purification followed RNAeasy (Qiagen, Hilden, Germany) mini prep kit manual.

Before constructing the sequencing library, rRNA was removed from all samples using Ribo-Zero rRNA Removal Kit (manufacturer specs). The library was made using TruSeq Stranded mRNA library prep kit from Illumina (manufacturer specs Cat. # 20020595). Sequencing was done using Illumina HiSeq2500. De-multiplexing was performed using Illumina's bcl2fastq software 2.20, and results were reported as FASTQ files. The reads were mapped to the reference genome (GCF_000005845.2_ASM584v2) using HISAT2 (174). The final per feature read counts were obtained using Rsubread (175). Analysis of differential expression using a generalized linear model, which is described in more detail in the text, was carried out with the aid of DESeq2 package (176).

Indole assay

Kovack's reagent was prepared fresh by dissolving 1 g of p-dimethyl aminobenzaldehyde in 15 ml of isoamyl alcohol and 5 ml of concentrated hydrochloric acid. Indole concentration was measured by adding 400µL of Kovack's reagent to a 3 ml culture of exponentially growing cells at OD_{600} of 0.3 ± 0.05. Cells were incubated with the reagent for 30 min at room temperature in the dark. From the 400µl of Kovack's reagent added to the culture, 200 µL of reacted product from the top layer was moved into a flat bottom 96 well plate and absorbance was measured at 535nm using SpectraMax plus-384 plate reader (Molecular Devices, Sunnyvale, CA). The standard curve was constructed using Kovack's reagent colorimetric assay with following concentrations of indole; 10, 25, 50, 100, 200, 400, 500 µM in LB.

Discussion

Bacteria adapt to antibiotic-containing environments by acquiring resistant mutations. Here, we have demonstrated that some of these mutations, including those that are highly prevalent in clinical isolates, can confer an additional benefit of increased persistence to bactericidal antibiotics. These high-persistence mutations resided in two regions of the beta subunit of the RNA polymerase: 1275-1304 and 531-533 and 526 *E. coli* equivalent in MRSA. Mutations in the first region can be readily selected at low concentrations of ciprofloxacin and those in the second are commonly occurring rifampicin-resistance mutations. Thus hip mutations can be fixed in a bacterial population not only through cyclical exposure to bactericidal antibiotics (177-180) but also as a result of pleiotropy of certain antibiotic resistance mutations.

The RpoB M1304R substitution resulted in two key phenotypes: reduced susceptibility to ciprofloxacin by 1.5-2-fold and increased persistence by a factor of 1,000. The two effects depend on different mechanisms, however. Among top 50 significantly over-expressed genes as a consequence of RpoB M1304R substitution, the function of only one of them, *mdtK*, which encodes a multi-antimicrobial extrusion transporter, could be directly linked to drug resistance (55) (Sup. File 3). When this work was in progress, Pietsch *et al.* found that similar *rpoB* mutations increased fluoroquinolone MIC by upregulating *mdtK* (139). However, while an *mdtK* knockout in RpoB M1304R strain resulted in the full reversal of the resistance phenotype (Table 3-1), it had no effect on persistence (Fig. S3-5), suggesting that the two phenotypes can be segregated.

MG1655 strain carrying RpoB L533P substitution, which confers rifampicin resistance, had no measurable effect on ciprofloxacin MIC. And yet it resulted in a striking persister phenotype; the frequency of persisters was independent of the growth phase (Fig. 3-4A).

Another relevant phenotype exhibited by the mutants is a slower growth. Decreasing the growth rate resulted in an increase of the number of persisters. However, the persister frequency of the *rpoB* rifampicin resistant mutant was 622 times higher when persistence was measured using ciprofloxacin and 88 times higher when using ampicillin, compared to what would be expected from the reduced growth rate alone in both ppGpp+ and null cells (Fig. 3-4A, Fig. S3-2). These findings strongly argue against the notion that a decreased target abundance, which should be a consequence of slowed growth, is sufficient to explain increase in persistence or that it confounds the phenomenon altogether.

The *rpoB* mutations completely overrode the ppGpp requirement for persister formation. This strongly suggests that the persister state is the result of a transcriptional program and ppGpp effects persistence primarily, if not solely, as a modulator of transcription. The mutants also illuminated the importance of differences in transcriptional activity among individual cells as an attribute of the hip phenotype: a sub-population of mutant cells had the promoter of the *tnaA* gene upregulated at least 10-fold, while most of the population showed only marginal shift in the promoter activity. We demonstrated that this *tnaA* activation resulted in accumulation of indole that accounted for 50-80% of the hip phenotype in the *rpoB* mutants. Although these results are qualitatively consistent with earlier observations of the effect of indole on persistence (181, 66), we also found that indole has no effect on persistence without ppGpp or its transcriptional mimics. The role of *tnaA* and indole in the persiter state formation may tie together the metabolic state of individual cells with transition to the dormant state. The low-affinity tryptophan transporter TnaA is activated when tryptophan is used as a carbon source (182, 183),

which happens only when all other preferred carbon sources in rich media have been exhausted (184,185). Transition to tryptophan, or other "lesser" carbon resources, may signal imminent starvation which, in combination with other yet unknown factors, establishes the persister state. In the *rpoB* mutants, *tnaA* transcription is constitutively upregulated in a number of cells, resulting in the "out-of-order" tryptophan utilization, starvation signaling by means of indole, and dormancy. This explanation also applies to indole-free species, where the "quality" of carbon and nitrogen source facilitates state transition. For example, Halsey *et al*. have suggested that histidine catabolism may be involved in regulation of CcpA response in *MRSA* (186-188), a major transcriptional regulator involved in metabolic regulation under suboptimal growth conditions, virulence, antibiotic resistance and biofilm formation (189,190).

The primary effect of rifampicin resistance mutations is to provide protection against the drug. With nearly a dozen of possible mutations conferring rifampicin resistance, slower growing mutants should be at a disadvantage. Yet, these mutations are frequently encountered in pathogenic species (191,192), suggesting that stringent mutations can provide survival advantage(s), likely in the form of persistence. Since rifampicin is almost always used in combinations with other bactericidal antibiotics against some of the more antibiotic-recalcitrant bacteria (33), selecting for *rpoB*-dependent persisters, may promote the establishment of chronic infections (193), rather than subverting them, in a long run.

Supplementary tables:

Supplementary table 3-1S: Antibiotics.

Antibiotic	Cat #	Manufacturer	Concentration of stock	Stock age	Final dilution
Ampicillin	BP176025	Fisher BioReagents	100mg/ml (water)	≤ 1 months (-20C) or 4 freeze cycles	100µg/ml
Kanamycin	100218-998	VWR Lifescience	50mg/ml (water)	≤ 3 months (-20C)	50µg/ml
Chloramphenicol	TCC2255	TCI	25 mg/ml (70% ethanol)	≤ 2months (-20C)	0.63µg/ml 25µg/ml
Rifampicin	R3501	Sigma-Aldrich	50mg/ml (methanol)	≤ 2months (-20C)	100µg/ml
Ciprofloxacin	NC9553331	Lkt Laboratories	20, 10, 1, 0.1, 0.01mg/ml (water)	≤ 1 months (-20C) or 4 freeze cycles	1µg/ml or 4µg/ml

Supplementary table 3-2S: Strains.

Name	Relevant amino acid substitution	Genotype	Source /Derivation
MG1655	-	F^-, $lambda^-$, rph-1	Plunkett,G. III
OKR5	RpoB L533P	MG1655, *rpoB*1598 T>C	This Study
OKR13	RpoB M1304R	MG1655, *rpoB*3911 T>G, *ΔAceB*	This Study
MG1655, pDJJ11		MG1655, pDJJ11	This Study
OKR5, pDJJ11	RpoB L533P	MG1655, *rpoB*1598 T>C, pDJJ11	This Study
OKR13, pDJJ11	RpoB M1304R	MG1655, *rpoB*3911 T>G, *ΔAceB,* pDJJ11	This Study
OKR1	GyrB S464Y	MG1655, *gyrB*1391 C>A	This Study
OKR1, pUA66-M	GyrB S464Y	MG1655, *gyrB*1391 C>A, pUA66 (*mdtK-p:GFP, kanR)*	This Study
OKR1, pUA66-I	GyrB S464Y	MG1655, *gyrB*1391 C>A, pUA66 (*ilvL-p:GFP, kanR)*	This Study
OKR1, pUA66-H	GyrB S464Y	MG1655, *gyrB*1391 C>A, pUA66 (*hisL-p:GFP, kanR)*	This Study
OKR2, pUA66-M	RpoB M1304R, GyrB S464Y	MG1655, *gyrB*1391 C>A, *rpoB*3911 T>G, pUA66 (*mdtK:GFP, kanR)*	This Study
OKR2, pUA66-I	RpoB M1304R, GyrB S464Y	MG1655, *gyrB*1391 C>A, *rpoB*3911 T>G, pUA66 (*ilvL:GFP, kanR)*	This Study
OKR2, pUA66-H	RpoB M1304R, GyrB S464Y	MG1655, *gyrB*1391 C>A, *rpoB*3911 T>G, pUA66 (*hisL:GFP, kanR)*	This Study
OKR2	RpoB M1304R, GyrB S464Y	MG1655, *gyrB*1391 C>A, *rpoB*3911 T>G	This Study
OKR3	RpoB E1279A, GyrB S464Y	MG1655, *gyrB*1391 C>A, *rpoB*3836 A>C	This Study
OKR4	RpoB V1275G, GyrB S464Y	MG1655, *gyrB*1391 C>A *rpoB*3824 T>G*:kanR*	This Study
MG1655(p)	-	*ΔdgoR, ΔrelA, ΔspoT*	This Study
OKR5(p)	RpoB L533P	MG1655, *ΔdgoR, ΔrelA, ΔspoT ΔaceB:kanR, rpoB*1598 T>C	This Study
OKR13(p)	RpoB M1304R	MG1655, *ΔdgoR, ΔrelA, ΔspoT ΔaceB:kanR ,rpoB*3911 T>G	This Study

OKR1(p)	GyrB S464Y	MG1655, *gyrB*1391 C>A, *ΔrelA, ΔspoT*	This Study
OKR15(p)	GyrB S464Y, RpoB L533P	MG1655, *gyrB*1391 C>A, *ΔrelA, ΔspoT, ΔAceB:kanR, rpoB*1598 T>C	This Study
OKR113(p)	GyrB S464Y, RpoB M1304R	MG1655, *gyrB*1391 C>A, *rpoB*3911 T>G, *ΔrelA, ΔspoT*	This Study
OKR1135(p)	GyrB S464Y, RpoB M1304R, RpoB L533P	MG1655, *gyrB*1391 C>A, *rpoB*3911 T>G, *ΔrelA, ΔspoT, rpoB*1598 T>C	This Study
OKR6	GyrA S83L	MG1655, *gyrA248* C>T	This Study
OKR65	RpoB L533P, GyrA S83L	MG1655, *rpoB*1598 T>C, *gyrA248* C>T	This Study
OKR613	RpoB M1304R, GyrA S83L	MG1655, *rpoB*3911 T>G, *gyrA248* C>T, *ΔAceB:kanR*	This Study
WCUH29	-	HA-MRSA	(194)
WCUH29-5	RpoBS486L	*rpoB*1457 C>T	This Study

Supplementary table 3-3S: Plasmids.

Name	**Relevant components**	**Source**
pDJJ11	Wt *rpoB*	(159)
pKD46	λ-red recombination	(162)
pCP20	FLP recombinase	(162)
pUA66	*mdtK-p:GFP/ ilvL-p:GFP/ hisL-p:GFP, kanR*	(168)

Supplementary table 3-4S: Primers.

Primer name	Sequence	Description
ΔSpoT F	TGC TGA AGG TCG TCG TTA ATC ACA AAG CGG GTC GCC CTT GGT GTA GGC TGG AGC TGC TTC	SpoT knockout-F amplified with FRT from pKD3
ΔSpoT R	GTG TTG GGT TCA TAA AAC ATT AAT TTC GGT TTC GGG TGA CAT GGG AAT TAG CCA TGG TCC	SpoT knockout-R amplified with FRT from pKD3
SpoT i F	CGC ACC GTT TAG GTA TCC AC	SpoT confirmation internal F
SpoT i R	GCT CAT TGC GTT ACC AAG TCC	SpoT confirmation internal R
SpoT e F	CAG GAA CAG CAA GAG CAG GA	SpoT confirmation external F
SpoT e R	CCA TGC AGA CGG TCA GAT CA	SpoT confirmation external R
RelA F	TGT AGA TAC GAG CAA ATT TCG GC	relA confirmation F
RelA R	GGC AGG TCT GGT CCC TAA AG	relA confirmation R
RpoB end F	GACGGTGCGAAAGAAGCAGA	C-terminal confirmation
RpoB end R	GCAGTGACCTGTTTGAGCGA	C-terminal confirmation / C-terminal seq
RifR F	GTCTGAGCGCACTGGTAGAA	Rif resistance F
RifR R	CTG AAC AAG CTG GAT TCG CC	Rif resistance R
RifR seq	GTC TCA GTT TAT GGA CCA GAA C	Rif resistance seq
1275 1F	CCT GAG TAC CTT CAG CGA TG	RpoB 1275 mut 1F
1275 1R	GCT TCC AGC GCC CAC CCT TCC ATC TCC	RpoB 1275 mut 1R
1275 2F	CGG GGA GAT GGA AGG GTG GGC GCT GGA	RpoB 1275 mut 2F
KanR F	GGAGTTAGCACTTAGAAGAACTCGTCAAGAAG	KanR flip F
Link 1R	TTGATCCCCTTACTCGTCTTCCAGTTCGATG	Link 1
KanR R	GACGAGTAAGGGGATCAAGATCTGATCAAG	KanR flip R
Link 2F	GTTCTTCTAAGTGCTAACTCCGACGGGAG	Link 2
Uni 2R	TGGTTTGAACGTACGGTAGTTGA	RpoC homology arm
1224 1F	TGACCTGAGTACCTTCAGC	RpoB 1224 mut 1F
1224 1R	ACA TGT AAC CAA CGG TTA CTG GAC GCT	RpoB 1224 mut 1R
1224 2F	TCG AGC GTC CAG TAA CCG TTG GTT ACA	RpoB 1224 mut 2F
Uni rpoB R	CAT CTT GGT ACG ACC GTT C	RpoB mut 2R
S RpoB F	AAT TCA TGG ACC AAG CAA ACC	S aureus RpoB Rif F
S RpoB R	CCA TAA CTG TAT TGT TAC CAC GG	S aureus RpoB Rif R
GyrA F	GCCATACCTACGGCGATACC	GyrA F
GyrA R	AGCGACCTTGCGAGAGAAAT	GyrA R

Supplementary figures:

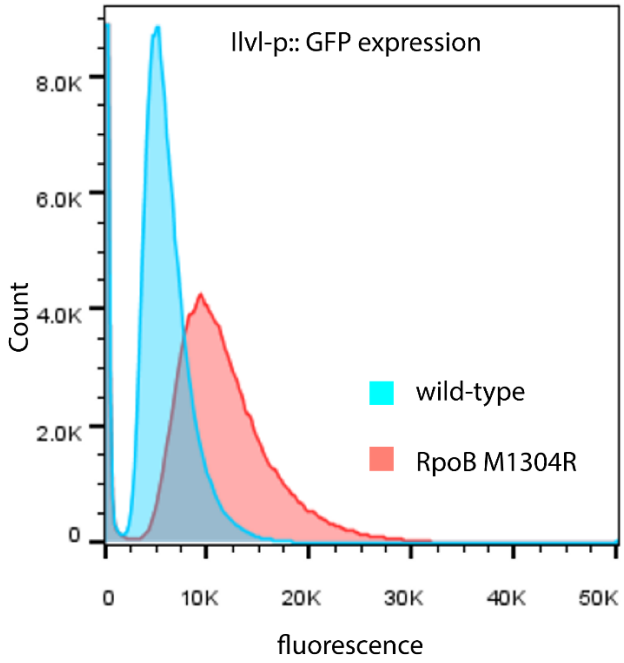

Supplementary figure S3-1: Flow cytometry of ilvL(p):GFP reporter: Cells grown in MOPS medium supplemented with all 0.2% glucose and all 20 amino acids. Samples for flow cytometry were taken after culture had reached OD_{600} of 0.3 and diluted down using the same pre-warmed media to 0.03±0.01. Comparison is between MG1655 GyrB S464Y (●) and RpoB M1304R (●) in the same backgrounds.

Supplementary figure 2

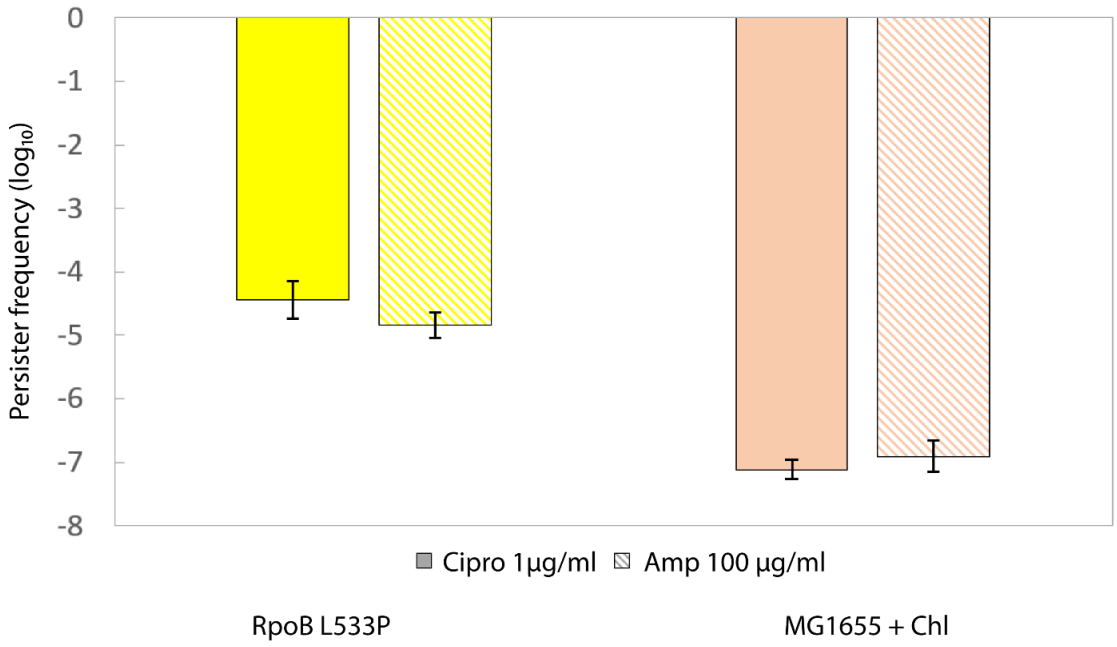

Supplementary figure S3-2: Stringent mutant persistence is not a consequence of slowed growth: Comparison of persistence between MG1655 RpoB L533P (●) and MG1655 (●) slowed to 30 min doubling time using chloramphenicol. The left bar represents persister frequency when strains were treated by ciprofloxacin, and the right bar shows persister frequency following ampicillin treatment. All treatments were performed on exponentially growing cultures at OD_{600} of 0.5.

Supplementary figure 3

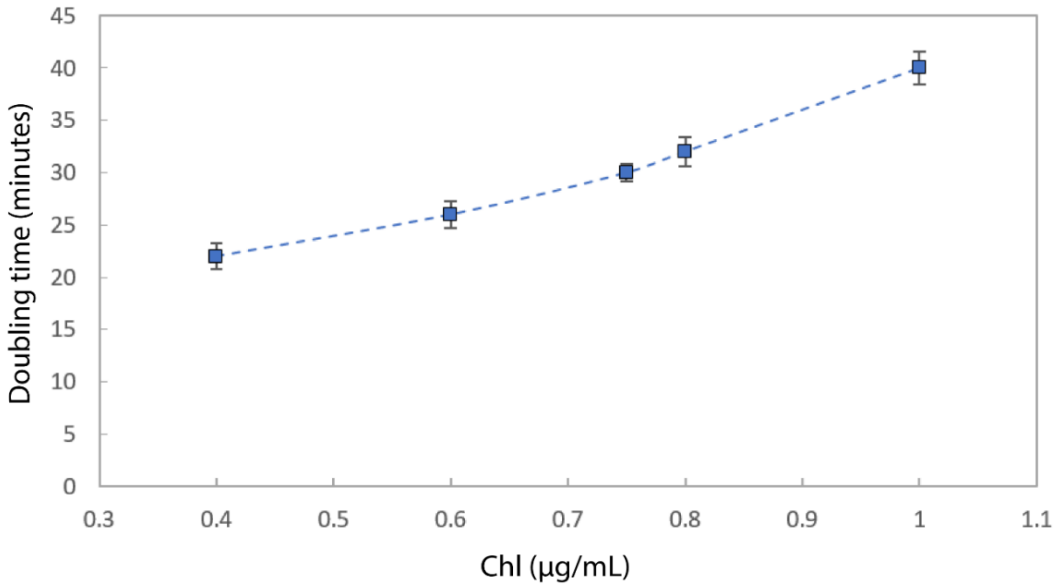

Supplementary figure S3-3: Effects of sub-inhibitory concentrations of chloramphenicol on growth of E. coli: MG1655 was grown in presence of 0.4, 0.6, 0.75, 0.8 and 1µg/mL of chloramphenicol and the doubling time at each concentration was determined using CFU/ml.

Supplementary figure 4

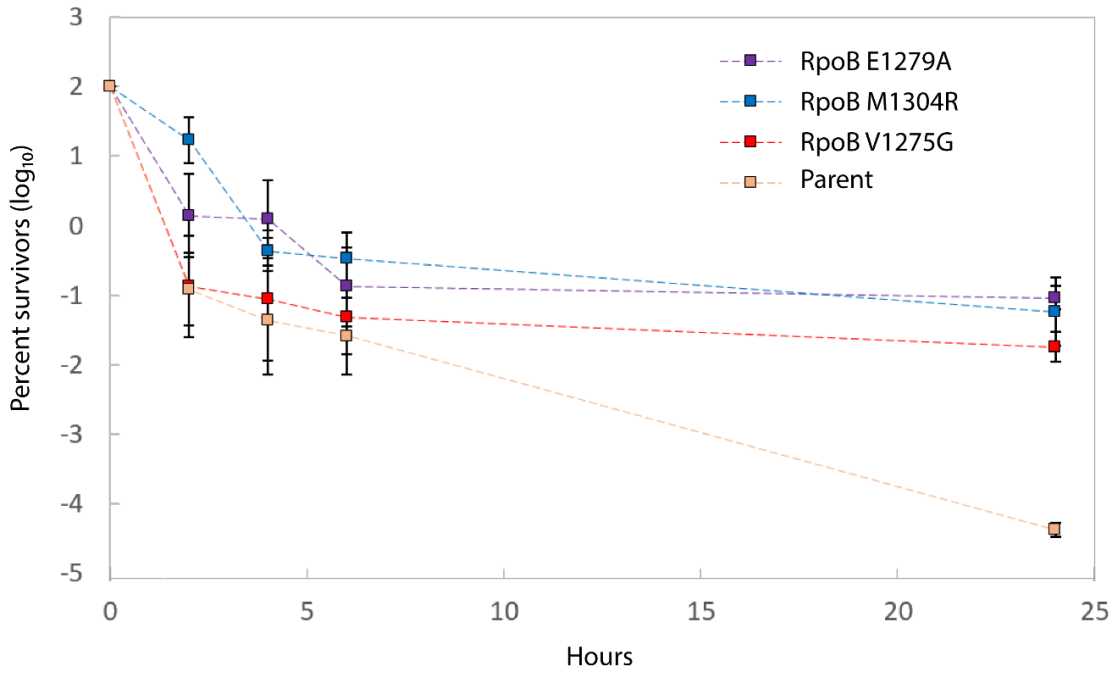

Supplementary figure S3-4: The *rpoB* mutations co-occurring with gyrase mutations from clinical isolates confer increased persistence: Ciprofloxacin (4µg/mL) 24h kill curves comparing the parent strain with a GyrB S464Y substitution (●) to the mutants in the same background carrying E1279A (●), M1304R (●) and V1275G (●) RpoB substitutions.

Supplementary figure 5

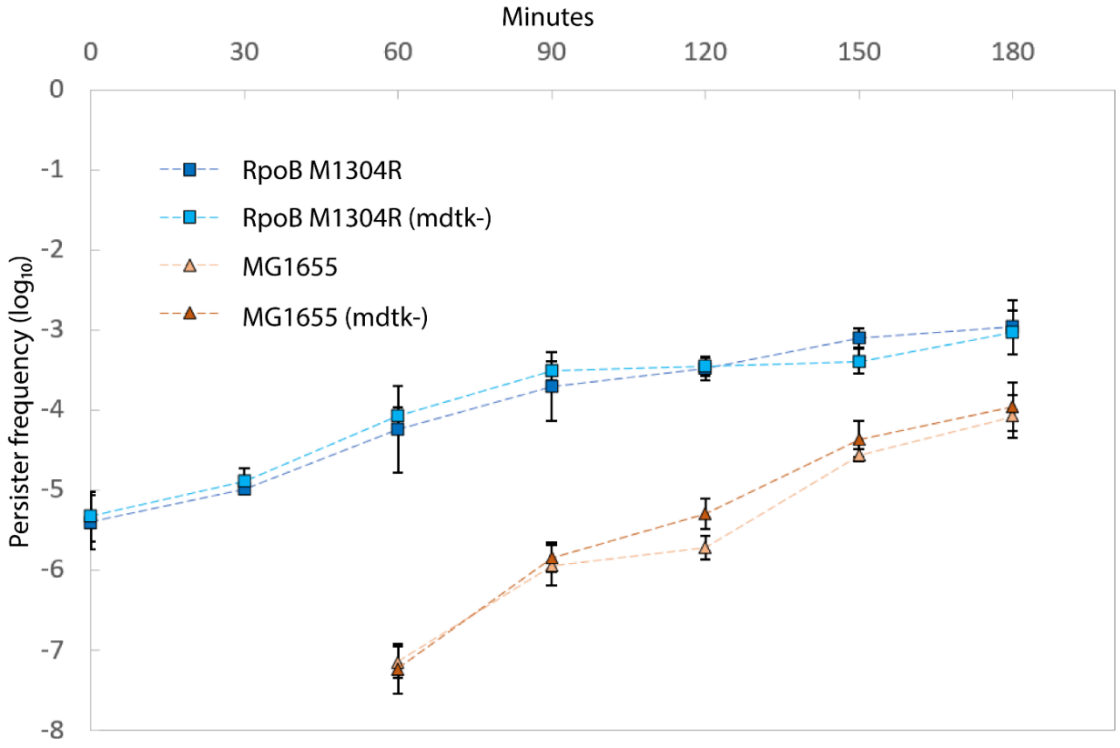

Supplementary figure S3-5: Deletion of *mdtK* has no effect on persistence: Comparison of persistence between MG1655 RpoB M1304R / MG1655 RpoB M1304R Δ*mdtk* (●) and MG1655 /MG1655 Δ*mdtk* (●) along the growth curve.

Chapter 4

Characterization of the unculturable state of the bacterium *Escherichia coli* during thymineless death

This chapter, while unlikely to be published due to a technological limitation, may still be submitted to BioRxvi. The major limitation of the chapter is that it is near impossible to determine if the DNA damage sustained during thymine starvation is fully reversible, and that no DNA near the origin of replication becomes permanently lost. While on macro scale (microarray/ microscopy) it appears that DNA is fully restored, on an individual cell level it is still possible that DNA fragments are getting lost. To address this, a single cell-based sequencing study will need to be conducted, since on average (population sequencing) does not provide high enough resolution to make a definitive call. Unfortunately, the interest in this subject does not justify the time and money investment that would be required for such study.

The idea for this chapter as well as the experiments described in this chapter were performed by me, with an exception of temporal profile of DNA degradation (Fig. 4-3S). The microarrays to measure DNA degradations were done by D. Sangurdekar as a part of his thesis project. Additionally, Dr.W. Margolin and Dr. R. Schaaper provided us with some of the key strains that we required to perform this research. As an advisor, Dr. A. Khodursky contributed to the development of the idea and preparation of the manuscript. Using my and D. Sangurdekar's data Dr. Khodursky also generated figure 4-4 and 4-2S.

Abstract

Thymine starvation causes inhibition of DNA replication, DNA damage and eventual cell demise known as thymineless death. We discovered a cellular hallmark of the thymine starvation: sequential deposition of FtsZ rings on both sides of the incompletely replicated nucleoid. Such cells, capped at both poles by the anucleate compartment, can grow, place internal FtsZ rings and repair their DNA but they cannot divide. Moreover,

the phenotype can be rescued by a temperature sensitive *ftsZ* allele implying that the bactericidal effect of thymine starvation is an inevitable consequence of an internal process, the division cycle.

Introduction

When *Escherichia coli* bacteria are starved for thymine they rapidly lose viability in a process known as thymineless death (TLD) (195). TLD was observed in all organisms that could be starved for thymine, including *Deinococcus radiodurans* (196), which can sustain extremely high levels of DNA damage. Cells undergoing TLD have been examined in numerous studies from multiple angles, establishing physiological, genetic and genomic parameters of the phenomenon (most recently reviewed in (197)). And yet, a path leading to cell demise remained obscure.

Thymine starvation causes DNA damage which in turn triggers SOS response (198,199). As part of the response, SulA inhibits FtsZ, leading to a cell division block (200, 201). If DNA damage persists, which should be the case in the absence of TTP in thymine starved cells, the division block should also continue. An extended division block via FtsZ inactivation or repression would result in a loss of viability as evidenced by irreversible temperature sensitivity of some *ftsZ* mutants (202. 203). This straightforward explanation of the nature of TLD was bolstered by findings (204, 205) that the loss-of-function mutations in Lon protease, which degrades SulA (206), accelerated onset and kinetics of TLD. However, a *sulA*$^{-}$ mutation protects from TLD only 5-10% of a population of the starved cells (82), which means that 90-95% of the TLD effect is unrelated to the SulA-mediated division block.

An alternative possibility was raised in previously established work (84): it was proposed that the loss of viability was due to the loss of essential genetic information at and/or near the origin of replication. It was hypothesized that cells whose chromosomes lack essential functionality, such as the origin of replication, would not be able to replicate upon return of thymine and thus won't generate progeny. However, further experiments revealed that thymine starved cells lose DNA around the origin only on one chromatid (207, 208). Although a formal possibility remains that the second chromatid has also been corrupted during TLD, it is more likely that the immediate cause of the cell demise lies elsewhere.

Return of thymine to a starved culture down-regulates SOS response (198) and allows resumption of DNA synthesis but without cell division (209). These observations, along with independence of TLD from SulA, prompted us to re-examine the nature of the division block caused by thymine starvation. We found that the starvation leads to a terminal cellular state which is characterized by entrapment of an under-replicated nucleoid between two FtsZ rings. The entrapment is caused by the failure of the rings to constrict. This phenotype is directly linked to the characteristic loss of colony counts in the course of TLD. Moreover, we found that a temperature sensitive *ftsZ* allele protects thymine starved cells from TLD at restrictive temperature.

Results and discussion

1. Observation of the nucleoid confinement in thymine starved cells

Early microscopy studies have established that bacterial cells starved for thymine underwent filamentation (210) and occasionally threw off anucleate cells (199, 211). The filamentation was interpreted to be the result of the DNA damage inducible, SulA-

mediated division block (204) and anucleate cells - the consequence of partial release of the block (199). However the frequency of anucleate cells reported even under the conditions where SulA was inactivated or un-inducible, and therefore unable to inhibit FtsZ and cause the division block (201), was always significantly less than 50% and the number of anucleate cells was always significantly smaller than the number of concomitantly observed filamentous cells (212, 199). Since anucleate cells most likely pinch off of the DNA free ends of filaments (213), the discrepancies in counts may imply that despite more than 90% prevalence of long filaments in a population of the thymine starved cells, only a subset of those filaments either contain DNA free ends or can pinch them off. The former would indicate a substantial degree of nucleoid unraveling in starved cells, which would have to be accounted for in assessing the TLD phenotype. The latter would point at a division block that either does not depend on SulA or supersedes it.

We used phase contrast and fluorescence light microscopy to follow changes in cell and nucleoid morphology accompanying thymine starvation. To bring out morphological features at the membrane – cell wall interface, the microscopy was carried out under mild plasmolysis conditions where cells were washed in 0.15 M NaCl solution and visualized in PBS. The assay revealed that cells started elongating within minutes after thymine withdrawal and by 2 h of starvation more than quadrupled in length, consistent with the expectation (197). Additionally, at 2 h starvation, 87% of all cells contained one plasmolysis bay between the nucleoid and the cell pole and 12% featured two bays, one on either side of the nucleoid (Fig. S4-1, Table 4-1). By the 3 h time point, the absolute majority of cells contained two bays. The spaces between the bay and the nearest cell

pole were devoid of DNA. After 5 h of starvation, the bays became less visible and within the next two hours disappeared altogether, leaving behind cells filled with amorphous protoplast (data not shown).

Table 4-1: Development of plasmolysis bays in thymine starved cells.

Time of starvation	Bay site configuration, % of cells [a]		
	0 bays	1 bay	2 bays
0 h	100	0	0
2 h	0	87.6	12.4
3 h	3.7	25.9	70.4

Cells were pre-cultured in thymine-containing media, and starved for 0, 2 and 3 hour for thymine. At given time points, bacteria was removed from the media and stained with DAPI. Percentage of plasmolysis bays was determined via microscopy, with a minimal sample size of 90 cells.

[a] – only DAPI positive cells, i.e., only those cells that contained DNA were included in the counts.

Because of the physical and geometric properties of the cytoplasmic membrane, the plasmolysis bay formation may be favored at the poles and constriction sites, i.e., future poles (214, 215). To determine if the plasmolysis bays were associated with the constriction sites in the thymine starved cells, we localized FtsZ rings, Z-rings from here on, in a thymine deficient strain carrying the IPTG inducible FtsZ-GFP protein fusion (216). The cultures were pre-induced with 0.5 mM IPTG 40 min prior to thymine withdrawal and samples were taken for microscopy right before the onset of starvation and at 30 min intervals thereafter. Cells growing exponentially with thymine in the

medium contained only one Z-ring in the middle along with 1-2 nucleoids per cell (Fig. 4-1A, left panel). By 2 h of starvation about 90% of the cells had at least 1 ring separating the nucleoid from a cell pole, with 45-60% containing 2 rings, and by 3 h, more than 80% had two rings segmenting the cell into 3 compartments in the following order: anucleate, nucleoid containing compartment and another anucleate compartment (Fig. 4-1A, right panel). We measured the distances between the rings as well as the rings and the poles, and found that the positions of the rings, expressed as absolute distance normalized to the length of the cell, coincided, within an error, with the positions of the mid-points of the plasmolysis bays (data not shown).

We tested the viability of cells that were subjected to microscopy by counting colonies on agar plates supplemented with thymine and observed that the decrease in CFU counts closely followed the increase in the frequency of cells with anucleate compartments on both sides of the nucleoid (Fig. 4-2).

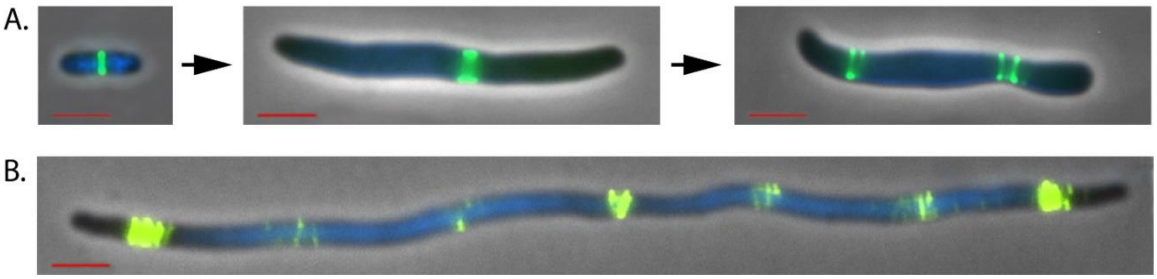

Figure 4-1: Z-ring deposition during unbalanced growth: DNA was visualized using DAPI, and Z-rings were visualized via *ftsZ*::GFP fusion. (**A**) *E. coli* during mid-exponential growth phase with a division ring deposited in-between two nucleoids. (**B**) Two hour of thymine starvation, a single ring is deposited, forming the first anucleated appendage. (**C**) By three hour starvation Z-ring are deposited at both poles, trapping the nucleus between two appendages. (**D**) At three hour starvation followed by one hour recovery, cells resume DNA synthesis, yet are unable to shed anucleate appendages to resume normal cell division.

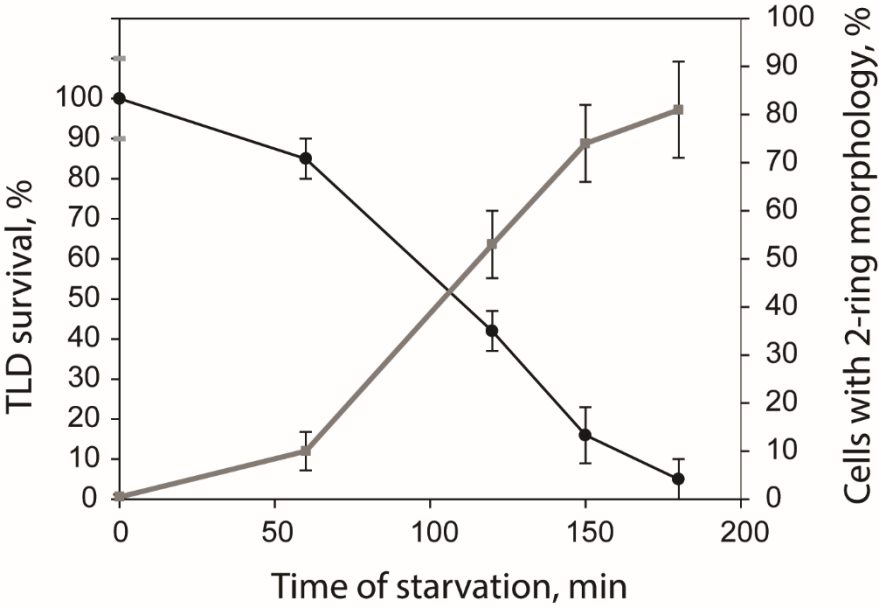

Figure 4-2: Inverse correlation between Z-ring deposition and survival during thymine starvation: Black circle (●) represents percentage of survivors, Grey square (▪) represents percentage of cells with Z-rings deposited at both poles. Number of survivors (CFU/ml) at 0, 60, 120, 150 and 180 minutes was determined by plating. Survival percentage was determined as a ratio of survivors/starting population. Error bars represent three standard deviations from the four independently performed starvations. The number of Z-rings at corresponding time points was determined in the manner described in materials and methods.

2. Reversibility of DNA damage in thymine starved cells

The results presented above suggest that by the time thymine starved cells lost their ability to form colonies, the un-replicated nucleoid was surrounded by two Z-rings that did not constrict. If arrested Z-rings on both side of the nucleoid is the irreversible event, then it could sufficiently explain the loss of viability on this stage of thymine starvation

because such cells won't divide even upon return to favorable conditions, i.e., restoration of thymine. Alternatively, the septation block is fully reversible but other injuries sustained by the cell during starvation, including DNA damage, are not. The starved cells maintained membrane integrity: their membranes retracted in response to osmotic pressure and they were refractory to propidium iodide (data not shown), which is commonly used to assess the viability of bacterial cells (217). They also remained metabolically competent, accumulating biomass for at least 1-1.5 doubling periods after CFU counts declined 120 times. However it was possible that thymine starvation caused irreparable DNA damage, as was proposed earlier (84, 218).

To directly test this hypothesis, we followed the replication origin- and terminus-proximal foci in strains carrying ParS/ParB-GFP constructs (219) during the course of thymine starvation and recovery. The ParB-GFP fusion protein was induced in *thyA*$^-$ strains carrying the *parS* locus near the origin of replication or near the terminus. The cells were induced with 0.05 mM IPTG for 1.5h before imaging. The *parS,thyA*$^-$ cells expressing ParB-GFP fusion were elongated even when thymine was present in the medium and increased in size only about 50% during 3 h of thymine starvation. However these cells lost their ability to form colonies at about the same rate as cells that did not carry the *parS* locus and did not express the fusion. At the beginning of starvation, the average number of origin-proximal foci was 2.91 ± 0.18 per cell and the average of terminus-proximal foci was 1.28 ± 0.07, with an oriC:ter ratio of 2.26 (Fig. 4-3 and Fig. 4-2S). By 3 h of starvation the characteristic loss of the origin-proximal region was evident: 1.31 ± 0.08 of origin-proximal and 0.94 ± 0.07 of terminus-proximal foci per cell, with an oriC:ter ratio of 1.39. Starvation phase was followed by a 2 h recovery in the

presence of thymine. The recovery resulted in an increase of the number of origin and terminus foci, 16.74 ± 1.04 and 7.98 ± 0.48 per cell, respectively, with an oriC:ter ratio of 2.10. To evaluate DNA dosage along the entire chromosome in a population of thymine recovering cells, we carried out microarray analysis of abundances of genomic sequences representing more than 98% of all *E. coli* ORF's in cells sampled 1 h after restoration of thymine. We found that the characteristic for thymine starved cells loss of DNA in about 600 kbp region of the chromosome surrounding the origin of replication has been nearly completely reversed (Fig. S4-3).

In an independent experiment, we induced FtsA-GFP fusion 1 h before thymine recovery (i.e., 2 h into starvation) and followed Z-rings in cells recovering from thymine starvation for up to 5 hours. During first 2 hours of recovery, we observed continued elongation of the cells, corresponding to about 3 doublings, and placement of Z-rings at near equal intervals along the elongated cell (Fig. 4-1B). All cells with visible Z-rings contained DAPI negative territories at the both poles demarcated by the most terminal rings. Additionally, not a single ParB-GFP focal point, origin- or terminus-specific, was observed in recovering cells within 10% of the cell length from the poles.

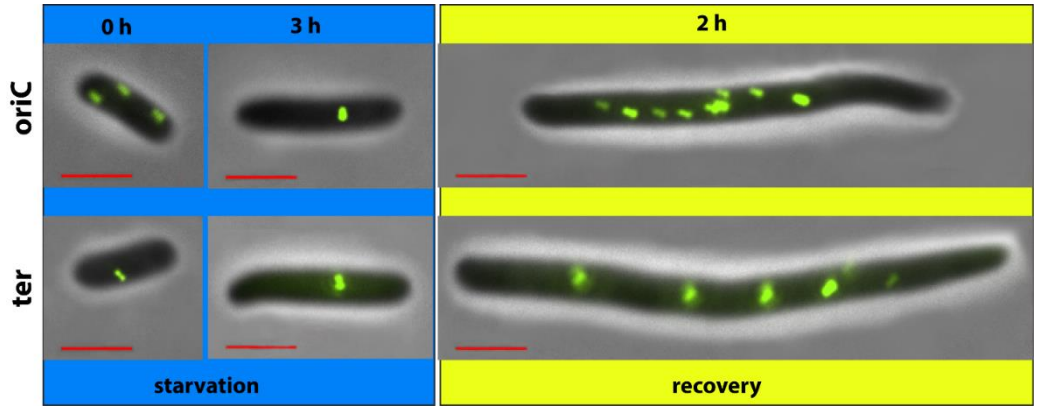

Figure 4-3: Changes in origin of replication and termini abundance during thymine starvation and recovery: Origins and termini were tagged using *parS*/ParB-GFP system. Prior to starvation exponentially gowning cells contain 2-3 origins per cell, and 1-2 termini. As starvation progresses to uncluturalble state number of origins drastically decreases, while number of termini does not change. Upon recovery the ratio of origins to termini are restored.

3. TLD kinetics and the deposition of Z-rings in TLD suppressing mutants

Thus thymine starved cells were arrested at the division stage and this arrest was associated with two morphological features: 1) confinement of the nucleoid between two unproductive Z-rings and 2) formation of anucleate compartments at the poles. One of the distinctive characteristics of TLD is its dependence on the initiation of chromosomal replication (220, 221). We reasoned that if the confinement is a true causative event, then inhibition of replication should alleviate it and thereby rescue cells from TLD.

We used a *dnaC*2 (222) derivative of the *thyA-ftsZ*::*gfp* strain to visualize the placement of Z-rings during the course of starvation. At permissive temperature of 30 °C, thymine withdrawal resulted in a typical, exponential decline in colony counts which was closely paralleled by the deposition of Z-rings on both sides of the nucleoid (Table 4-2). However, when starvation was carried out at restrictive temperature of 42 °C, the cells were significantly protected from TLD: about 90% formed colonies after 2 h starvation, 60% - after 3 h and 15% - after 5 h. We directly compared cell morphologies between 2 h starvation samples when both were expected to have live and "dead" cells in double digit percentages, which made the comparisons more robust. Cells that were starved at permissive temperature and whose viable counts declined by about 50% had deposited Z-rings on both sides of the nucleoid in 42% of the population. At the same time, 10% of

the cells starved at restrictive temperature lost ability to form colonies and 9.4% of cells starved at the restrictive temperature had their nucleoids surrounded by two rings. Thus inhibition of replication initiation significantly delayed the appearance of the two-ring morphology. The delay was even greater when starvation was imposed not concomitantly with the transition to restrictive temperature but after the initiation of replication was fully inhibited at restrictive temperature (data not shown). However interpretation of the latter observations was confounded by the dual ring morphology and viability loss in *dnaC*^{ts}, as was also observed in (223), that were independent of thymine starvation.

Another distinctive feature of TLD is its dependence on the activity of RecQ and RecF: a loss-of -function mutation in the corresponding genes significantly slows down the rates of killing of thymine starved cells (224, 225). We observed that thymine starved *recF*- and *recQ*- mutants started depositing Z-rings later than the parent and by 3 h starvation they had, respectively, 50% and 30% fewer cells with double Z-rings than the corresponding parental strain. Moreover, the extent of the origin-proximal DNA degradation directly correlated with the frequency of double-ringed cells (Fig. 4-4).**Table 4-2: Effect of dnaC(ts) on Z-ring deposition and TLD.**

Time of starvation	Starvation effects, %			
	30 °C		42 °C	
	TLD	dual Z-rings	TLD	dual Z-rings
0 h	0	0	0	0
2 h	54.2 ± 10.4	42.4 ± 15.1	9.1 ± 2.1	9.2 ± 4.2
3 h	87.5 ± 10.1	75.1 ± 14.2	40.3 ± 10.1	35.1 ± 7.3

The survival rate and formation of double anucleate appendages are shown under DNA replication permissive and inhibited conditions. The Z-ring formation was measured via microscopy using inducible *ftsZ*::GFP fusion. Survival rate was determined by plating 10 fold serial dilution. Data shown is the mean of three independent experiments and ± indicates a standard deviation.

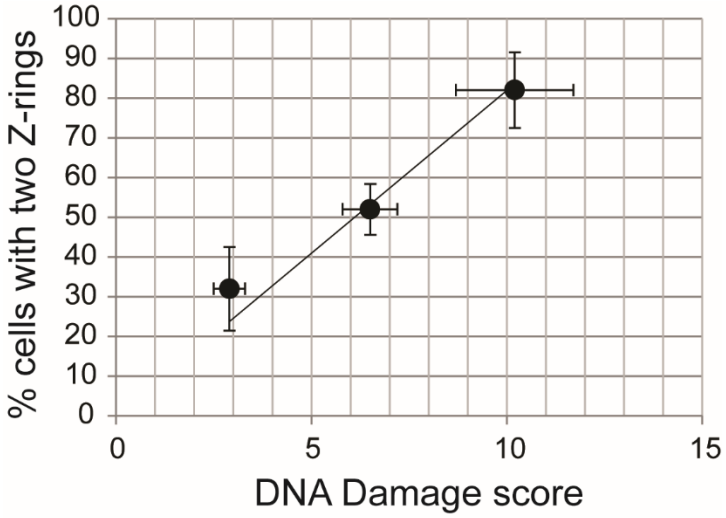

Figure 4-4: Positive correlation of DNA degradation and a double Z-ring formation: DNA degradation was measured using microarrays. Vertical error bars represent standard deviation from six independent samples. Z-ring accumulation was measured using microscopy. Horizontal error bars represent standard deviation of four or more samples that were used at each corresponding time point. Each sample consisted of at least 90 cells.

4. The effect of a temperature sensitive *ftsZ* allele on TLD

If the confinement of the nucleoid by unproductive Z-rings is the basis of the irreversible division arrest, then inhibition of the ring formation should prevent the arrest and protect cells from TLD. To test that, we constructed a temperature sensitive BW25113 *ftsZ*84^{ts} *thyA*- strain. The culture was maintained in MOPS medium supplemented with 0.2% glucose, 0.2% casamino acids and thymine at 25 µg/ml in early exponential phase (OD_{600} of 0.05 - 0.4) for 4-6 generations at 30 °C and then starved for thymine at 42 °C. After 2

h starvation cell biomass increased 50% (as measured by OD_{600} and dry weight, data not shown) and CFU counts declined by 93.9% (Fig. 4-5). At this point thymine was returned for one hour, while keeping the culture at 42 °C. It resulted in the 10.6-times increase of CFU counts from 6.1% to 64.9%. This increase of the viable counts could not be due to proliferation of survivors because the mutant does not divide at restrictive temperature. In fact, when thymine was available, the CFU counts of the Δ*thyAftsZ84*^{ts} mutant strain decreased 17.3% in 1 hour between 2 h and 3 h time points at restrictive temperature. This is in contrast with the thymine recovery of *thyA*$^{-}$*ftsZ* $^{+}$, where the CFU increase was entirely due to multiplication of survivors (data not shown). Therefore, since *thyA*$^{-}$*ftsZ84*^{ts} cells did not divide at restrictive temperature, the observed recovery was due to the extended capacity of the thymine starved *ftsZ* temperature sensitive mutant to form colonies. Thus, inhibition of Z-ring formation conferred very significant protection from TLD; 76.1% (64.9% - 6.1% + 17.3%) of the CFU variation could be explained by the FtsZ activity. Of note, if CFU counts in the thymine recovered samples are normalized directly to the viable counts at a corresponding time point that depended only on the *ftsZ84*^{ts}, the recovery would result in more than 90% survival (Fig. 4-5).

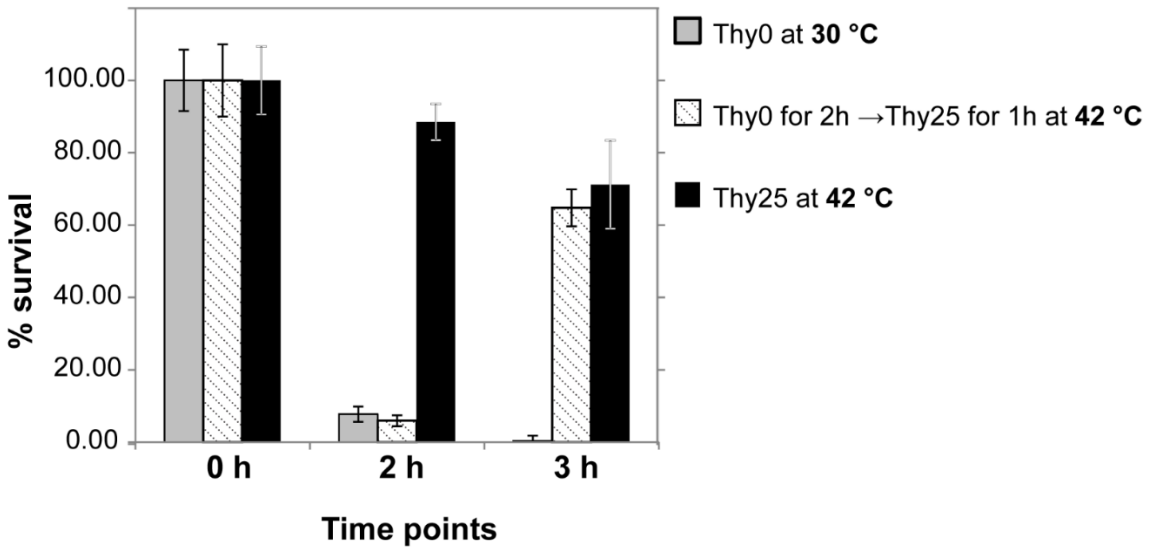

Figure 4-5: Inhibition of Z-ring formation during thymine starvation improves cell survival: (▫) At 30 °C cells were not inhibited for Z-ring formation throughout starvation and recovery. (▪) At 42 °C cells were inhibited for Z-ring formation throughout starvation and recovery. (⧈) Cells were not inhibited for Z-ring formation prior to and during the thymine starvation. Following a 2-hour starvation cells were inhibited for Z-ring formation by shifting temperature to 42 °C. The loss of viability associated with prolonged inhibition of Z-ring formation results in a 15% per hour or 5% per doubling time loss of viability. Error bars show a single standard deviation determined from at least three independent replicates. Bars represent mean percentage of survivors, as was determined by plating.

5. A model

In rapidly dividing *E. coli*, because of the fixed time required for chromosome synthesis and cytokinesis, the division site must be established during a preceding cell cycle, i.e., in a mother or even "grandmother" cell, with septation taking place promptly after replication is completed and daughter chromosomes are segregated (226, 227). The division site formation is initiated and controlled by the activity of FtsZ (36, 37) whose

levels are also likely set during the preceding cell cycle(s). We postulate that in thymine-starved cells, when FtsZ is active and available in sufficient amount, Z-rings will form at division sites but won't constrict, blocking the normal process of binary fission. The ring deposition is controlled only by the activity of FtsZ and availability of the sites. Cells entering thymine starvation have at least one septation site pre-formed and the Z-ring will deposit at that site as soon as the effect of SulA is alleviated. We hypothesize that another site is established as a result of the replication origin activation (230), which may serve as a positive cue for the division event (231, 232). However, the site likely stays sequestered until one of the sister chromatid DNA branches in the vicinity of the origin is degraded. Upon the degradation, the second Z-ring is deposited, effectively trapping the nucleoid for a period of time during which cells are fully viably but unculturable. It is possible that such site-specific constriction requires either the signal that the replication cycle has been completed or an input from fully segregated nucleoids on both sides of the nascent septum.

The model (Fig. 4-6) is based on the following observations that are organized in the chronological order of events that thymine starved cells go through: 1) cessation of replicative DNA synthesis (233); 2) SOS induction (210, 198); 3) activation of the replication at *oriC* or in its close proximity (230, 234); 4) beginning of visible (across a population) degradation of one of the chromatids on both sides of the replication origin (84, 207), appearance of cells with Z-rings

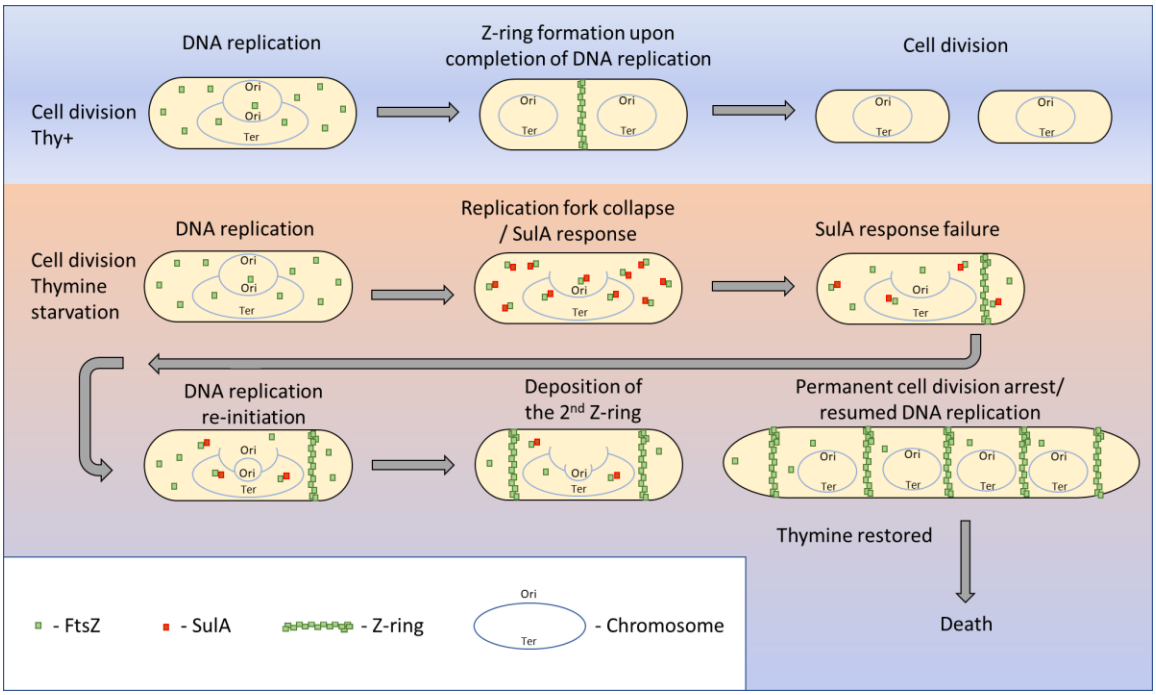

Figure 4-6: Model of thymine starvation-based killing: The top section depicts a normal, synchronized chromosomal replication and cells division. The bottom section depicts the loss of DNA at the origin in the early stages of thymine starvation, which triggers an SOS response which in turn results in a production of SulA. For a while (several doubling times) sulA is sufficient to keep Z-ring from depositing, however once it fails a single FtsZ ring is free to polymerize at the pole. The cycle of replication re-initiation failure will repeat one more time, eventually resulting in a deposition of the 2nd Z-ring. Once two Z-rings are deposited at both poles bacteria becomes locked inside its own membrane. While still alive, and capable of DNA replication upon return of thymine to the system, these cells are no longer capable of cell division. Eventually, inability to divide results in death.

on both sides of the nucleoid, and commencement of exponential decline in colony counts (current study); 5) complete degradation of one of the chromatids between the stalled forks and the maximum count of cells with two Z-rings surrounding the nucleoid (84, 208). We also observed that inhibition of Z-rings in thymine starved cells is only transient. Before starvation Z-rings could be observed in more than 99% of cells and within 40 minutes of the thymine withdrawal less 1% of cells contained Z-rings.

However Z-rings re-appeared within 80 min after that. Additionally, TLD occurs only in actively replicating cells. TLD depends on transcription insofar as transcription is required for initiation of DNA replication (221) and it does not depend on de novo protein synthesis (235). Formation of Z-rings outside of the nucleoid also does not require protein synthesis and inhibition of transcription by the antibiotic rifampicin, which is not bactericidal against *E. coli*, results in the ring deposition over the nucleoid (236).

TLD is an exponential process with a characteristic half-life which does not depend on the culture density. This implies that each cell loses ability to form the colony independent of other cells in a population. The half-life is determined by the nature of an underlying process leading to the loss of colony counts. The colony count of thymine starved cells halves every 18 ± 4 minutes. Notably, the length of the division phase of the bacterial cell cycle is of the same scale. Cell cycle of rapidly dividing bacteria consists of two main phases: *C* period, during which chromosomal DNA doubles in amount, and *D* period, during which the cell that has completed replication of the entire chromosome undergoes division by binary fission (226). As soon as chromosome replication is completed, the cell enters the *D* period, or the cytokinesis phase, during which the septum is formed and its constriction yields two daughter cells. The *D* period is 20 ± 2 minutes long in cells with doubling times between 24 and 60 min (226), similar to the rate of TLD in cells doubling faster than every 60 min. The observation that *D. radiodurans*, which is remarkably resistant to any external types of DNA damage, is as susceptible to TLD as *E. coli* (196) also supports, albeit rather circumstantially, the notion that TLD is mediated by an intrinsic process.

Some observations and interpretations presented herein are in qualitative agreement with findings reported in several other studies (82, 223, 237, 238). Gullbrand and Nordstrom demonstrated that unreplicated nucleoids in the inviable cells of a *dnaC*^{ts} mutant were occluded by Z-rings on both sides (223). Rudner and colleagues suggested that a one-sided replication roadblock in *Bacillus subtilis* results in the formation of nonfunctional Z-rings (238). Rosenberg (82), Levin (237) and their co-workers postulated the existence of a viable but unculturable state in bacterial cells with blocked DNA replication. Seemingly contradictory to the presented results, inhibition of DNA replication that followed synchronization of the initiation in a population of *E. coli* cells interfered with the Z-ring formation (239). However, the fact that the reported condition did not result in a loss of viability during the span of the experiment when the ring deposition was blocked bolsters our assertion that placement of unproductive Z-rings is an essential step toward cell demise.

Material and Methods

Bacterial strains, media and growth conditions

Escherichia coli strains (Table S4-1) were grown at 30 °C or 37 °C in Luria-Bertani (LB) medium; M9 rich, supplemented with 0.01% thiamine, glucose at 0.4% and either 0.2% or 1% CAA and 0.05% tryptophan and proline; MOPS (240) rich, supplemented with 0.4% glucose, 1% CAA, 0.05% tryptophan and proline. The cultures of *ftsZ*^{ts} mutants were starved in low salt LB (0.05-0.5% NaCl) and MOPS rich medium (0.1% NaCl). Frozen stocks (in 10% DMSO) were set up from over-night cultures grown in LB supplemented with the required antibiotic. Strains were propagated on LB or M9 agar (1.5%) plates. For each experiment, fresh colonies were streaked from the frozen stock

and 2-3 average size colonies were used for the sub-culture. Antibiotics were used in the following concentrations: kanamycin (Kan) – 50 μg/ml; ampicillin (Amp) – 100 μg/ml and Tetracycline (Tet) – 10 μg/ml and Chloramphenicol (Cm) - 12.5 μg/ml. For P1 transductions, cell lysates were obtained in liquid cultures grown in P1 broth (LB supplemented with 0.2% glucose and 5 mM CaCl). Isogenic MG1655 and BW25113 strains were constructed by generalized transduction using P1vir phage (241).

All mutations linked to critical phenotypes under the investigation have been verified by PCR and/or sequencings.

Thymine starvation assay

Strain cultures were streaked out on LB plates supplemented with thymine at a final concentration of 25 μg/ml. 2-3 average size colonies were cultured for 12-16 hours in M9 or MOPS rich media, supplemented with 1% CAA, 0.05%Trp, 0.4% glucose, 25 μg/ml thymine and appropriate antibiotics, at which point the cultures were diluted to a final OD_{600} of 0.05 and were maintained in the exponential phase of growth (OD_{600} between 0.1-0.3) for at least 6 generations by repeated dilution. The exponential, steady-state culture was washed 3 times (using centrifugation or filtration) in the same medium but without thymine and glucose, or in 0.85% NaCl. Following the wash, thymine starvation was established by resuspending cells to a final OD_{600} of 0.05-0.1 in the same medium as prior to starvation but without thymine. Starved cultures were aerated at the same rate as during the exponential growth before starvation, 250-275 rpm. The temperature of starvation was determined by a specific strain background and experimental design (see “Results” section for details). The colony formation of starved cultures was measured, following serial dilution, by plating on M9 or MOPS rich media

agar plates supplemented with 25 µg/ml thymine. Colonies were counted after 48 h incubation at 30 °C or 37 °C, depending on the strain.

Microarray analysis of DNA damage profiles

RNA-free, whole-genome DNA samples were obtained from thymine starved and thymine recovered cells using silica-gel based QiaAMP DNA mini kit (Qiagen). Extracted DNA was sonicated using Branson Digital Sonifier (30% power, 3 pulses of 10 s each, final size range 200–1000 bp). Purified and concentrated DNA was labelled using BioPrime Array Labeling Kit (Invitrogen, Carlsbad, CA) for hybridization on *E. coli* cDNA microarray as described earlier (242). The DNA damage score was calculated as described elsewhere (84).

Microscopy

Cultures of *thyA*- cells carrying the *ftsZ-gfp* construct were prepared for live microscopy as described in the thymine starvation section. The FtsZ-GFP protein fusion was induced with 0.5 mM of IPTG 40 minutes prior to visualization. Nucleoid staining was done by adding 5 µl of DAPI (10 mg/ml) to 990 µl of cell culture and incubating the mixture at room temperature in the dark for 5 min. Cells were then washed twice with M9 medium (lacking glucose and thymine). Following DAPI staining, cells were concentrated in 50-80 µl suspension; 8.5 µl of the suspension was placed onto 2% agarose pad, air dried for 20 sec and covered with a degreased coverslip.

For the simultaneous visualization of plasmolysis bays and nucleoids, cells were prepared and stained as described above. Following the 5 min staining, cells were washed twice and re-suspended in 80 µl of PBS (pH 7.4). 10 µl of the cell suspension was placed on the

poly-L-lysine (Sigma, > 98% purity) treated coverslip and air-dried for 10-15 min, sealed with nail polish and analyzed. To prepare poly-L-lysine coated coverslips, coverslips were washed twice in ddH_2O and 1M NaOH, followed by a 15 min long wash in 95% ethanol. Once dry, coverslips were layered over with 10 µl of 0.1% (v/v, in PBS) poly-L-lysine for 10 min, poly-L-lysine was then removed, and coverslips dried overnight.

Cells containing ParS/B localization system were starved as described above, except that the plasmid encoded ParB-GFP protein fusion was induced 1.5 hours prior to microscopy with 0.05 mM IPTG. Following induction, 1 ml of culture was concentrated to 50 µl, and 8.5 µl of cells suspension was directly deposited onto 2% agarose pad, air dried for 20 s and covered with a degreased coverslip.

Images were taken using Nikon e800 and i90 equipped with Nikon 100 x PlanFluor 1.3 N.A. Ph3 DLL 0.2 WD Oil Immersion objective, GFP and DAPI cube filters, Photometrics CoolSNAP Myo (CCD) monochromatic camera and Lumencor Sola Light Engine. Image quantification was done using Nikon Elements and Fiji software. The contrast and brightness of images were further adjusted using Adobe Photoshop Elements.

Supplementary Figures/ Tables

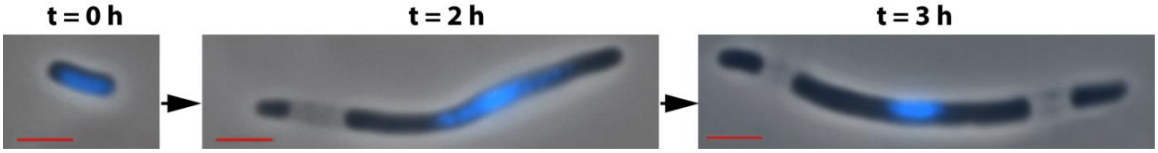

Supplementary figure S4-1: Plasmolysis bays in cells undergoing thymine starvation: Time of sampling is shown above each panel. DAPI stained nucleoids are in blue. Scale bar is 2 µm

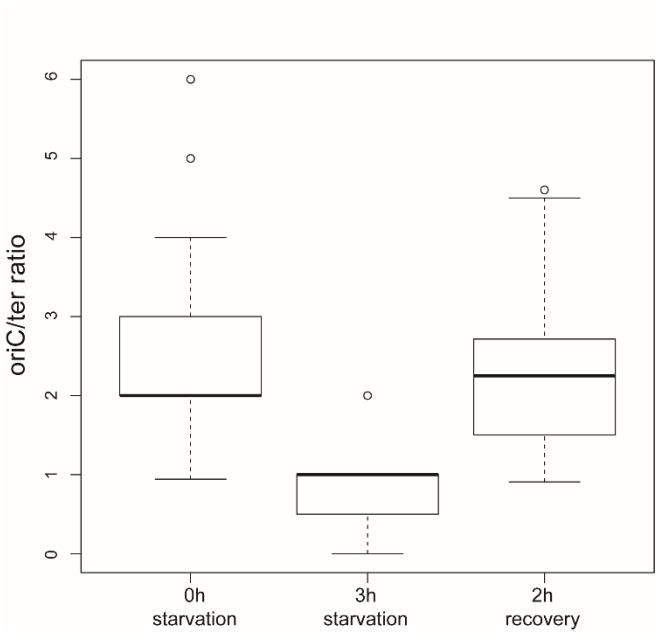

Supplementary figure S4-2: Boxplots of distributions of *oriC:ter* ratios in the samples of cells starved for thymine for indicated amounts of time: The ratios were obtained from the counts of ParB-GFP foci in cells carrying *parS* site near either *oriC* or *ter* locus.

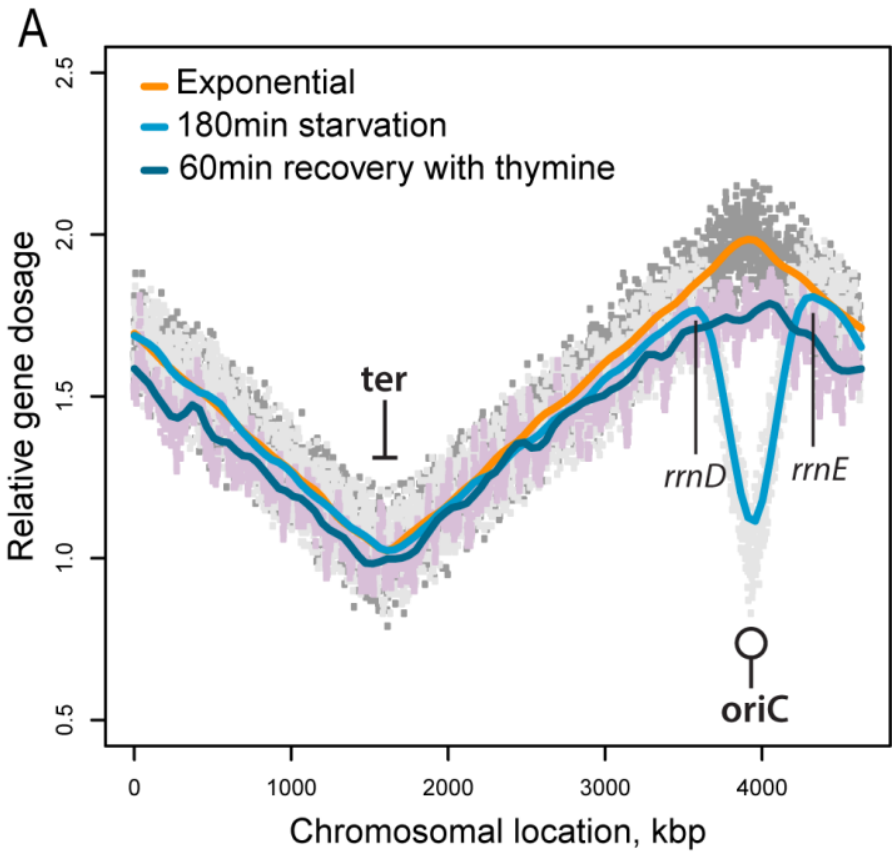

Supplementary figure S4-3: Reversibility of the origin-centric fragile site in the chromosome of thymine starved *E. coli*: Positions of the origin, terminus and ribosomal RNA clusters are shown. The exponential and starvation profiles were smoothed using 6 samples (3 biological x 2 technical replicates), the recovery profile was smoothed over 3 biological replicates.

Supplementary Table 4-1S: Strains used in the study.

Name	Background and genotype	Source; reference or derivation
BW25113	*rrnB3, ΔlacZ4787, hsdR514, Δ(araBAD)567, Δ(rhaBAD)568 , rph-1*	CGSC, Yale; (163)
CC4711	W3110 *pstA*::P1*parS (*kanR*)*	S. Lovett; (219)
CC4713	W3110 *gadB*::P1*parS (*kanR*)*	S. Lovett; (219)
DH5α (pALA2705)	GFP-Δ30ParB, *ampR*	S. Lovett; (219)
JW0941	BW25113 *ΔsulA::kan*	CGSC, Yale; (163)
JW5855-2	BW25113 *ΔrecQ::kan*	CGSC, Yale; (163)
JW3677	BW25113 *ΔrecF::kan*	CGSC, Yale; (163)
MCZ84	*leu-260::Tn10*, *ftsZ844*(ts)	CGSC, Yale; (203)
NR17642	BW25113*ΔthyA::kan*	R. Schaaper ; (243)
WM2026	MG1655 *lacY-*, *ftsZ-gfp*(ampR)	W. Margolin; (216)
PC1	*leuB6*(Am), λ^-, *thyA47*, *rpsL153*(strR), *dnaC1*(ts), *deoC3*	Laboratory stock; (222)
OK1	BW25113 *ΔthyA::kan*	Kan^R P1(NR17642) x BW25113
OK2	BW25113 *ΔthyA*	Kan^S OK1[a]
OK3	WM2026 *ΔthyA::kan*	Kan^R P1(OK1) x WM2026
OK4	WM2026 *ΔthyA*	Kan^S OK3[a]
OK5	PC1 *leuB6*(Am), λ^-, *thyA47*, *rpsL153*(strR), *dnaC1*(ts), *deoC3*, *ftsZ-GFP*(ampR)	Amp^R P1(WM2026) x PC1
OK6	WM2026 *ΔthyA, ΔrecF::kan, ftsZ-gfp*(ampR)	Kan^R P1(JW3677) x OK3
OK7	WM2026 *ΔthyA, ΔrecQ::kan, ftsZ-gfp*(ampR)	Kan^R P1(JW5855-2) x OK3
OK8	BW25113 *ΔthyA,*P1*parS*(kanR), pALA2705(ampR)	$Kan^R Amp^R$ P1(CC4711) x OK2 + pALA2705
OK9	BW25113 *ΔthyA*, P1*parS*(kanR), pALA2705(ampR)	$Kan^R Amp^R$ P1(CC4713) x OK2 + pALA2705
OK10	BW25113 *ΔthyA, leu-260::Tn10*, *thiE1*, *deo-73*	Tet^R P1(MCZ84) x OK2

a- strains were obtained by curing kanamycin resistance cassette between two FRT sites using pCP20 plasmid as described in (162).

Acknowledgements

We thank J. Courcelle, N.P. Higgins, A. Kuzminov, S. Lovett, J. Lutkenhaus , W. Margolin, R. Schaaper for strains, reagents, suggestions and clarifications, and Q. Ran for technical assistance with some experiments. Thu Tran was supported by an ASM undergraduate fellowship and by REU NSF/ MCB-1344188.

Chapter 5

Conclusion

Work presented in this thesis addressed an overall question of bacterial survival under stringent conditions. However, the investigations presented here were performed in a different order then described above. The first project I worked on was thymineless death, followed by the drug resistance and persistence projects in parallel. The discoveries made along the way helped to guide and inform following projects. I would like to finish this dissertation, not simply by summarizing the findings, but by offering some of my general thoughts on the topics discussed above and possible future directions.

In chapter four we were able to identify the likeliest cause of thymine starvation induced death. We determined that bacteria experience a permanent cell division block when starved for thymine. Just over mid-way through the thymine starvation (2h) SOS (DNA damage stress response) induced cell division inhibitor SulA likely begins to fail, and a single ring gets deposited at one pole. Within the following hour the second ring is deposited at the opposite pole, resulting in a formation of anucleate appendages at both ends of the cell. Once both sides of the cell become blocked, internal safeguards proteins MinC/MinD prevent cells from shedding said appendages, resulting in a permanent cell division block. A second major finding was that following the loss of DNA at the origin during thymine starvation, at least one chromosome remains fully intact and capable of replication. Moreover, proportional recovery of chromosomal origins and termini indicates that DNA damage induced during starvation is likely reversible. More questions, however, still need to be answered regarding these observations, such as what happens to the giant (division-blocked) cells, and what causes them to die? Also, and more importantly, is the recovered DNA following thymine starvation still viable in most cells? Since damage sites vary from cell to cell, bulk sequencing cannot be used, while a

single-cell approach would be way too costly. Hopefully in the near future, technology will be available to allow us to answer these questions.

While working on the thymineless death project, we wanted to know if it is possible to select for thymine starvation resistant mutants (data not included in the thesis). After nearly a dozen rounds of mutagenesis, starvation, and recovery, we selected a mutant that was 100-times more resistant to thymine starvation than its parent. After sequencing said mutant, amongst nearly one hundred mutations, one in particular stood out: a mutation in a toxin-antitoxin pair RelE/RelB. This particular toxin-antitoxin pair likely induces a persister state preemptively, before cells were subjected to DNA-damaging conditions. Since DNA replication does not take place in non-dividing cells, these cells become resistant to thymine starvation. This theory still needs to be tested; however, it will likely fall to the next generations of graduate students.

In chapter three, we explored a secondary effect that ciprofloxacin and rifampicin resistance mutations have on overall microbial survival. We showed that such mutations cause a population-wide transcriptional re-programming by mimicking ppGpp stress response in a ppGpp-independent manner. We have also demonstrated that transcriptional change disrupts the normal order of amino acid consumption by the cells. Premature consumption of certain amino acids creates byproducs that in turn help to induce a persister state. In the case of *E. coli*, indole (a byproduct of tryptophan consumption) explains 50-80% of the high persistence phenotype in hip RpoB mutants. With nearly 700 genes getting differentially expressed as a result of RpoB mutations, it is likely that a number of other pathways are also contributing to the overall persistence phenotype, such as genes belonging to the *LeuO, ppGpp* and *rpoS* regulons (Fig. 5-1).

Persistence scheme

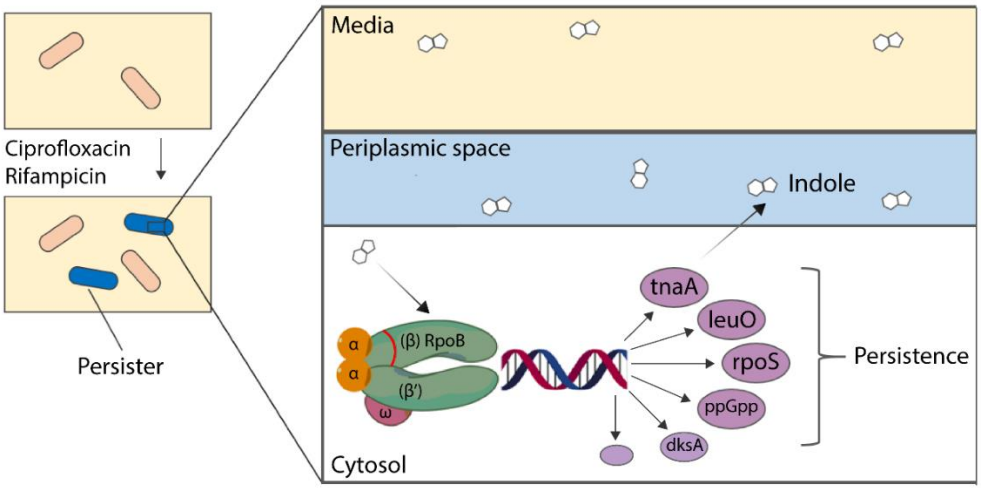

Figure 5-1: Proposed model of RpoB-based persistence: RpoB mutations that confer resistance to rifampicin and ciprofloxacin cause a significant increase in the number of persisters. Part of the mechanism can be explained by overproduction of TnaA, which catalyzes L-tryptophan into indole. Accumulation of indole then drives cells towards the persister state. At the same time other major regulons associated with starvation become active in RpoB mutants such as *rpoS, leuO, ppGpp* and others. Activation of each one of these regulons is likely contributing to the overall persistence observed. This is evidenced by the fact that knocking out *tnaC* does not completely eliminate persistence in RpoB mutants.

Despite the mechanistic complexity of the persistence phenomenon, the plain fact is that RpoB, ciprofloxacin and rifampicin resistance mutations unequivocally improved the rate of persister formation by 1000-10,000. Thus, the next logical question is: how can this

newly identified problem be addressed? Since these antibiotics cannot be taken off the market, alternative solutions are needed. One possible approach is to force persister cells back into the growth phase by interfering with the persister state. Indeed, according to our preliminary data, sub-inhibitory concentrations of ribosome inhibitors seem to reactivate persister cells, making them susceptible to antibiotics. It is my suspicion that minor inhibition of ribosomes compensates for the transcriptional changes imposed by RpoB mutations.

Assuming that the expression of genes contributing to induction of a persister state has to reach a certain threshold to induce the phase switch, compromising the ability of a cell to reach this threshold, even by a small fraction, will have a drastic effect on the persistence phenotype (Fig. 5-2). In other words, addition of ribosome inhibitor will result in two outcomes; i. fast growing cells will grow a bit slower, and ii. cells destined to become persisters will not go through phase change and will stay as slow growing cells. Hence, the culture will become normalized, consisting of slower exponentially growing cell that are uniformly susceptible to the drug treatment (Fig. 5-2).

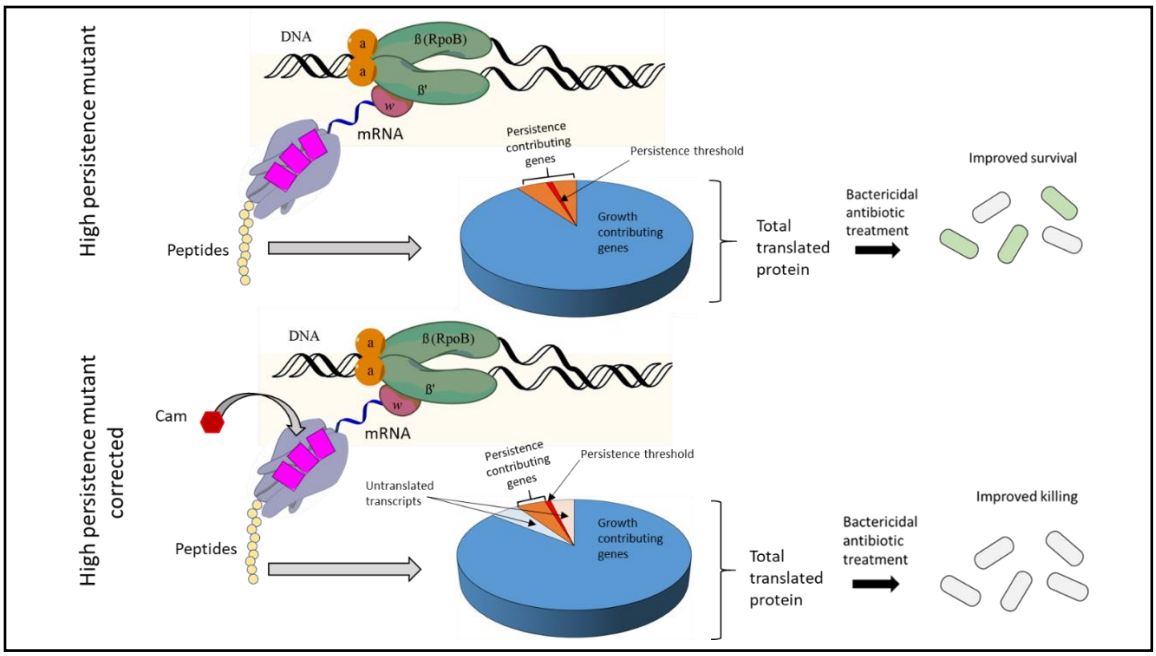

Figure 5-2: Proposed mechanism of RpoB mutation-based persistence correction via ribosomal inhibitors: The top section represents overall transcription taking place in RpoB high persistence mutants. The blue section are the genes being transcribed that are cell requires for growth and proliferation, while orange are the genes that are not contributing to growth and may be contributing to persister formation. The red line indicates the minimum threshold that transcripts not contributing to growth need to reach to induce persister state. The bottom section shows how proportional elimination of transcripts from growth and persister groups results in the inability of a cell to reach the needed threshold to induce persistence. The transcriptional threshold to induce persister state is high, as indicated by the infrequency of persistence phenomenon. Hence, proportional inhibition of translation will have a greater effect on persister formation than growth, placing cells back into growth state and improving killing.

Chapter two highlights two important points. First is the large gap between clinical reality and laboratory observations. Under laboratory conditions, it is possible to select for mutations outside the drug target that are going to confer antibiotic resistance (47). However, as we had determined (at least with quinolones) in the clinical setting, antibiotic resistance tends to take a predetermined path, the path that offers the highest

resistance in the least amount of mutations. To identify the mutational path taken by different microbial pathogens in order to gain quinolone resistance, we examined thousands of genomes from clinical isolates. We analyzed the data using chi-square and conditional probability measurements to determine dependence and the order of the mutations. According to our findings, in most cases a handful (1-3) of mutations is sufficient to determine whether clinical levels of resistance have been or are going to be reached.

The second point highlighted is the underutilization of large genome databases. Not only were we able to establish mutational patterns that can be used to predict the development of quinolone resistances in nearly 20 species, but we were also able to make some unexpected discoveries along the way. For instance, using our data set we were able to identify rampant improper use of quinolones to treat *Vibrio cholera* in India and South-East Asia. Thus, not only can this information be implemented by healthcare providers but also by public health officials to curb the improper use of antimicrobials in specific communities and to limit the spread of antibiotic resistance.

In conclusion, we have made several key findings dealing with antibiotic resistance, chronic infections, as well as discovering a potentially new mode of killing bacteria. By addressing clinically relevant topics, we did our best to ground our research in reality. As with most research, at the end of the day we have more questions than when we started. Yet, it is my hope that these studies can inform future researchers on how to better predict and prevent the emergence of new antibiotic-resistant strains and ways to treat highly persistent infection.

Citations:

1. Fleming, A. On the Antibacterial Action of Cultures of a *Penicillium*, with Special Reference to their Use in the Isolation of B. influenza. *Br J Exp Pathol.* **10**, 226–236 (1929).

2. Ventola, C. L. The antibiotic resistance crisis: causes and threats. *Pharmacy and Therapeutics*. **40**, 277–83 (2015).

3. The Center for Disease, Dynamics Economics & Policy. ResistanceMap: Antibiotic resistance. (2020). Available at: https://resistancemap.cddep.org/AntibioticResistance.php.

4. de Kraker, M. E. A., Stewardson, A. J. & Harbarth, S. Will 10 Million People Die a Year due to Antimicrobial Resistance by 2050? *PLoS Med.* **13**, (2016).

5. Pankey, G. A. & Sabath, L. D. Clinical Relevance of Bacteriostatic versus Bactericidal Mechanisms of Action in the Treatment of Gram-Positive Bacterial Infections. *Clin. Infect. Dis.* **38**, 864–870 (2004).

6. Tuomanen, E., Cozens, R., Tosch, W., Zak, O. & Tomasz, A. The rate of killing of Escherichia coli by β-lactam antibiotics is strictly proportional to the rate of bacterial growth. *J. Gen. Microbiol.* **132**, 1297–1304 (1986).

7. Regoes, R. R., Wiuff, C., Zappala, R. M., Garner, K. N., Baquero, F., & Levin, B. R. Pharmacodynamic functions: A multiparameter approach to the design of antibiotic treatment regimens. *Antimicrob. Agents Chemother* **48**, 3670–3676 (2004).

8. Horn, D. L., Zabriskie, J. B., Austrian, R. & Cleary, P. P. Why Have Group A Streptococci Remained Susceptible to Penicillin? Report on a Symposium. *Clin. Infect. Dis*. **26**, 1341–1345 (1998).

9. Gutmann, L. & Tomasz, A. Penicillin-resistant and penicillin-tolerant mutants of group A Streptococci. *Antimicrob. Agents Chemother.* **22**, 128–36 (1982).

10. De Muri, G. P., Sterkel, A. K., Kubica, P. A. & Duster, M. N. *et al.* Macrolide and clindamycin resistance in group a streptococci isolated from children with pharyngitis. *Pediatr. Infect. Dis. J.* **36**, 342–344 (2017).

11. Cohen, S. P., McMurry, L. M. & Levy, S. B. *marA* locus causes decreased expression of OmpF porin in multiple-antibiotic-resistant (Mar) mutants of *Escherichia coli*. *J. Bacteriol.* **170**, 5416–5422 (1988).

12. Pagès, J. M., James, C. E. & Winterhalter, M. The porin and the permeating antibiotic: A selective diffusion barrier in Gram-negative bacteria. *Nat. Rev. Microbiol.* **6**, 893–903 (2008).

13. Nau, R. & Eiffert, H. Modulation of release of proinflammatory bacterial compounds by antibacterials: Potential impact on course of inflammation and outcome in sepsis and meningitis. *Clin. Microbiol. Rev.* **15**, 95–110 (2002).

14. Blaser, M. Antibiotic overuse: Stop the killing of beneficial bacteria. *Nature* **476**, 393–394 (2011).

15. Brown, K. A., Khanafer, N., Daneman, N. & Fisman, D. N. Meta-analysis of antibiotics and the risk of community-associated *Clostridium difficile* infection. *Antimicrob. Agents Chemother.* **57**, 2326–2332 (2013).

16. Smits, W. K., Lyras, D., Lacy, D. B., Wilcox, M. H. & Kuijper, E. J. *Clostridium difficile* infection. *Nat. Rev. Dis. Prim.* **2**, 1–20 (2016).

17. CDC. Nearly half a million Americans suffered from Clostridium difficile infections in a single year. (2015). https://www.cdc.gov/media/releases/2015/p0225-clostridium-difficile.html

18. Kohanski, M. A., Dwyer, D. J. & Collins, J. J. How antibiotics kill bacteria: From targets to networks. *Nat. Rev. Microbiol.* **8**, 423–435 (2010).

19. Quinlivan, E. P., McPartlin, J., Weir, D. G. & Scott, J. Mechanism of the antimicrobial drug trimethoprim revisited. *FASEB J.* **14**, 2519–2524 (2000).

20. Pérez-Cobas, A. E., Artacho, A., Knecht, H., Ferrús, M. L. *et al.* Differential effects of antibiotic therapy on the structure and function of human gut microbiota. *PLoS One* **8**, (2013).

21. Yoshida, M., Takada, T., Kawarada, Y. & Tanaka, A.*et al.* Antimicrobial therapy for acute cholecystitis: Tokyo Guidelines. *J. Hepatobiliary. Pancreat. Surg.* **14**, 83–90 (2007).

22. Lobritz, M. A., Belenky, P., Porter, C. B. M., Gutierrez, A. *et al.* Antibiotic efficacy is linked to bacterial cellular respiration. *Proc. Natl. Acad. Sci. U. S. A.* **112**, 8173–8180 (2015).

23. Schauf, V., Green, D. C., van der Stuyf, L. & Riff, L. Chloramphenicol kills Haemophilus influenzae more rapidly than does ampicillin or cefamandole. *Antimicrob. Agents Chemother.* **23**, 364–8 (1983).

24. Feldman, W. E. & Zweighaft, T. Effect of ampicillin and chloramphenicol against *Streptococcus pneumoniae* and *Neisseria meningitidis*. *Antimicrob. Agents Chemother.* **15**, 240–242 (1979).

25. Langdon, A., Crook, N. & Dantas, G. The effects of antibiotics on the microbiome throughout development and alternative approaches for therapeutic modulation. *Genome Medicine* **8**, (2016).

26. Jakobsson, H. E., Jernberg, C., Andersson, A. F., Sjölund-Karlsson, M. *et al.* Short-term antibiotic treatment has differing long- term impacts on the human throat and gut microbiome. *PLoS One* **5**, (2010).

27. Baker, S. J., Payne, D. J., Rappuoli, R. & De Gregorio, E. Technologies to address antimicrobial resistance. *Proc. Natl. Acad. Sci. U.S.A.* **115**, 12887–12895 (2018).

28. Ratcliff, W. C. & Denison, R. F. Microbiology. Alternative actions for antibiotics. *Science.* **332**, 547–548 (2011).

29. Barka, E. A., Vatsa, P., Sanchez, L., Gaveau-Vaillant, N. *et al.* Taxonomy, Physiology, and Natural Products of Actinobacteria. *Microbiol. Mol. Biol. Rev.* **80**, 1–43 (2016).

30. Alexander, D. C. & Jensen, S. E. Investigation of the *Streptomyces clavuligerus* cephamycin C gene cluster and its regulation by the CcaR protein. *J. Bacteriol.* **180**, 4068–4079 (1998).

31. Chow, J. W. & Yu, V. L. Combination antibiotic therapy versus monotherapy for gram-negative bacteraemia: a commentary. *Int. J. Antimicrob. Agents* **11**, 7–12 (1999).

32. Ahmed, A., Azim, A., Gurjar, M. & Baronia, A. K. Current concepts in combination antibiotic therapy for critically ill patients. *Indian J. Crit. Care Med.* **18**, 310–314 (2014).

33. Forrest, G. N. & Tamura, K. Rifampin combination therapy for nonmycobacterial infections. *Clin. Microbiol. Rev.* **23**, 14–34 (2010).

34. WHO. WHO treatment guidelines for isoniazid-resistant tuberculosis. (2018). https://apps.who.int/iris/bitstream/handle/10665/260494/9789241550079-eng.pdf

35. Chamberlin, J., Story, S., Ranjan, N., Chesser, G. & Arya, D. P. Gram-negative synergy and mechanism of action of alkynyl bisbenzimidazoles. *Sci. Rep*. **9**, (2019).

36. Dcosta, V. M., King, C. E., Kalan, L., Morar, M. *et al.* Antibiotic resistance is ancient. *Nature* **477**, 457–461 (2011).

37. Modi, S. R., Collins, J. J. & Relman, D. A. Antibiotics and the gut microbiota. *J. Clin. Invest.* **124**, 4212–4218 (2014).

38. Blair, J. M. A., Webber, M. A., Baylay, A. J., Ogbolu, D. O. & Piddock, L. J. V. Molecular mechanisms of antibiotic resistance. *Nat. Rev. Microbiol.* **13**, 42–51 (2015).

39. Macheboeuf, P., Contreras-Martel, C., Job, V., Dideberg, O. & Dessen, A. Penicillin binding proteins: Key players in bacterial cell cycle and drug resistance processes. *FEMS Microbiol. Lett.* **30**, 673–691 (2006).

40. Campbell, E. A., Korzheva, N., Mustaev, A., Murakami, K. *et al.* Structural mechanism for rifampicin inhibition of bacterial RNA polymerase. *Cell* **104**, 901–912 (2001).

41. Hooper, D. C. & Jacoby, G. A. Topoisomerase inhibitors: Fluoroquinolone mechanisms of action and resistance. *Cold Spring Harb. Perspect. Med.* **6**, (2016).

42. Wang, J.C. DNA Topoisomerases. *Annu. Rev. Biochem.* **65**, 635-692 (1996).

43. Snyder, M. & Drlica, K. DNA gyrase on the bacterial chromosome: DNA cleavage induced by oxolinic acid. *J. Mol. Biol.* **131**, 287–302 (1979).

44. Hiasa, H., Yousef, D. O. & Marians, K. J. DNA strand cleavage is required for replication fork arrest by a frozen topoisomerase-quinolone-DNA ternary complex. *J. Biol. Chem.* **271**, 26424–26429 (1996).

45. Khodursky, A. B., Zechiedrich, E. L. & Cozzarelli, N. R. Topoisomerase IV is a target of quinolones in *Escherichia coli*. *Proc. Natl. Acad. Sci. U. S. A.* **92**, 11801–11805 (1995).

46. Zhang, Q., Lambert, G., Liao, D., Kim, H. *et al.* Acceleration of emergence of bacterial antibiotic resistance in connected microenvironments. *Science.* **333**, 1764–1767 (2011).

47. Baym, M., Lieberman, T. D., Kelsic, E. D., Chait, R. *et al.* Spatiotemporal microbial evolution on antibiotic landscapes. *Science.* **353**, 1147–1151 (2016).

48. Blanco, P., Hernando-Amado, S., Reales-Calderon, J., Corona, F. *et al.* Bacterial Multidrug Efflux Pumps: Much More Than Antibiotic Resistance Determinants. *Microorganisms* **4**, 14 (2016).

49. Venter, H., Mowla, R., Ohene-Agyei, T. & Ma, S. RND-type drug efflux pumps from Gram-negative bacteria: Molecular mechanism and inhibition. *Front Microbiol* **6**, 377-385 (2015).

50. Elkins, C. A. & Nikaido, H. Substrate specificity of the RND-type multidrug efflux pumps AcrB and AcrD of Escherichia coli is determined predominantly by two large periplasmic loops. *J. Bacteriol.* **184**, 6490–8 (2002).

51. Alvarez-Ortega, C., Olivares, J. & Martínez, J. L. RND multidrug efflux pumps: What are they good for? *Front Microbiol* **4**, (2013) doi: 10.3389/fmicb.2013.00007.

52. Kuroda, T. & Tsuchiya, T. Multidrug efflux transporters in the MATE family. *Biochim. Biophys. Acta* **1794**, 763–768 (2009).

53. Lange, R. & Hengge-Aronis, R. The cellular concentration of the σ(S) subunit of RNA polymerase in Escherichia coli is controlled at the levels of transcription, translation, and protein stability. *Genes Dev.* **8**, 1600–1612 (1994).

54. Erickson, J. W., Vaughn, V., Walter, W. A., Neidhardt, F. C. & Gross, C. A. Regulation of the promoters and transcripts of *rpoH*, the *Escherichia coli* heat shock regulatory gene. *Genes Dev.* **1**, 419–432 (1987).

55. Morita, Y., Kodama, K., Shiota, S., Mine, T. *et al.* NorM, putative multidrug efflux protein, of Vibrio parahaemolyticus and its homolog in *Escherichia coli*. *Antimicrob. Agents Chemother.* **42**, 1778–1782 (1998).

56. Balaban, N. Q., Helaine, S., Lewis, K., Ackermann, M. *et al.* Definitions and guidelines for research on antibiotic persistence. *Nat. Rev. Microbiol.* **17**, 441–448 (2019).

57. Brauner, A., Fridman, O., Gefen, O. & Balaban, N. Q. Distinguishing between resistance, tolerance and persistence to antibiotic treatment. *Nat. Rev. Microbiol.* **14**, 320–330 (2016).

58. Cohen, N. R., Lobritz, M. A. & Collins, J. J. Microbial persistence and the road to drug resistance. *Cell Host Microbe* **13**, 632–642 (2013).

59. Windels, E. M. Windels, E. M., Michiels, J. E., Fauvart, M., Wenseleers, T. *et al.* Bacterial persistence promotes the evolution of antibiotic resistance by increasing survival and mutation rates. *ISME J.* **13**, 1239–1251 (2019).

60. Bigger, J. W. TREATMENT OF STAPHYLOCOCCAL INFECTIONS WITH PENICILLIN BY INTERMITTENT STERILISATION. *Lancet* **244**, 497–500 (1944).

61. Radzikowski, J. L., Vedelaar, S., Siegel, D., Ortega, Á. D. *et al*. Bacterial persistence is an active σ S stress response to metabolic flux limitation. *Mol. Syst. Biol.* **12**, 882 (2016).

62. Kwan, B. W., Valenta, J. A., Benedik, M. J. & Wood, T. K. Arrested protein synthesis increases persister-like cell formation. *Antimicrob. Agents Chemother.* **57**, 1468–1473 (2013).

63. Zeiler, H. J. Evaluation of the in vitro bactericidal action of ciprofloxacin on cells of Escherichia coli in the logarithmic and stationary phases of growth. *Antimicrob. Agents Chemother.* **28**, 524–527 (1985).

64. Shah, D. Shah, D., Zhang, Z., Khodursky, A., Kaldalu, N. *et al.* Persisters: A distinct physiological state of E. coli. *BMC Microbiol.* **6**, (2006) doi: 10.1186/1471-2180-6-53.

65. Kaldalu, N. & Tenson, T. Slow growth causes bacterial persistence. *Sci. Signal.* **12**, (2019) doi: 10.1126/scisignal.aay1167.

66. Wu, N., He, L., Cui, P., Wang, W. *et al.* Ranking of persister genes in the same *Escherichia coli* genetic background demonstrates varying importance of individual persister genes in tolerance to different antibiotics. *Front. Microbiol.* **6**, (2015). doi: 10.3389/fmicb.2015.01003

67. Kussell, E., Kishony, R., Balaban, N. Q. & Leibler, S. Bacterial persistence: A model of survival in changing environments. *Genetics* **169**, 1807–1814 (2005).

68. Dörr, T., Vulić, M. & Lewis, K. Ciprofloxacin causes persister formation by inducing the TisB toxin in *Escherichia coli*. *PLoS Biol.* **8**, (2010).

69. Yamaguchi, Y. & Inouye, M. Regulation of growth and death in *Escherichia coli* by toxin-antitoxin systems. *Nature Reviews Microbiology* **9**, 779–790 (2011).

70. Amato, S. M., Orman, M. A. & Brynildsen, M. P. Metabolic Control of Persister Formation in *Escherichia coli*. *Mol. Cell* **50**, 475–487 (2013).

71. Korch, S. B., Henderson, T. A. & Hill, T. M. Characterization of the hipA7 allele of Escherichia coli and evidence that high persistence is governed by (p)ppGpp synthesis. *Mol. Microbiol.* **50**, 1199–1213 (2003).

72. Murray, K. D. & Bremer, H. Control of spoT-dependent ppGpp synthesis and degradation in *Escherichia coli*. *J. Mol. Biol.* 259, 41–57 (1996).

73. Hansen, M. T., Pato, M. L., Molin, S., Fill, N. P. & von Meyenburg, K. Simple downshift and resulting lack of correlation between ppGpp pool size and ribonucleic acid accumulation. *J. Bacteriol.* **122**, 585–591 (1975).

74. Gentry, D. R., Hernandez, V. J., Nguyen, L. H., Jensen, D. B. & Cashel, M. Synthesis of the stationary-phase sigma factor σ(s) is positively regulated by ppGpp. *J. Bacteriol.* **175**, 7982–7989 (1993).

75. Moyed, H. S. & Bertrand, K. P. hipA, a newly recognized gene of *Escherichia coli* K-12 that affects frequency of persistence after inhibition of murein synthesis. *J. Bacteriol.* **155**, 768–775 (1983).

76. Girgis, H. S., Harris, K. & Tavazoie, S. Large mutational target size for rapid emergence of bacterial persistence. *Proc. Natl. Acad. Sci. U. S. A.* **109**, 12740–12745 (2012).

77. Schumacher, M. A., Balani, P., Min, J., Chinnam, N. B. *et al.* HipBA-promoter structures reveal the basis of heritable multidrug tolerance. *Nature* **524**, 59–66 (2015).

78. LaFleur, M. D., Qi, Q. & Lewis, K. Patients with long-term oral carriage harbor high-persister mutants of *Candida albicans*. *Antimicrob. Agents Chemother.* **54**, 39–44 (2010).

79. Novak, R., Henriques, B., Charpentier, E., Normark, S. & Tuomanen, E. Emergence of vancomycin tolerance in *Streptococcus pneumoniae*. *Nature* **399**, 590–593 (1999).

80. Spanu, T., Romano, L., D'Inzeo, T. & Masucci, L. Recurrent Ventriculoperitoneal Shunt Infection Caused by Small-Colony Variants of *Staphylococcus aureus*. *Clin. Infect. Dis.* **41**, e48–e52 (2005).

81. Cohen, S. S. & Barner, H. D. STUDIES ON UNBALANCED GROWTH IN ESCHERICHIA COLI. *Proc. Natl. Acad. Sci. U.S.A.* **40**, 885–893 (1954).

82. Fonville, N. C., Bates, D., Hastings, P. J., Hanawalt, P. C. & Rosenberg, S. M. Role of RecA and the SOS response in thymineless death in *Escherichia coli*. *PLoS Genet.* **6**, (2010).

83. Longley, D. B., Harkin, D. P. & Johnston, P. G. 5-Fluorouracil: Mechanisms of action and clinical strategies. *Nat. Rev. Cancer* **3**, 330–338 (2003).

84. Sangurdekar, D. P., Hamann, B. L., Smirnov, D., Srienc, F. *et al.* Thymineless death is associated with loss of essential genetic information from the replication origin. *Mol. Microbiol.* **75**, 1455–1467 (2010).

85. Hong, Y., Li, L., Luan, G., Drlica, K. & Zhao, X. Contribution of reactive oxygen species to thymineless death in *Escherichia coli*. *Nat. Microbiol.* **2**, 1667–1675 (2017).

86. Owusu-Ofori, A. & Scheld, W. M. Treatment of *Salmonella meningitis*: Two case reports and a review of the literature. *Int. J. Infect. Dis.* **7**, 53–60 (2003).

87. Davis, A., Meintjes, G. & Wilkinson, R. J. Treatment of Tuberculous Meningitis and Its Complications in Adults. *Curr Treat Options Neurol* **20**, (2018) doi: 10.1007/s11940-018-0490-9.

88. Yamamoto, S., Higuchi, Y. & Nojima, M. Current therapy of acute uncomplicated cystitis. *Int. J. Urol.* **17**, 450–456 (2010).

89. Hiasa, H. DNA topoisomerases as targets for antibacterial agents. in *Methods in Molecular Biology* **1703**, 47–62 (Humana Press Inc., 2018).

90. Pommier, Y. Drugging topoisomerases: Lessons and Challenges. *ACS Chemical Biology* **8**, 82–95 (2013).

91. Collin, F., Karkare, S. & Maxwell, A. Exploiting bacterial DNA gyrase as a drug target: Current state and perspectives. *Appl. Microbiol. Biotechnol.* **92**, 479–497 (2011).

92. Chen, S. H., Chan, N.-L. & Hsieh, T. New Mechanistic and Functional Insights into DNA Topoisomerases. *Annu. Rev. Biochem.* **82**, 139–170 (2013).

93. Nitiss, J. L. DNA topoisomerase II and its growing repertoire of biological functions. *Nat. Rev. Cancer* **9**, 327–337 (2009).

94. Corbett, K. D. & Berger, J. M. Structure, molecular mechanisms, and evolutionary relationships in DNA topoisomerases. *Annu. Rev. Biophys.* **33**, 95–118 (2004).

95. Aldred, K. J., Kerns, R. J. & Osheroff, N. Mechanism of quinolone action and resistance. *Biochemistry* **53**, 1565–1574 (2014).

96. Yoshida, H., Bogaki, M., Nakamura, M. & Nakamura, S. Quinolone resistance-determining region in the DNA gyrase *gyrA* gene of *Escherichia coli*. *Antimicrob. Agents Chemother.* **34**, 1271–1272 (1990).

97. Hooper, D. C. & Jacoby, G. A. Mechanisms of drug resistance: Quinolone resistance. *Ann. N. Y. Acad. Sci.* **1354**, 12–31 (2015).

98. Wohlkonig, A., Chan, P. F., Fosberry, A. P., Homes, P. *et al.* Structural basis of quinolone inhibition of type IIA topoisomerases and target-mediated resistance. *Nat. Struct. Mol. Biol.* **17**, 1152–1153 (2010).

99. Blower, T. R., Williamson, B. H., Kerns, R. J. & Berger, J. M. Crystal structure and stability of gyrase-fluoroquinolone cleaved complexes from *Mycobacterium tuberculosis*. *Proc. Natl. Acad. Sci. U. S. A.* **113**, 1706–1713 (2016).

100. Laponogov, I., Pan, X. S., Veselkov, D. A., Mcauley, K. E. *et al.* Structural basis of gate-DNA breakage and resealing by type II topoisomerases. *PLoS One* **5**, (2010).

101. Ferrero, L., Cameron, B. & Crouzet, J. Analysis of *gyrA* and *grlA* mutations in stepwise-selected ciprofloxacin- resistant mutants of *Staphylococcus aureus*. *Antimicrob. Agents Chemother.* **39**, 1554–1558 (1995).

102. Wattam, A. R., Abraham, D., Dalay, O., Disz, T. L. *et al.* PATRIC, the bacterial bioinformatics database and analysis resource. *Nucleic Acids Res.* **42**, (2014).

103. Wattam, A. R., Davis, J. J., Assaf, R., Boisvert, S. *et al.* Improvements to PATRIC, the all-bacterial bioinformatics database and analysis resource center. *Nucleic Acids Res.* **45**, D535–D542 (2017).

104. Henikoff, S. & Henikoff, J. G. Amino acid substitution matrices from protein blocks. *Proc. Natl. Acad. Sci. U. S. A.* **89**, 10915–10919 (1992).

105. Pfeiffer, E. S. & Hiasa, H. Determination of the primary target of a quinolone drug and the effect of quinolone resistance-conferring mutations by measuring quinolone sensitivity based on its mode of action. *Antimicrob. Agents Chemother.* **51**, 3410–3412 (2007).

106. Blanche, F., Cameron, B., Bernard, F. X., Maton, L. *et al.* Differential behaviors of Staphylococcus aureus and *Escherichia coli* type II DNA topoisomerases. *Antimicrob. Agents Chemother.* **40**, 2714–20 (1996).

107. Pan, X. S. & Fisher, L. M. *Streptococcus pneumoniae* DNA gyrase and topoisomerase IV: Overexpression, purification, and differential inhibition by fluoroquinolones. *Antimicrob. Agents Chemother.* **43**, 1129–1136 (1999).

108. Takei, M., Fukuda, H., Kishii, R. & Hosaka, M. Target preference of 15 quinolones against *Staphylococcus aureus*, based on antibacterial activities and target inhibition. *Antimicrob. Agents Chemother.* **45**, 3544–3547 (2001).

109. Pan, X. S. & Fisher, L. M. Targeting of DNA gyrase in *Streptococcus pneumoniae* by sparfloxacin: selective targeting of gyrase or topoisomerase IV by quinolones. *Antimicrob. Agents Chemother.* **41**, 471–4 (1997).

110. H, F. & K, H. Primary Targets of Fluoroquinolones in *Streptococcus pneumoniae*. *Antimicrob. Agents Chemother.* **43**, (1999).

111. Belland, R. J., Morrison, S. G., Ison, C. & Huang, W. M. Neisseria gonorrhoeae acquires mutations in analogous regions of *gyrA* and *parC* in fluoroquinolone-resistant isolates. *Mol. Microbiol.* **14**, 371–380 (1994).

112. Pan, X. S., Ambler, J., Mehtar, S. & Fisher, L. M. Involvement of topoisomerase IV and DNA gyrase as ciprofloxacin targets in *Streptococcus pneumoniae*. *Antimicrob. Agents Chemother.* **40**, 2321–2326 (1996).

113. Probability theory: the logic of science. *Math. Intell.* **27**, 83–83 (2005).

114. Li, X., Mariano, N., Rahal, J. J., Urban, C. M. & Drlica, K. Quinolone-resistant Haemophilus influenzae: Determination of mutant selection window for ciprofloxacin, garenoxacin, levofloxacin, moxifloxacin. *Antimicrob. Agents Chemother.* **48**, 4460–4462 (2004).

115. Morgan-Linnell, S. K. & Zechiedrich, L. Contributions of the combined effects of topoisomerase mutations toward fluoroquinolone resistance in *Escherichia coli*. *Antimicrob. Agents Chemother.* **51**, 4205–4208 (2007).

116. Swick, M. C., Evangelista, M. A., Bodine, T. J., Easton-Marks, J. R. *et al.* Novel Conserved Genotypes Correspond to Antibiotic Resistance Phenotypes of *E. coli* Clinical Isolates. *PLoS One* **8**, e65961 (2013) doi: 10.1371/journal.pone.0065961.

117. Conley, Z. C., Bodine, T. J., Chou, A. & Zechiedrich, L. Wicked: The untold story of ciprofloxacin. *PLoS Pathog.* **14**, e1006805 (2018) doi: 10.1371/journal.ppat.1006805.

118. Al-Emran, H. M., Eibach, D., Krumkamp, R., Ali, M. *et al.* A Multicountry Molecular Analysis of *Salmonella enterica* Serovar Typhi with Reduced Susceptibility to Ciprofloxacin in Sub-Saharan Africa. *Clin. Infect. Dis.* **62**, s42–s46 (2016).

119. Ito, H., Yoshida, H., Bogaki-Shonai, M., Niga, T. *et al.* Quinolone resistance mutations in the DNA gyrase *gyrA* and *gyrB* genes of Staphylococcus aureus. *Antimicrob. Agents Chemother.* **38**, 2014–2023 (1994).

120. Brisse, S., Milatovic, D., Fluit, A. C., Verhoef, J. *et al.* Comparative in vitro activities of ciprofloxacin, clinafloxacin, gatifloxacin, levofloxacin, moxifloxacin, and trovafloxacin against *Klebsiella pneumoniae*, *Klebsiella oxytoca*, *Enterobacter cloacae*, and *Enterobacter aerogenes* cl. *Antimicrob. Agents Chemother.* **43**, 2051–5 (1999).

121. Brisse, S. & Verhoef, J. Phylogenetic diversity of *Klebsiella pneumoniae* and *Klebsiella oxytoca* clinical isolates revealed by randomly amplified polymorphic DNA, *gyrA* and *parC* genes sequencing and automated ribotyping. *Int. J. Syst. Evol. Microbiol.* **51**, 915–924 (2001).

122. Deguchi, T., Fukuoka, A., Yasuda, M., Nakano, M. *et al.* Alterations in the GyrA subunit of DNA gyrase and the ParC subunit of topoisomerase IV in quinolone-

resistant clinical isolates of *Klebsiella pneumoniae*. *Antimicrob. Agents Chemother.* **41**, 699–701 (1997).

123. Deguchi, T., Yasuda, M., Nakano, M., Ozeki, S. *et al.* Detection of mutations in the *gyrA* and *parC* genes in quinolone-resistant clinical isolates of Enterobacter cloacae. *J. Antimicrob. Chemother.* **40**, 543–549 (1997).

124. Ferrero, L., Cameron, B., Manse, B., Lagneaux, D. *et al.* Cloning and primary structure of *Staphylococcus aureus* DNA topoisomerase IV: a primary target of fluoroquinolones. *Mol. Microbiol.* **13**, 641–653 (1994).

125. Grad, Y. H., Harris, S. R., Kirkcaldy, R. D., Green, A. G. *et al.* Genomic epidemiology of gonococcal resistance to extended-spectrum cephalosporins, macrolides, and fluoroquinolones in the United States, 2000-2013. *J. Infect. Dis.* **214**, 1579–1587 (2016).

126. Heisig, P. Genetic evidence for a role of *parC* mutations in development of high-level fluoroquinolone resistance in *Escherichia coli*. *Antimicrob. Agents Chemother.* **40**, 879–85 (1996).

127. Janoir, C., Zeller, V., Kitzis, M. D., Moreau, N. J. & Gutmann, L. High-level fluoroquinolone resistance in *Streptococcus pneumoniae* requires mutations in *parC* and *gyrA*. *Antimicrob. Agents Chemother.* **40**, 2760–2764 (1996).

128. Kong, L. C., Gao, D., Gao, Y. H., Liu, S. M. & Ma, H. X. Fluoroquinolone resistance mechanism of clinical isolates and selected mutants of *Pasteurella multocida* from bovine respiratory disease in China. *J. Vet. Med. Sci.* **76**, 1655–1657 (2014).

129. Morgan-Linnell, S. K., Boyd, L. B., Steffen, D. & Zechiedrich, L. Mechanisms accounting for fluoroquinolone resistance in *Escherichia coli* clinical isolates. *Antimicrob. Agents Chemother.* **53**, 235–241 (2009).

130. Ng, E. Y., Trucksis, M. & Hooper, D. C. Quinolone resistance mutations in topoisomerase IV: Relationship to the *flqA* locus and genetic evidence that topoisomerase IV is the primary target and DNA gyrase is the secondary target of fluoroquinolones in *Staphylococcus aureus*. *Antimicrob. Agents Chemother.* **40**, 1881–1888 (1996).

131. Oizumi, N. . Relationship between mutations in the DNA gyrase and topoisomerase IV genes and nadifloxacin resistance in clinically isolated quinolone-resistant *Staphylococcus aureus*. *J. Infect. Chemother.* **7**, 191–194 (2001).

132. Schmitz, F. J., Jones, M. E., Hofmann, B., Hansen, B. *et al.* Characterization of *grlA*, *grlB*, *gyraA* and *gyrB* mutations in 116 unrelated isolates of *Staphylococcus*

aureus and effects of mutations on ciprofioxacin MIC. *Antimicrob. Agents Chemother.* **42**, 1249–1252 (1998).

133. Su, X. & Lind, I. Molecular basis of high-level ciprofloxacin resistance in *Neisseria gonorrhoeae* strains isolated in Denmark from 1995 to 1998. *Antimicrob. Agents Chemother.* **45**, 117–123 (2001).

134. Tanaka, M., Nakayama, H., Haraoka, M. & Saika, T. Antimicrobial resistance of *Neisseria gonorrhoeae* and high prevalence of ciprofloxacin-resistant isolates in Japan, 1993 to 1998. *J. Clin. Microbiol.* **38**, 521–5 (2000).

135. Vila, J., Ruiz, J., Goñi, P. & De Anta, T. J. Quinolone-resistance mutations in the topoisomerase IV *parC* gene of *Acinetobacter baumannii*. *J. Antimicrob. Chemother.* **39**, 757–762 (1997).

136. Vila, J. Activity of clinafloxacin, compared with six other quinolones, against *Acinetobacter baumannii* clinical isolates. *J. Antimicrob. Chemother.* **49**, 471–477 (2002).

137. Lewis, K. Persister cells, dormancy and infectious disease. *Nat. Rev. Microbiol.* **5**, 48–56 (2007).

138. Drlica, K., Malik, M., Kerns, R. J. & Zhao, X. Quinolone-mediated bacterial death. *Antimicrob. Agents. Chemother.* **52**, 385–392 (2008).

139. Pietsch, F., Bergman, J. M., Brandis, G., Marcusson, L. L. *et al.* Ciprofloxacin selects for RNA polymerase mutations with pleiotropic antibiotic resistance effects. *J. Antimicrob. Chemother.* **72**, 75–84 (2017).

140. Vinué, L., Hooper, D. C. & Jacoby, G. A. Chromosomal mutations that accompany qnr in clinical isolates of *Escherichia coli*. *Int. J. Antimicrob. Agents* **51**, 479–483 (2018).

141. Mukhopadhyay, J., Das, K., Ismail, S., Koppstein, D. *et al.* The RNA Polymerase 'Switch Region' Is a Target for Inhibitors. *Cell* **135**, 295–307 (2008).

142. Srivastava, A., Talaue, M., Liu, S., Degen, D. *et al.* New target for inhibition of bacterial RNA polymerase: 'switch region'. *Curr. Opin. Microbiol.* **14**, 532–543 (2011).

143. Kim, C., Mwangi, M., Chung, M., Milheirço, C. *et al.* The mechanism of heterogeneous beta-lactam resistance in MRSA: Key role of the stringent stress response. *PLoS One* **8**, e82814 (2013). doi: 10.1371/journal.pone.0082814

144. Kaspy, I., Rotem, E., Weiss, N., Ronin, I. *et al.* HipA-mediated antibiotic persistence via phosphorylation of the glutamyl-tRNA-synthetase. *Nat. Commun.* **4**, (2013).

145. Shan, Y., Gandt, A. B., Rowe, S. E., Deisinger, J. P. *et al.* ATP-Dependent persister formation in *Escherichia coli*. *MBio* **8**, e02267-16 (2017) doi: 10.1128/mBio.02267-16.

146. Tripathi, A., Dewan, P. C., Siddique, S. A. & Varadarajan, R. MazF-induced growth inhibition and persister generation in *Escherichia coli*. *J. Biol. Chem.* **289**, 4191–4205 (2014).

147. Rotem, E., Loinger, A., Ronin, I., Levin-Reisman, I. *et al.* Regulation of phenotypic variability by a threshold-based mechanism underlies bacterial persistence. *Proc. Natl. Acad. Sci. U. S. A.* **107**, 12541–12546 (2010).

148. Chant, E. L. & Summers, D. K. Indole signalling contributes to the stable maintenance of *Escherichia coli* multicopy plasmids. *Mol. Microbiol.* **63**, 35–43 (2007).

149. Santos-Zavaleta, A., Salgado, H., Gama-Castro, S., Sánchez-Pérez, M. *et al.* RegulonDB v 10.5: Tackling challenges to unify classic and high throughput knowledge of gene regulation in *E. coli* K-12. *Nucleic Acids Res.* **47**, D212–D220 (2019).

150. Keseler, I. M., Mackie, A., Santos-Zavaleta, A., Billington, R. *et al.* The EcoCyc database: reflecting new knowledge about *Escherichia coli* K-12. *Nucleic Acids Res.* **45**, D543–D550 (2017).

151. Kuroda, A., Tanaka, S., Ikeda, T., Kato, J. *et al.* Inorganic polyphosphate kinase is required to stimulate protein degradation and for adaptation to amino acid starvation in *Escherichia coli*. *Proc. Natl. Acad. Sci. U. S. A.* **96**, 14264–14269 (1999).

152. Koch, A. L. The Adaptive Responses of *Escherichia coli* to a Feast and Famine Existence. *Adv. Microb. Physiol.* **6**, 147–217 (1971).

153. Zhou, Y. N. & Jin, D. J. The *rpoB* mutants destabilizing initiation complexes at stringently controlled promoters behave like ‘stringent’ RNA polymerases in *Escherichia coli*. *Proc. Natl. Acad. Sci. U. S. A.* **95**, 2908–2913 (1998).

154. Xiao, H., Kalman, M., Ikehara, K., Zemel, S. *et al.* Residual guanosine 3’,5’-bispyrophosphate synthetic activity of *relA* null mutants can be eliminated by *spoT* null mutations. *J. Biol. Chem.* **266**, 5980–90 (1991).

155. Potrykus, K., Murphy, H., Philippe, N. & Cashel, M. ppGpp is the major source of growth rate control in *E. coli*. *Environ. Microbiol.* **13**, 563–575 (2011).

156. Yoshida, H., Bogaki, M., Nakamura, M., Yamanaka, L. M. & Nakamura, S. Quinolone resistance-determining region in the DNA gyrase *gyrB* gene of *Escherichia coli*. *Antimicrob. Agents Chemother.* **35**, 1647–1650 (1991).

157. Lindgren, P. K., Marcusson, L. L., Sandvang, D., Frimodt-Møller, N. & Hughes, D. Biological cost of single and multiple norfloxacin resistance mutations in *Escherichia coli* implicated in urinary tract infections. *Antimicrob. Agents Chemother.* **49**, 2343–2351 (2005).

158. Ostrer, L., Khodursky, R. F., Johnson, J. R., Hiasa, H. & Khodursky, A. Analysis of mutational patterns in quinolone resistance-determining regions of GyrA and ParC of clinical isolates. *Int. J. Antimicrob. Agents* **53**, 318–324 (2019).

159. Jin, D. J. & Gross, C. A. Mapping and sequencing of mutations in the *Escherichia coli rpoB* gene that lead to rifampicin resistance. *J. Mol. Biol.* **202**, 45–58 (1988).

160. Missiakas, D. M. & Schneewind, O. Growth and laboratory maintenance of *Staphylococcus aureus*. *Curr. Protoc. Microbiol.* Chapter 9: Unit–9C.1 (2013).

161. Riley, M., Abe, T., Arnaud, M. B., Berlyn, M. K. B. *et al. Escherichia coli* K-12: A cooperatively developed annotation snapshot - 2005. *Nucleic Acids Res.* **34**, 1–9 (2006).

162. Datsenko, K. A. & Wanner, B. L. One-step inactivation of chromosomal genes in *Escherichia coli* K-12 using PCR products. *Proc. Natl. Acad. Sci. U. S. A.* **97**, 6640–6645 (2000).

163. Baba, T., Ara, T., Hasegawa, M., Takai, Y. *et al.* Construction of *Escherichia coli* K-12 in-frame, single-gene knockout mutants: the Keio collection. *Mol. Syst. Biol.* **2**, 2006-2008 (2006) doi: 10.1038/msb4100050.

164. Jin, D. J. & Gross, C. A. Characterization of the pleiotropic phenotypes of rifampin-resistant *rpoB* mutants of *Escherichia coli*. *J. Bacteriol.* **171**, 5229–5231 (1989).

165. Wiegand, I., Hilpert, K. & Hancock, R. E. W. Agar and broth dilution methods to determine the minimal inhibitory concentration (MIC) of antimicrobial substances. *Nat. Protoc.* **3**, 163–175 (2008).

166. Jensen, K. F., Houlberg, U. & Nygaard, P. Thin-layer chromatographic methods to isolate 32P-labeled 5-phosphoribosyl-α-1-pyrophosphate (PRPP): Determination of cellular PRPP pools and assay of PRPP synthetase activity. *Anal. Biochem.* **98**, 254–263 (1979).

167. Schindelin, J., Arganda-Carreras, I., Frise, E., Kaynig, V. *et al.* Fiji: an open-source platform for biological-image analysis. *Nat. Methods* **9**, 676–682 (2012).

168. Zaslaver, A., Bren, A., Ronen, M., Itzkovitz, S. A. *et al.* A comprehensive library of fluorescent transcriptional reporters for *Escherichia coli*. *Nat. Methods* **3**, 623–628 (2006).

169. Langmead, B. Aligning short sequencing reads with Bowtie. *Curr. Protoc. Bioinforma.* Chapter 11: Unit 11.7 (2010).

170. Langmead, B. & Salzberg, S. L. Fast gapped-read alignment with Bowtie 2. *Nat. Methods* **9**, 357–359 (2012).

171. Li, H., Handsaker, B., Wysoker, A., Fennell, T. *et al.* The Sequence Alignment/Map format and SAMtools. *Bioinformatics* **25**, 2078–2079 (2009).

172. Quinlan, A. R. & Hall, I. M. BEDTools: a flexible suite of utilities for comparing genomic features. *Bioinformatics* **26**, 841–842 (2010).

173. Deatherage, D. E. & Barrick, J. E. Identification of mutations in laboratory-evolved microbes from next-generation sequencing data using breseq. *Methods Mol. Biol.* **1151**, 165–188 (2014).

174. Pertea, M., Kim, D., Pertea, G. M., Leek, J. T. & Salzberg, S. L. Transcript-level expression analysis of RNA-seq experiments with HISAT, StringTie and Ballgown. *Nat. Protoc.* **11**, 1650–1667 (2016).

175. Liao, Y., Smyth, G. K. & Shi, W. The R package Rsubread is easier, faster, cheaper and better for alignment and quantification of RNA sequencing reads. *Nucleic Acids Res.* **47**, e47 (2019).

176. Love, M. I., Huber, W. & Anders, S. Moderated estimation of fold change and dispersion for RNA-seq data with DESeq2. *Genome Biol.* **15**, (2014).

177. Van Den Bergh, B., Michiels, J. E., Wenseleers, T., Windels, E. M. *et al.* Frequency of antibiotic application drives rapid evolutionary adaptation of Escherichia coli persistence. *Nat. Microbiol.* **1**, (2016).

178. Fridman, O., Goldberg, A., Ronin, I., Shoresh, N. & Balaban, N. Q. Optimization of lag time underlies antibiotic tolerance in evolved bacterial populations. *Nature* **513**, 418–421 (2014).

180. Tuomanen, E., Durack, D. T. & Tomasz, A. Antibiotic tolerance among clinical isolates of bacteria. *Antimicrob. Agents Chemother.* **30**, 521–527 (1986).

181. Vega, N. M., Allison, K. R., Khalil, A. S. & Collins, J. J. Signaling-mediated bacterial persister formation. *Nat. Chem. Biol.* **8**, 431–433 (2012).

182. Gong, F., Ito, K., Nakamura, Y. & Yanofsky, C. The mechanism of tryptophan induction of tryptophanase operon expression: Tryptophan inhibits release factor-mediated cleavage of TnaC-peptidyl-tRNAPro. *Proc. Natl. Acad. Sci. U. S. A.* **98**, 8997–9001 (2001).

183. Hopkins, F. G. & Cole, S. W. A contribution to the chemistry of proteins. *J. Physiol.* **29**, 451–466 (1903).

184. Lacour, S. & Landini, P. S-Dependent Gene Expression at the Onset of Stationary Phase in *Escherichia coli*: Function of S-Dependent Genes and Identification of Their Promoter Sequences. *J. Bacteriol.* **186**, 7186–7195 (2004).

185. Prub, B. M., Nelms, J. M., Park, C. & Wolfe, A. J. Mutations in NADH: Ubiquinone oxidoreductase of *Escherichia coli* affect growth on mixed amino acids. *J. Bacteriol.* **176**, 2143–2150 (1994).

186. Halsey, C. R., Lei, S., Wax, J. K., Lehman, M. K. *et al.* Amino acid catabolism in *Staphylococcus aureus* and the function of carbon catabolite repression. *MBio* **8**, e01434-16 (2017) doi: 10.1128/mBio.01434-16.

187. Nuxoll, A. S., Halouska, S. M., Sadykov, M. R., Hanke, M. L. *et al.* CcpA Regulates Arginine Biosynthesis in *Staphylococcus aureus* through Repression of Proline Catabolism. *PLoS Pathog.* **8**, page numbers(2012).

188. Stanley, N. R. & Lazazzera, B. A. Environmental signals and regulatory pathways that influence biofilm formation. *Mol. Microbiol.* **52**, 917–924 (2004).

189. Reed, J. M., Olson, S., Brees, D. F., Griffin, C. E. *et al.* Coordinated regulation of transcription by CcpA and the *Staphylococcus aureus* two component system HptRS. *PLoS One* **13**, e0207161 (2018) doi: 10.1371/journal.pone.0207161.

190. Seidl, K., Goerke, C., Wolz, C., Mack, D. *et al.* Staphylococcus aureus CcpA affects biofilm formation. *Infect. Immun.* **76**, 2044–2050 (2008).

191. Wichelhaus, T. A., Schäfer, V., Brade, V. & Böddinghaus, B. Molecular characterization of *rpoB* mutations conferring cross-resistance to rifamycins on methicillin-resistant *Staphylococcus aureus*. *Antimicrob. Agents Chemother.* **43**, 2813–2816 (1999).

192. Telenti, A., Imboden, P., Marchesi, F., Lowrie, D. *et al.* Detection of rifampicin-resistance mutations in *Mycobacterium tuberculosis*. *Lancet* **341**, 647–651 (1993).

193. Fisher, R. A., Gollan, B. & Helaine, S. Persistent bacterial infections and persister cells. *Nat. Rev. Microbiol.* **15**, 453–464 (2017).

194. Lei, T., Zhang, Y., Yang, J., Silverstein, K. & Ji, Y. Complete Genome Sequence of Hospital-Acquired Methicillin-Resistant *Staphylococcus aureus* Strain WCUH29. *Microbiol. Resour. Announc.* **8**, e00551-19 (2019). doi: 10.1128/MRA.00551-19

195. BARNER, H. D. & COHEN, S. S. The induction of thymine synthesis by T2 infection of a thymine requiring mutant of *Escherichia coli*. *J. Bacteriol.* **68**, 80–88 (1954).

196. Little, J. G. & Hanawalt, P. C. Thymineless death and ultraviolet sensitivity in *Micrococcus radiodurans*. *J. Bacteriol.* **113**, 233–240 (1973).

197. Khodursky, A., Guzmán, E. C. & Hanawalt, P. C. Thymineless Death Lives On: New Insights into a Classic Phenomenon. *Annu. Rev. Microbiol.* **69**, 247–263 (2015).

198. Casaregola, S., D'Ari, R. & Huisman, O. Quantitative evaluation of *recA* gene expression in *Escherichia coli*. *MGG Mol. Gen. Genet.* **185**, 430–439 (1982).

199. Howe, W. E. & Mount, D. W. Production of cells without deoxyribonucleic acid during thymidine starvation of lexA- cultures of *Escherichia coli* K-12. *J. Bacteriol.* **124**, 1113–1121 (1975).

200. George, J., Castellazzi, M. & Buttin, G. Prophage induction and cell division in *E. coli*. III. Mutations *sfiA* and *sfiB* restore division in *tif* and *lon* strains and permit the expression of mutator properties of *tif*. *Mol. Gen. Genet.* **140**, 309–332 (1975).

201. Huisman, O., D'Ari, R. & Gottesman, S. Cell-division control in *Escherichia coli*: Specific induction of the SOS function SfiA protein is sufficient to block septation. *Proc. Natl. Acad. Sci. U. S. A.* **81**, 4490–4494 (1984).

202. Burdett, I. D. J. & Murray, R. G. E. Septum formation in *Escherichia coli*: characterization of septal structure and the effects of antibiotics on cell division. *J. Bacteriol.* **119**, 303–324 (1974).

203. Dai, K. & Lutkenhaus, J. *ftsZ* Is an essential cell division gene in *Escherichia coli*. *J. Bacteriol.* **173**, 3500–3506 (1991).

204. Huisman, O., D'Ari, R. & George, J. Inducible *sfi* dependent division inhibition in *Escherichia coli*. *MGG Mol. Gen. Genet.* **177**, 629–636 (1980).

205. Walker, J. R. & Smith, J. A. Cell division of the *Escherichia coli lon*-mutant. *MGG Mol. Gen. Genet.* **108**, 249–257 (1970).

206. Mizusawa, S. & Gottesman, S. Protein degradation in *Escherichia coli*: the *lon* gene controls the stability of SulA protein. *Proc. Natl. Acad. Sci. U. S. A.* **80**, 358–362 (1983).

207. Kuong, K. J. & Kuzminov, A. Disintegration of nascent replication bubbles during thymine starvation triggers RecA- and RecBCD-dependent replication origin destruction. *J. Biol. Chem.* **287**, 23958–23970 (2012).

208. Ostrer, L., Hamann, B. L. & Khodursky, A. Perturbed states of the bacterial chromosome: A thymineless death case study. *Front. Microbiol.* **6**, (2015). doi: 10.3389/fmicb.2015.00363

209. Vidal, J., Perrelet, A. & Sicard, N. Morphology and DNA synthesis of cells recovering from thymineless death in *E. coli* K12. *Experientia* **30**, 1262–1264 (1974).

210. Bazill, G. W. Lethal unbalanced growth in bacteria. *Nature* **216**, 346–349 (1967).

211. Sargent, M. G. Anucleate cell production and surface extension in a temperature-sensitive chromosome initiation mutant of *Bacillus subtilis*. *J. Bacteriol.* **123**, 1218–34 (1975).

212. Martin, C.M. *Role of DNA replication initiation on the lethality caused by thymine starvation*. (Universidad de Extremadura, Badajoz, 2014).

213. Hirota, Y., Jacob, F., Ryter, A., Buttin, G. & Nakai, T. On the process of cellular division in *Escherichia coli*. I. Asymmetrical cell division and production of deoxyribonucleic acid-less bacteria. *J. Mol. Biol.* **35**, 175-192 (1968).

214. Cook, W. R., MacAlister, T. J. & Rothfield, L. I. Compartmentalization of the periplasmic space at division sites in Gram-negative bacteria. *J. Bacteriol.* **168**, 1430–1438 (1986).

215. Koch, A. L. The Biophysics of the Gram-Negative Periplasmic Space. *Crit. Rev. Microbiol.* **24**, 23–59 (1998).

216. Geissler, B., Shiomi, D. & Margolin, W. The *ftsA** gain-of-function allele of *Escherichia coli* and its effects on the stability and dynamics of the Z ring. *Microbiology* **153**, 814–825 (2007).

217. Breeuwer, P. & Abee, T. Assessment of viability of microorganisms employing fluorescence techniques. *Int. J. Food Microbiol.* **55**, 193–200 (2000).

218. Nakayama, K., Kusano, K., Irino, N. & Nakayama, H. Thymine starvation-induced structural changes in *Escherichia coli* DNA Detection by pulsed field gel

electrophoresis and evidence for involvement of homologous recombination. *J. Mol. Biol.* **243**, 611–620 (1994).

219. Li, Y., Sergueev, K. & Austin, S. The segregation of the *Escherichia coli* origin and terminus of replication. *Mol. Microbiol.* **46**, 985–995 (2002).

220. Bouvier, F. & Sicard, N. Interference of DNA *ts* mutations of *Escherichia coli* with thymineless death. *J. Bacteriol.* **124**, 1198–204 (1975).

221. Hanawalt, P. Involvement of Synthesis of RNA in Thymineless Death. *Nature* **198**, (1963). DOI:10.1038/198286a0

222. Carl, P. L. *Escherichia coli* mutants with temperature-sensitive synthesis of DNA. *MGG Mol. Gen. Genet.* **109**, 107–122 (1970).

223. Gullbrand, B. & Nordström, K. FtsZ ring formation without subsequent cell division after replication runout in *Escherichia coli*. *Mol. Microbiol.* **36**, 1349–1359 (2000).

224. Nakayama, K., Kusano, K., Irino, N., Nakayama, H.*et al.* Isolation and genetic characterization of a thymineless death-resistant mutant of *Escherichia coli* K12: Identification of a new mutation (*recQ1*) that blocks the RecF recombination pathway. *MGG Mol. Gen. Genet.* **195**, 474–480 (1984).

225. Nakayama, K., Shiota, S. & Nakayama, H. Thymineless death in *Escherichia coli* mutants deficient in the RecF recombination pathway. *Can. J. Microbiol.* **34**, 905–907 (1988).

226. Cooper, S. & Helmstetter, C. E. Chromosome replication and the division cycle of *Escherichia coli*. *J. Mol. Biol.* **31**, 519–540 (1968).

227. Kornberg, T. & Baker, A. *DNA replication*. (University Science Books, 2005).

228. Bi, E. & Lutkenhaus, J. FtsZ regulates frequency of cell division in *Escherichia coli*. *J. Bacteriol.* **172**, 2765–2768 (1990).

229. Ward, J. E. & Lutkenhaus, J. Overproduction of FtsZ induces minicell formation in *E. coli*. *Cell* **42**, 941–949 (1985).

230. Martín, C. M., Viguera, E. & Guzmán, E. C. Rifampicin suppresses thymineless death by blocking the transcription-dependent step of chromosome initiation. *DNA Repair (Amst).* **18**, 10–17 (2014).

231. Lies, M., Visser, B. J., Joshi, M. C., Magnan, D. & Bates, D. MioC and GidA proteins promote cell division in *E. coli*. *Front. Microbiol.* **6**, (2015). doi: 10.3389/fmicb.2015.00516

232. Morigen, M., Flåtten, I. & Skarstad, K. The Escherichia coli datA site promotes proper regulation of cell division. *Microbiol. (United Kingdom)* **160**, 703–710 (2014).

233. Hanawalt, P. C. Macromolecular synthesis in *E. coli* under conditions of unbalanced growth. (Yale University, New Haven, 1958).

234. Pritchard, R. H. & Lark, K. G. Induction of replication by thymine starvation at the chromosome origin in Escherichia coli. *J. Mol. Biol.* **9**, 288–307 (1964).

235. Maaløe, O. & Hanawalt, P. C. Thymine deficiency and the normal DNA replication cycle. I. *J. Mol. Biol.* **3**, 144–155 (1961).

236. Sun, Q. & Margolin, W. Effects of perturbing nucleoid structure on nucleoid occlusion-mediated toporegulation of FtsZ ring assembly. *J. Bacteriol.* **186**, 3951–3959 (2004).

237. Arjes, H. A., Kriel, A., Sorto, N. A., Shaw, J. T.*et al.* Failsafe mechanisms couple division and DNA replication in bacteria. *Curr. Biol.* **24**, 2149–2155 (2014).

238. Bernard, R., Marquis, K. A. & Rudner, D. Z. Nucleoid occlusion prevents cell division during replication fork arrest in *Bacillus subtilis*. *Mol. Microbiol.* **78**, 866–882 (2010).

239. Cambridge, J., Blinkova, A., Magnan, D., Bates, D. & Walker, J. R. A Replication-inhibited unsegregated nucleoid at mid-cell blocks Z-ring formation and cell division independently of SOS and the SlmA nucleoid occlusion protein in *Escherichia coli*. *J. Bacteriol.* **196**, 36–49 (2014).

240. Neidhardt, F. C., Bloch, P. L. & Smith, D. F. Culture medium for *Enterobacteria*. *J. Bacteriol.* **119**, 736–747 (1974).

241. Thomason, L. C., Costantino, N. & Court, D. L. E. coli Genome Manipulation by P1 Transduction, in *Curr. Protoc. Mol. Biol.* Chapter 1: Unit 1.17 (2007).

242. Khodursky, A. B., Peter, B. J., Schmid, M. B., DeRisi, J. *et al.* Analysis of topoisomerase function in bacterial replication fork movement: Use of DNA microarrays. *Proc. Natl. Acad. Sci. U. S. A.* **97**, 9419–9424 (2000).

243. Itsko, M. & Schaaper, R. M. The dgt gene of *Escherichia coli* facilitates thymine utilization in thymine-requiring strains. *Mol. Microbiol.* **81**, 1221–1232 (2011).